https://doi.org/10.15388/vu.thesis.55

VILNIUS UNIVERSITY

Indrė
LAPEIKAITĖ

Effect of amino acids and NMDA on electrical signalling parameters of Charophyte *Nitellopsis obtusa*

DOCTORAL DISSERTATION
Natural Sciences,
Biophysics N 011

VILNIUS 2020

This dissertation was written between 2014 and 2019 at Vilnius University. The Research Council of Lithuania supported the research.

Academic supervisor:
Osvaldas Ruksenas PhD prof. (Vilnius University, Natural Sciences, Biophysics – N 011).

https://doi.org/10.15388/vu.thesis.55

VILNIAUS UNIVERSITETAS

Indrė
LAPEIKAITĖ

Amino rūgščių ir NMDA įtaka menturdumblių *Nitellopsis obtusa* ląstelių elektrinių signalų parametrams

DAKTARO DISERTACIJA

Gamtos mokslai,
Biofizika N 011

VILNIUS 2020

Disertacija rengta 2014–2019 metais Vilniaus Universitete.
Mokslinius tyrimus rėmė Lietuvos mokslo taryba.

Mokslinis vadovas:

Prof. dr. Osvaldas Rukšėnas (Vilniaus universitetas, gamtos mokslai, biofizika – N 011).

TABLE OF CONTENTS

LIST OF ABBREVIATIONS

AA – amino acids
Ala – alanine
AMPA – α-amino-3-hydroxy-5-methyl-4-isoxazole propionate
AP – action potential
AP-5 – DL-2-Amino-5-phosphonopentanoic acid
AP-7 – DL-2-Amino-7-phosphonoheptanoic acid
APW – artificial pond water
Asn – L-asparagine
Asp – aspartate
*At*GLR – *Arabidopsis thaliana* Glutamate-like Receptor
CNQX – 6-cyano-7- nitroquinoxaline-2,3-dione
DNQX – 6,7-Dinitroquinoxaline-2,3(1H,4H)-dione
E_{th} – excitation threshold of action potential (mV of membrane potential)
Gly – L-glycine
Gln – glutamine
GLR – glutamate receptor-like channels in plants
Glu – L-glutamate
HEPES – 4-(2-hydroxyethyl)-1-piperazineethanesulfonic acid
I_{-90} – Cl^- current transient amplitude at -90 mV (voltage-clamp)
I-Asn – isoasparagine
I_{max} – maximum Cl^- current transient amplitude (voltage-clamp)
IP_3 – inositol trisphosphate
IP_6 – inositol hexakisphosphate
Lys – lysine
Met – methionine
MP – membrane potential
NMDA – N-Methyl-D-aspartic acid
Pro – proline
RP – membrane resting potential
$t_{act.}$ – current transient activation duration
$t_{inact.}$ – current transient inactivation duration
TRIS – tris(hydroxymethyl)aminomethane

INTRODUCTION

In order to survive in ever-changing environment, plants optimize their physiological functions. Environmental inputs – a plethora of physical, biological and chemical constantly varying cues – evoke well-tuned responses. Information about locally acting stimuli is transmitted via chemical, hydraulic or electrical signals of whom the latter ones are the fastest means of communication in plants (Fromm and Lautner 2007). Over the years electrical signalling unfolded as an integral part of plant physiology. Bioelectrical responses range from local cell membrane potential alterations to several types of propagating systemic signals whose primary purpose is to transduce information to distant parts of the plant body (Trebacz *et al.* 2006, Pyatygin *et al.* 2008). Electrical signals are the primary responses to such environmental factors as changes in illumination, temperature, touch, also to biotic factors such as microbes and pathogens (Fromm and Lautner 2007, Pyatygin *et al.* 2008) and, equally important – to internal/external signalling molecules (Kisnieriene *et al.* 2018). Universal among *Plantae*, and most extensively characterized type are action potentials (APs) – transmittable through long distances, distinctly shaped, self-propagating signals (Dziubinska, 2003). APs were first discovered in Characeaen algae (reviewed in Beilby 2007) and over the years described not only in "sensitive" plants, such as *Mimosa* or *Dionaea* but also in conventional food crops and *Arabidopsis* (Sukhov *et al.* 2019). Propagation of APs leads to modulation of vital physiological functions such as photosynthesis, respiration, gene expression, regulation of phytohormones' activity and many others (reviewed by Pyatygin *et al*. 2008, Sukhov *et al.* 2019,). Thus electrical signals' regulatory/transduction function is prominent throughout *Plantae*. Electrical signals are highly variable among different plants, yet in a particular tissue of a species APs are considered to be uniform responses regardless of the modality of the causing stimulus. However, emerging research reveals that the variability of APs is not only an intrinsic property of plants, but that it also can be related to the effect of environment (Beilby and Shepherd 2001, Krol *et al.* 2007, Kisnieriene *et al.* 2009, Sevriukova *et al.* 2014, Kisnieriene *et al.* 2018).

It has been revealed that amino acids (AA) are exploited by plants as signalling molecules (Miller *et al.* 2008) – among whom glutamate so far holds the most elucidated regulatory function. It has been well-described that root development is responsive to Glu content in the soil. Later it has been documented that external Glu elicits cytoplasmic Ca^{2+} oscillations and plasma membrane depolarization in *Arabidopsis* root hair in a dose-dependent manner

(Dennison and Spalding 2000, Sivaguru *et al.* 2003, Vincill *et al.* 2013). Calcium signalling is intertwined with AP generation since an increase in cytoplasmic calcium initiates AP generation – a mechanism thought to be common to all plants (reviewed in Fromm and Lautner 2007). In some cases, exogenously applied Glu can elicit spontaneous action potentials, as reported in various species (Felle and Zimmermann 2007, Krol *et al.* 2007, Stolarz *et al.* 2010). Also, APs elicited upon AA effect possess such altered characteristics as amplitude and duration (Krol *et al.* 2007). These findings fuelled further research on Glu and AA signalling in plants.

Signal transduction mechanism of Glu as an environmental signal was elucidated when GLRs (glutamate receptor-like receptors) were characterized in plants. GLRs are the homologs to animal ionotropic glutamate receptors (iGluRs). Upon activation by neurotransmitters (Glu/Gly), iGluRs permeate cations, including calcium, thus predicating signal transduction in neurons (Dennison and Spalding 2000) – transduction mechanism now known also, to some extent, to be inherent to plants (Qi *et al.* 2006, Stephens *et al.* 2008). GLR channel genes have been found in genomes of flowering plants, ferns, mosses and chlorophytes. GLRs (depending on clade) are activated by Glu and other amino acids (Wudick *et al*. 2018).

Characterization of GLR-mediated Ca^{2+} fluctuations puts GLRs in a crucial position in plant physiology regarding calcium signalling and forming of calcium signals together with other Ca^{2+}-permeable channels (Mousavi *et al.* 2013, Demidchik *et al.* 2018, Medvedev 2018). A transient rise in the cytoplasmic calcium concentration is an early step in the process by which many signals are transduced into a physiological response. GLR-mediated responses are calcium-based and have plant-specific physiological functions ranging from carbon and nitrogen metabolism (Kang *et al.* 2004), abscisic acid biosynthesis and signalling (Kong *et al.* 2015), immune responses (Kwaaitaal *et al.* 2011), wound-induced leaf-to-leaf electrical signalling (Mousavi *et al.* 2013), to systemic reactive oxygen species signalling (Choi *et al.* 2017).

Although GLRs have a wide range of agonists and action targets, it is generally agreed that GLR-mediated responses are suppressed by classical iGluR antagonists such as AP-5 and DNQX (reviewed by Weiland *et al.* 2016). Pharmacological approach supports the GLR receptor as a mediator of various AA effects. Unexpectedly, despite the wide range of GLR agonists, classical synthetic NMDA-type iGluR agonist NMDA (binding to the Glu site in the iGluR) was demonstrated to be inactive in higher plants (Dennison and Spalding 2000, Qi *et al.* 2006), with only one exception (Sivaguru *et al.* 2003). However, NMDA action was demonstrated in the liverwort *Conocephalum conicum* (Krol *et al.* 2007): NMDA application induced APs, and this effect

was inhibited by AP-5, thus NMDA is a potential synthetic agonist at least in some plant species.

The components of glutamatergic system – AA-activated ionotropic receptors, involvement of electrical signals and extensive physiological outputs – in plants have been relatively well-described, yet the interlinks are yet to be elucidated. Thus, a fully active synthetic agonist would allow to distinguish GLR-mediated responses, apply pharmacological approaches excluding crosstalk with internal AA signalling while investigating glutamatergic transduction pathway.

Current knowledge of the glutamatergic system in plants is mainly based on *Arabidopsis* and vascular plant research (Weiland *et al.* 2016). The electrical signals recorded in tissues do not accurately regard the excitation of single cell. Following, in tissues it is almost unattainable to perform voltage clamp recordings of ion fluxes in single cell during excitation due to cell connections via plasmodesmata, thus such parameters as chloride efflux dynamics and AP threshold potential are also uncharted. Precise multi-parametrical analysis of both current- and voltage-clamp recording of the same cell upon exposure to AA and NMDA has never been reported. Also, inhibition of the excitatory effect of NMDA by iGluR antagonists in plants was reported in only one instance (Krol *et al.* 2007), so it is unclear whether this agonist is effective in *Plantae* research. The effect of NMDA and its inhibition in other than *Conocephalum* taxa is yet to be determined.

Considering the variability of excitation parameters among plant species and variety of previously used electrophysiological approaches, characterization of plant APs, even among Characeaen, is not standardized and still requires robust multi-parametrical analysis. Characeaen internodal cell provides a robust single plant cell model system for electrical signalling investigation. APs of giant Characeaen cell exhibit relatively consistent characteristics in comparison to composite tissue APs (Sukhov *et al.* 2019). The possibilities of various electrophysiological approaches toward Characeaen internodal cell enable detailed investigation of electrical signalling alterations on a single cell level, including those of excitation threshold (E_{th}), AP peak, amplitude and repolarization dynamics in free-running MP and fluxes' dynamics in clamped MP (Kisnieriene *et al.* 2018). These properties enable characterization of excitation upon various environmental stimuli (Sevriukova *et al.* 2014, Kisnieriene *et al.* 2018, Kisnieriene *et al.* 2019). Prior to this study, the AA or NMDA effect has not been investigated in Characeaen, thus using advantages of this model system, presented research aims to describe modulation of electrical signalling upon

exposure to AA, a synthetic iGluR agonist NMDA, and propose criteria for evaluation of AP parameters.

The aim and the objectives of the study:

The aim of the study:

determine whether electrical signalling parameters of a single plant cell of Characeaen are modulated by putative glutamate receptor-like channels' agonists, quantifying the possible effect and examining its inhibition by ionotropic glutamate receptors' antagonists.

The objectives of the study:

1) Determine the effect and dose-dependency of Asn, Glu and NMDA on electrical signalling parameters:
   a. Membrane potential and resistance in steady-state
   b. Action potential excitation threshold, amplitude and duration
   c. Cl^- efflux amplitude and temporal dynamics during excitation
2) Determine whether the effect of glutamate receptor-like channels' agonists is reversible.
3) Determine the effect of ionotropic glutamate receptor antagonists AP-5 and DNQX
4) Determine whether the putative effect of NMDA is inhibited by ionotropic glutamate receptors' antagonists.

Novelty and significance. The study:

a) for the first time presents correlations between excitation parameters obtained by current-clamp and voltage-clamp approaches in single Characeaen cells in standard conditions,
b) reports the first standardized determination of AP excitation threshold potential in plants,

c) introduces quantified chloride efflux temporal dynamics as viable electrophysiological parameters altered by glutamate receptor-like channels' agonists,

d) presents a detailed quantitative description of Glu and Asn excitatory effect pattern on a single plant cell,

e) defines NMDA as an active excitation-altering compound in *Characeaen*, exhibiting the same effect pattern as AA and inhibited by both NMDA and non-NMDA type ionotropic glutamate receptors' antagonists.

Statements to be defended:

1) Multiparametric analysis of excitation parameters in a single plant cell obtained by current-clamp and voltage-clamp approaches allows detailed evaluation of glutamatergic system-mediated electrical signalling alterations.

2) Exposure to amino acids Glu and Asn enhances *Nitellopsis obtusa* cell excitability and alters electrical signalling parameters in a dose-dependent manner.

3) In *Nitellopsis obtusa* modulation of electrical signalling parameters by a synthetic compound NMDA and AA follows the same pattern, yet NMDA effect exceeds that of AA.

4) NMDA effect is prevented by both NMDA-type and non-NMDA type ionotropic glutamate receptors' synthetic antagonists AP-5 and DNQX.

1. LITERATURE REVIEW

1.1 Electrical signalling in plants

1.1.1 General features

For years the physiological significance of electrical signalling in plants has been neglected, thus, many aspects of plant excitability are yet to be elaborated. Nowadays it is common knowledge that in animals as well as in plants ion fluxes through plasma membrane provide biophysical base for electrical signals - an integral part of plant physiology, ranging from local membrane potential alterations of the cell to several types of systemic propagating signals. Electrical signals are transient changes in the gradient of the electrical potential across the plasma membrane (Fromm and Lautner, 2007, Vodeneev *et al.* 2015, Sukhov 2016). To this date, there are three types of electrical signals discovered in plants: system potentials, variation potentials, and action potentials (APs). The least researched plant electrical signals are system potentials, characterized as propagating transitory hyperpolarization waves, observed only in higher plants (Sukhov *et al.* 2019). Variation potentials are elicited by damage and can be distinguished by steep depolarization and irregular repolarization with extended duration (exceeding tens of minutes). Universal and most extensively characterized are action potentials - a short-term (from seconds to tens of seconds) propagating depolarization and repolarization of the potential difference across the membrane (MP) (Trebacz *et al.* 2006, Beilby 2007, Fromm and Lautner 2007, Sukhov *et al.* 2016, Sukhov 2019). One of the first APs were observed in Characeaen algae (Blinks *et al.* 1929), and later research on this family led the field of plant physiology and electrophysiology (reviewed in Beilby 2007).

AP kinetics depend on the integrated activities of ion channels in the plasma membrane (Lunevsky *et al.* 1983, Fromm and Bauer 1994, Wayne 1994). It is thought that the mechanism of AP generation is to some extent common among plants (Lunevsky *et al.* 1983, Trebacz *et al.* 2006, Felle and Zimmermann 2007) and algae including Characeaen (Lunevsky *et al.* 1983, Okihara *et al.* 1991, Homann and Thiel 1994, Thiel *et al.* 1997). According to the generally accepted model, depolarization of MP during AP is initiated by calcium influx into the cytosol followed by Cl^- efflux through Ca^{2+} activated Cl^- channels (Williamson and Ashley 1982, Lunevsky *et al.* 1983). The MP depolarization activates voltage-gated potassium channels allowing K^+ efflux repolarizing MP, ATP-dependent proton efflux also contributes to MP repolarization. In cells of plants, both the plasmalemma and the tonoplast usually undergo excitation, with the tonoplast AP being slower and of smaller

amplitude (Findley 1970, Kikuyama 1986). The participation of two membranes, multiple ion transport systems therein and lack of specialization of cells account for the Characeaen AP shape being more variable than that of animal APs (Beilby and Casanova 2014). APs in Characeaen, mosses and higher plants hold the following characteristics (reviewed by Sukhov *et al.* 2019):

a) APs are induced by non-damaging stimuli, including electrical currents (Krol *et al.* 2006, Bulychev and Krupenina 2010, Sevriukova *et al.* 2014, Kisnieriene *et al.* 2016, 2018).
b) The generation of the action potential has an all-or-none character: the electrical response is not induced by sub-threshold stimuli, while the over-threshold stimuli induce APs with constant amplitude (Opritov *et al.* 1991, Trebacz *et al.* 2006, Sukhov 2016). APs exhibit species-specific excitation threshold (Beilby 2007, Sukhov *et al.* 2019).
c) AP is a self-propagating signal. It propagates through living tissues and has a constant rate, which usually equals a value between 0,1-10,0 cm/s in different plants (Sibaoka 1991, Trebacz *et al.* 2006, Favre and Agosti 2007, Huber and Bauerle 2016, Sukhov *et al.* 2019). However, the rate can be 10-20 cm/s in plants exhibiting rapid movements (Sibaoka 1991, Huber and Bauerle, 2016). The AP appears to propagate without decrement in velocity or magnitude (whereas the VP parameters decrease significantly with distance). APs can be transmitted only down the cell lines having low-resistance plasmodesmata connections (Trebacz *et al.* 2006). In Characeaen AP transmission velocity is 1,1-4,4 cm/s, depending on the species (Beilby 2007).
d) The generation and propagation of the action potential are limited by absolute and relative refractory periods (Trebacz *et al.* 2006, Favre and Agosti 2007). These periods can be extensive in higher plants: from 0,5 to 20 min (the absolute refractory period) and from 2 to 300 min (the relative refractory period) (Opritov *et al.* 2005, Favre and Agosti 2007). Carnivorous plants are an exception – with a refractory period of seconds (Król *et al.* 2010). The refractory periods in algae and mosses are equal a few minutes (Favre and Agosti, 2007). In Characeaen, however, the absolute refractory period is around 3 s and relative around 6-60 s (Beilby 2007).

APs are induced by cold (Fromm and Bauer 1994, Opritov *et al.* 2005, Krol *et al.* 2006), mechanical irritation (Kishimoto 1968, Sibaoka 1991, Shepherd *et al.* 2008), some chemical agents (Felle and Zimmermann 2007), including

amino acids (Felle and Zimmermann 2007, Krol *et al.* 2007, Stolarz *et al.* 2010) and the action of light or shadow (Trebacz *et al.* 2006).

1.1.2 Mechanism of excitation

Membrane resting potential (of Nitellopsis)

The electrical potential across a membrane is determined to a large extent by the difference in ion concentrations across and their permeabilities. The concentrations of Cl^-, Na^+, K^+, and Ca^{2+} in the external medium, cytoplasm, and vacuole of *Nitellopsis obtusa* cells, as reported by various studies, are summarized in Table 1. The distribution and the concentration gradients of these ions is considered to be universal in *Plantae* (Sukhov *et al.* 2019)

At the equilibrium, the net flow of charges through the membrane is zero, and the permeability of the membrane to relevant ions determines membrane resting potential. The equilibrium potentials of all the ions diffusing across a membrane contribute to the resting membrane potential (RP). The RP of the plasma membrane of Characeaen internodal cells is usually approximately -180 mV indicating that permeability coefficient $P_K >> P_{Na} > P_{Cl} > P_{Ca}$ and the membrane potential is determined to a large extent by the passive diffusion of K^+ (reviewed in Wayne 1994). The greater the permeability to K^+, the closer membrane potential is to E_K. However, the plasma membrane of Characeaen maintains electrogenic pumps that pump out cations at the expense of ATP and generate a more negative membrane potential. Thus, the membrane potential of the Characeaen plasma membrane is usually between -180 and -300 mV. (Wayne 1994, Beilby 2007, Kisnieriene *et al.* 2018).

The Characeaen plasma membrane has four stable states. Background state conductance is dominated by non-selective cation channels which supply micronutrients to the plant and contribute to signalling of osmotic changes (Demidchik and Maathuis 2007, Beilby and Casanova 2014). This state is entered upon exposure to salinity with reversal potential of ~ -100 mV (Beilby and Shepherd 2001). The others are the K^+-state (MP more positive than -180 mV) - determined predominantly by the diffusion of K^+, the pump state, where the electrogenic H^+-ATPase contributes to the hyperpolarization of MP (between -180 mV and -300 mV) and a fourth stable state which occurs at high pH, when the permeability to H^+ or OH^- becomes so large that the diffusion potential is determined by the permeability for H^+ or OH^-. MP in this state is more negative than -200 mV at pH_{out} 12 (Bisson and Walker 1981).

The vacuolar membrane of Characeaen cells also has an electrogenic H^+-ATPase and H^+-PPase (pyrophosphate powered pump), yet the vacuolar membrane potential (-10 mV) is similar to the equilibrium potential for K^+ and Cl^-, indicating that there is a large permeability to K^+ and Cl^- that effectively short-circuits the pumps (Beilby 2007).

Table 1. Concentrations of ions reported in *Nitellopsis obtusa* cytoplasm and vacuole, the ionic composition of artificial pond water and corresponding equilibrium potential for each ion across plasma membrane (E_{pl}) and tonoplast (E_{ton}) (based on concentrations reported by Katsuhara and Tazawa (1988) presented in bold) at room temperature. Other references are listed below.

	$[X]_{Cyt}$, mM				$[X]_{Vac}$, mM				APW, $[X]_{out}$, mM			
	K^+	Na^+	Cl^-	Ca^{2+}	K^+	Na^+	Cl^-	Ca^{2+}	K^+	Na^+	Cl^-	Ca^{2+}
									0,1	**1**	**1,3**	**0,1**
[1]			15		124	27		14				
[2]				**<1µM**								
[3]	**88**	**11**	**55**		**135**	**25**	**140**					
[4]					136	24	190	**9**				
E_{pl}, mV	**-170**	**-60**	**95**	**80**					$[X]_{out} = [X]_{out}$, $[X]_{in} = [X]_{Cyt}$			
E_{ton}, mV					**10**	**20**	**-25**	**135**	$[X]_{out} = [X]_{Vac}$, $[X]_{in} = [X]_{Cyt}$			

E_X - equilibrium potential for ion X (mV), following Nernst equation:
$E_X = (RT / z_X F) \ln ([X]_{out} / [X]_{in})$
z_X - valence of ion X
$[X]_{out}$ and $[X]_{in}$ - concentrations of an ion on the outside and inside medium, mM

[1] Lunevsky *et al.* 1983; [2] Mimura and Tazawa, 1983 (indirectly); [3] Katsuhara and Tazawa, 1988; [4] Wayne and Staves, 1991.

Cytoplasmic calcium increase – crucial part of AP initiation

The influx of Ca^{2+} in cytosolic space is one of the first steps in generating AP (Shiina and Tazawa 1986, Biskup *et al.* 1999, Wacke *et al.* 2003). Free cytoplasmic Ca^{2+} concentration ($[Ca^{2+}]_{cyt}$) during the AP increases many-fold (Trebacz *et al.* 2006, Felle and Zimmermann 2007): Williamson and Ashley (1982) estimated in *Chara* a 30-fold (from ~0,2 µM to 7 µM in *Chara*) and in *Nitella* a 42-fold increase during an AP. In *Conocephalum*, this increase is on average 2-6 fold (Trebacz *et al.* 1994). Excitation is generally inhibited by the Ca^{2+} channel blockers, e.g. La^{3+} or Ca^{2+} chelators - EGTA (Mimura and Tazawa 1983). Ca^{2+} flux into the cytoplasm is voltage dependant (Lunevsky *et al.* 1983, Kataev *et al.* 1984, Berestovski *et al.* 1987), thus activation of

voltage-dependent Ca^{2+} channels is presumed, yet they are not yet associated with any specific gene (Demidchik *et al.* 2018).

Even though the regulation of transient $[Ca^{2+}]_{cyt}$ increase during the AP is very precise and occurs according to the all-or-none rule (Wacke and Thiel 2001), the origin of calcium itself remains controversial.

In the extracellular origin theory, a Ca^{2+} influx through voltage-dependent Ca^{2+} permeable channels in plasmalemma is supposed (Berestovsky and Kataev 2005), this raised from observation that externally applied Mg^{2+} (3 mM) inhibits excitation in Characeaen (Findlay and Hope 1964). Also, depletion of Ca^{2+} from the external solution reduced the Cl^- efflux during excitation (Shiina and Tazawa 1987). Thiel-Beilby model also proposes that some of Ca^{2+} comes from the extracellular solution (Beilby and Al Khazaaly 2016).

Calcium concentration in internal stores – vacuole (~10 mM) and endoplasmic reticulum (~10 μM according to Thiel-Beilby model, Wacke and Thiel 2001) is high in comparison to cytoplasm (**Table 1**). It was reported that in Characeae, most of the Ca^{2+} in the cytoplasm at the time of the action potential comes from the internal stores (Kikuyama *et al.* 1993) and as Characeae are ancestral algae to land plants (Nishiyama *et al.* 2018), APs in land plants may have a similar mechanism.

The concept that intracellular calcium is the origin of cytoplasmic rise during excitation states, that the initial membrane depolarization, whether obtained by passing a current across the membrane or by mechanical stimulation, elevates the levels of the second messenger (inositol triphosphate (IP_3) as presumed at that time) in the cytoplasm, and second messenger-dependent Ca^{2+} release from internal stores takes place (Biskup *et al.* 1999). Microinjected IP_3 was shown to elicit an elevation in cytosolic Ca^{2+} of *C. communis* guard cells (Gilroy *et al.* 1990). Also, it has been documented that elevation of IP_3 is effective in triggering membrane excitation in *Chara* (Thiel *et al.* 1990) and that inhibition of IP_3 production suppresses the excitation (Biskup *et al.* 1999). However, Tazawa and Kikuyama (2003) attempted to cross-validate direct IP_3 involvement in *Chara* excitation but obtained contradictory results. It is known that IP_3 and IP_6 are interconvertible and IP_6 signalling rather than IP_3 is now clarified (at least in guard cells (reviewed in Munnik and Vermeer 2010). Mathematical modelling of *Chara* APs assumes participation of IP_3 or other second messenger (Wacke and Thiel 2001).

Second messenger concept could base the all-or-none excitation nature of APs (Wacke *et al.* 2003): if the second messenger level remains below a threshold, no Ca^{2+} is mobilized from the stores (vacuole or ER), above the critical value, IP_X causes acute mobilization from the internal stores. This view

of IP_X action is consistent with the fact that IP_3 causes an all-or-none type of calcium liberation from internal stores as reported for *Arabidopsis* guard cells and animal cells (Tazawa and Kikuyama 2003).

Combining these two sources of Ca^{2+} is also possible in the process of calcium-induced calcium release: a small portion of Ca^{2+} crossing the plasma membrane from the apoplast would lead to Ca^{2+} release from internal stores. The established Thiel-Beilby mathematical model of excitation in Characeaen supports this idea: the working model is based on two sources of Ca^{2+} in *Chara* AP: short transient inflow from outside through TRP-like (transient receptor potential-like) channels and at the same time IP_X-activated channel opening in the internal stores (Beilby and Al Khazaaly 2016, Berestovsky and Kataev 2005). In *Nitellopsis obtusa* Lunevskey *et al.* (1983) analyzed electric current flowing across the plasmalemma and tonoplast by clamping the voltage on each membrane separately and obtained results supporting the hypothesis that Ca^{2+} ions are entering the cytoplasm from both the external medium and the vacuole activating the Cl^- channels of the membranes. Thus, cytoplasmic calcium origin and the possible involvement of the second messenger is still to be unravelled.

Cl^- efflux – main depolarizing current

There is no doubt that the increase of the cytoplasmic Ca^{2+} concentration activates anion channels in plasmalemma (Trebacz *et al.* 2006, Felle and Zimmermann 2007). These channels are probable to be a voltage-dependent R-type anion channel QUAC1 (QUickly activating Anion Channel 1) or S-type Ca^{2+}-dependent and voltage-dependent anion channel SLAC1 (SLowly activating Anion Channel 1) (Hedrich *et al.* 2016, Cuin *et al.* 2018). In *Characeaen* there are no genes attributed to Ca^{2+}-dependent anion channels, but high amplitude efflux, following Ca^{2+} influx during excitation was well-described in voltage-clamp studies (Lunevsky *et al.* 1983). This current is voltage dependant, its peak current is of ~-30-50 $\mu A/cm^2$ (at voltages ~-100 mV) and it exhibits activation-inactivation kinetics (Kishimoto 1968, Kisnieriene *et al.* 2018). Although $[Ca^{2+}]_{cyt}$ is directly related to Cl^- efflux during excitation, its regulation is not trivial, and there are several directions by which efflux regulation could take place.

First and most straight-forward observation is that the amplitude of depolarizing Cl^- current is proportional to the square of the cytoplasmic Ca^{2+} concentration in Characeaen (Berestovsky and Kataev 2005). *Via* patch-clamp studies it was confirmed that current through chloride channels is only observed when the Ca^{2+} concentration on the protoplasmic side of the

membrane is about 1 μM (Okihara *et al.* 1991). By series of cell-attached patch-clamp studies on intact Characeaen cells, Thiel and co-workers drew some important observations on chloride channels (Thiel *et al.* 1997):

a) long periods of little channel activity are randomly interspersed with intervals of transient coordinated activation/inactivation of Cl^- channel activity.
b) voltages more positive than RP facilitate a transient rise in open probability, although the voltage is neither a necessary nor a sufficient condition for Cl^- transient activation.
c) Cl^- transients are caused by ensembles of two types of Cl^- channels which are abundant (10 to 20 channels/μm^2) in the plasma membrane - 15 pS and 38 pS (with 100 mM Cl^- in the pipette (Okihara *et al.* 1991, Homann and Thiel 1994)).
d) Individual Cl^- transients vary in size over one order of magnitude but have a limited range of durations (with a rising time about two times shorter than the trailing time).

Thiel applied calcium release from internal stores model, and based on patch-clamp data suggested that the individual relationship between the number of Ca^{2+} discharging stores released and the size of the affected ensemble of Cl^- channels determine the magnitude of the observed Cl^- transients. Also, the two channel types showed bursting behaviour – consequence of the quantal release of Ca^{2+} from stores in the vicinity of the plasmalemma (Thiel *et al.* 1993, Thiel and Dityatev 1998). Inactivation of Chloride channels (decay of current) was reported to coincide with decreasing calcium (Kataev *et al.* 1984, Okihara *et al.* 1991, Shiina and Tazawa 1987, Lunevsky *et al.* 1983) as it enters the known Ca^{2+} buffering system of *Chara* (Hayama and Tazawa 1980, Kikuyama and Tazawa 1983). Internodal cells of *Chara corallina* simultaneous recording of the membrane voltage and patch currents revealed that randomly activated Cl^- transients trailing kinetics coincides with AP generation (Homann and Thiel 1994).

Repolarization – outward potassium current and activation of H^+-ATPase

The presence of a Ca^{2+}-activated K^+ current in *Chara* points to a rise in cytoplasmic Ca^{2+} as a common activating step for both Cl^- and K^+ currents (Homan and Thiel 1994, Felle and Zimmermann 2007). Single ion channels with conductance of about 50 pS were reported in *Nitellopsis* plasma membrane (Azimov *et al.* 1987). In *Chara corallina* - K^+-conducting channel

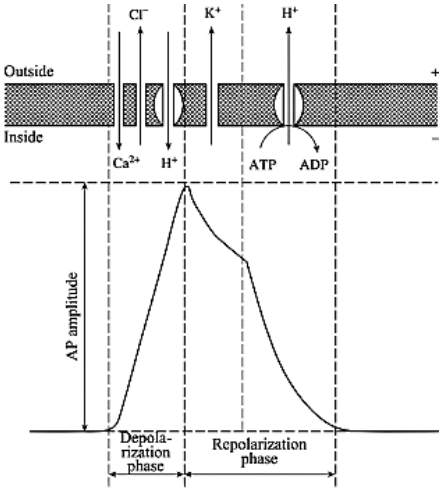

Fig 1.1 Supposed scheme of AP generation at the plasma membrane of an excitable cell of a higher plant. Depolarization phase is related to a threshold-type development of passive fluxes of Ca^{2+} and Cl^- and is partly caused by dissipation of E_m metabolic component due to switching off the H^+-pump (the H^+ flux through the channel of H^+-ATPase is shown). The phase of repolarization is caused by the initial passive efflux of K^+ and by subsequent active transport of H^+ mediated by H^+-ATPase. (Opritov *et al.* 2002)

(40 pS) activity during an AP could be identified as well (Homann and Thiel 1994). *Via* patch-clamp studies it was reported that these channels are opened just before the steady-state potential for Cl^- ions is reached. K^+ channels were observed to completely inactivate within 20 to 30 s after activation of the Cl^- currents (Homann and Thiel, 1994, Thiel *et al.* 1997). In plants outward K^+ channels are probable to be depolarisation-activated outward channels GORK (Gated Outwardly-Rectifying K^+ Channel) (Hedrich *et al.* 2016, Cuin *et al.* 2018).

According to the Thiel-Beilby model, calcium channels in the ER are inactivated by increased calcium concentration in the cytoplasm, this imposes negative feedback on calcium entrance (Beilby and Al Khazaaly 2016). The decrease in the Ca^{2+} concentration inactivates anion channels and re-activates H^+-ATPase, thus the repolarization phase is developed (Sukhov and Vodeneev 2009).

There are several mechanisms that return the cytoplasm to steady state low $[Ca^{2+}]_{cyt}$. Plant P-type 2B Ca^{2+} ATPases have been described in *Arabidopsis* (Roelfsema and Hedrich 2010). The pumps are likely to become active at high Ca^{2+} concentration and deactivate at low $[Ca^{2+}]$. There are also 2A P-type ATPases, located on ER. These transporters are thought to have stoichiometry of 2 Ca^{2+} per ATP and are thought to be responsible for the maintenance of a low cytoplasmic calcium content (Beilby and Casanova 2014, Roelfsema and Hedrich 2010).

Generalized scheme of AP ionic mechanism in plants is presented in **Fig 1.1** (Opritov *et al.* 2002), estimations of conductances of main ion currents are presented in **Fig 1.2**.

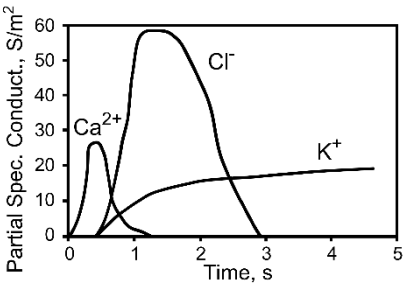

Fig 1.2 Plasmalemma partial specific conductances of AP-generating ions during action potential over time (estimated from Lunevsky *et al.* (1983) by Wayne (1994).

Tonoplast AP – accompanying small amplitude excitation

Findley (1970) recorded a tonoplast excitation of Characeaen – a positive-going change in tonoplast potential of 40-60 mV, reaching a peak in about 5 s. In plasma membrane permeabilized cells of *Chara*, the vacuolar membrane action potential can be activated by increasing the Ca^{2+} concentration of the external medium from 0 to 1 μM. The increased Ca^{2+} concentration on the protoplasmic side of the vacuole causes chloride efflux to cytoplasm and depolarization of tonoplast. The Cl^- current flows through a specific Cl^- channel, since the Cl^- channel blocker, anthracene- 9-carboxylic acid, completely eliminates the Ca^{2+}-induced depolarization of tonoplast (Kikuyama 1986). Later it has become evident that micromolar concentration of calcium in the cytoplasm activates tonoplast Cl^- channels - 37 pS/ 48 pS. Activation occurs as an increase in open probability of channels, even in the presence of high calcium concentrations. Tonoplast anion channels inactivate in 15-20 min, and it is not clear whether by themselves or by another factor (Berecki *et al.* 1999). It is thought that high-conductance (170 pS) tonoplast Ca^{2+}-dependent K^+ channels could be also involved in the generation of tonoplast action potential i.e. its repolarisation phase (Laver and Walker, 1991).

1.1.3 Physiological implications of APs

APs are transmittable signals elicited by a plethora of inputs – thus its transmission has to possess outputs - distant cells ought to receive information about locally acting stimuli (Trebacz *et al.* 2006). In *Characeaen*, AP generation is coupled with a sudden cessation of protoplasmic streaming, thought to act as a safety mechanism in the case of cell lesion. The streaming is inhibited by an increase in the cytoplasmic Ca^{2+} concentration (Williamson 1975, reviewed in Beilby 2007). Second direct consequence is that each action potential depletes the cell of K^+ and Cl^- and reduces turgor pressure of the cell (Beilby 2007). This is thought to be the basis of most apparent AP output - trap closures of carnivorous plants (*D. muscipula* and *A. vesiculosa*) (Sibaoka 1969, Iijima and Sibaoka 1982). One of systemic whole plant physiological

outputs of APs is an increase in respiration as demonstrated in *Incarvillea* upon AP excitation by mechanical stimulation exerted by a falling pollen grain on bilobal stigma (whose closure upon pollen is also AP-induced) (Sinyukhin and Britikov 1967). The significant increase of respiration following stimulation of the *C. conicum* thallus is well documented – a response dependant on AP transmission (Dziubinska *et al.* 1989) also reported in other species, e.g. barley (Felle and Zimmermann 2007). Respiration increase is followed by suppressed photosynthesis and pH banding system for about 20 min in *Characeae* (Bulychev *et al.* 2004). Photosynthesis suppression is also described in higher plants (Koziolek *et al.* 2004, Fromm and Lautner 2007). Other physiological consequences of plant excitation cover temporary decrease of the growth rate and susceptibility, enhancement of peroxidase activity, induction of jasmonic acid biosynthesis, increase of the ATP content in leaves (reviewed in Pyatygin *et al.* 2008). APs are also found to play a role in gene expression: e.g. PINII genes whose products (proteinase inhibitors) accumulate in tissues and play a key role in a systemic response to wounding (Fisahn *et al.* 2004).

The broad spectrum of responses following AP raise a question how a uniform signal evokes different responses or, to be direct, how can ion fluxes and membrane potential changes alter enzyme activities and even play the role of transcription factors. Many if not all of these physiological processes are fine-tuned by calcium signalling cascades (Medvedev 2018, Hetherington and Brownlee 2004). Ca^{2+} plays the central role in initiation of APs and regulation of activity of ion channels involved in AP generation. Different environmental/internal stimuli induce cytoplasmic Ca^{2+} oscillations unique in spatiotemporal properties, named calcium signatures, ranging from processes in the immediate vicinity of activated Ca^{2+} channels to large-scale propagating waves (Medvedev 2018). Such waves commonly intertwine with APs and probably activate physiological responses (Fisahn *et al.* 2004, Felle and Zimmermann 2007) and the kind of response and its degree depends on the susceptibility of individual cells or tissues to Ca^{2+} fluxes (Trebacz *et al.* 2006).

1.1.4 Alterations of APs in response to environmental stimuli

Generally, APs are uniform signals independent of the stimuli that initiated them (Trebacz *et al.* 2006, Sukhov 2016). Although, plant APs are much more variable than their animal counterparts. In plant cells both plasma membrane and the tonoplast are excitable, which probably accounts for the Characeaen AP shape being more variable than that of animal APs (Beilby 2007). Also,

temporal characteristics and amplitudes of transient currents in *Nitellopsis* cell membranes, according to Lunevsky *et al.* (1983), vary from year to year and depend on the "shelf life" in artificial media. Other basic and well-described changes of AP shape in Characeaen result from physical conditions of environment.

The AP and Cl^- current transient duration and amplitude are temperature-dependant. The duration of both membrane and tonoplast AP, as well as the clamped excitation currents increased 30-fold when temperature was decreased from 40°C to 3,5°C in *Chara* (Beilby and Coster 1976a). Consequently, the amplitude of the AP decreased with temperature but the AP form did not change. AP refractory period also is temperature-dependant, it decreases in higher temperatures (Beilby and Coster 1976b).

Repolarization rate is one of highly variable parameters of AP in plants (Kisnieriene *et al.* 2012). It was reported that in *Nitellopsis* – a salt-sensitive Characeaen – a mild salinity of 50 mM NaCl had a profound effect on the AP shape and extended the AP duration from 2 to up to 60 s (Kisnieriene *et al.* 2018). In salt-sensitive *Chara australis*, exposure to additional 50 mM NaCl led to altered AP threshold and almost doubled durations of AP (Beilby and Khazaaly 2017).

In Characeaen AP parameters were demonstrated to be altered by various substances. 1 mM of aluminium applied exogenously for 30 min increased AP peak value and prolonged the slow phase of repolarization. It is noteworthy that aluminium effect was reversible (Kisnieriene and Sakalauskas 2005). Sevriukova *et al.* (2014) reported ~35% prolonged repolarization phase of the action potential and ~27% decreases of Cl^- and Ca^{2+} effluxes during excitation due to tritium exposure for half an hour. In *Conocephalum conicum* Favre *et al.* (1999) described APs of longer durations induced by light, heat and cold in comparison to electrically induced APs.

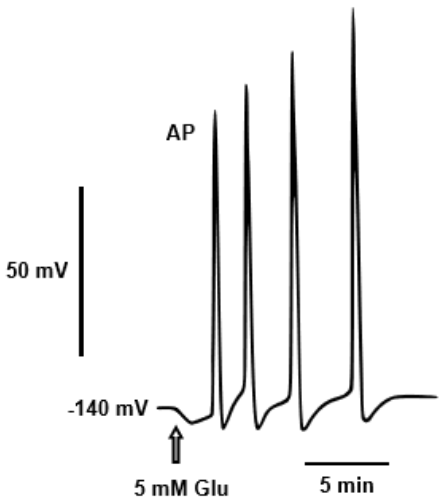

Fig 1.3. Spontaneous Glu-induced AP series recorded in *Conocephalum conicum* using intracellular microelectrodes (Krol *et al.* 2007)

In *Nitellopsis* and *Nitella flexilis* acetylcholine - a signalling molecule in plants - caused an increase in duration of AP repolarization of cells in K^+ state. Also, exposure to 5 mM of acetylcholine led to depolarization of MP and spontaneous generation of APs (Kisnieriene *et al.* 2012). Gong and Bisson (2002) reported that ACh increases Cl^- channels open probability in tonoplast of *Chara*.

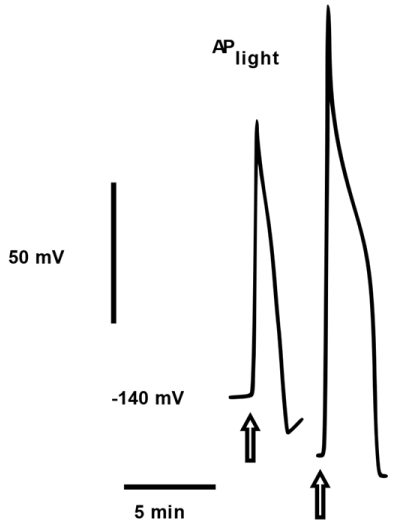

Fig 1.4. APs recorded in *Conocephalum conicum* using intracellular micro-electrodes. APs were elicited by light, first – in standard conditions, second – after incubation for an hour in 5 mM glutamate. The arrows are the moments of stimulations (Krol *et al.* 2007).

A novel signalling molecule glutamate, not only induce APs – reported in *Helianthus annuus* (Stolarz *et al.* 2010), barley *Hordeum vulgare* (Felle and Zimmermann 2007), *Conocephalum (*Krol *et al.* 2007) (**Fig 1.3**) – but Glu triggered APs had significantly increased half-time duration (up to 3-fold). Presence of Glu and Gly heightened amplitude of APs elicited by other stimuli (~1,5 fold) (Krol *et al.* 2007) (**Fig 1.4**). Modulation of AP shape and excitatory action of glutamate and asparagine is reported in this study on Characeaen.

1.2 Amino acids and their signalling role in plants

1.2.1 Amino acids in plant physiology

Plant growth is limited by nutrients, among key ones - nitrogen (N). The availability of N has a profound short- and long-term effect on plant physiology, thus nitrogen-sensing mechanisms that allow adjustments are essential for the fitness of plants (Price *et al.* 2012). Genome-wide studies on plant responses to amino acids (AA) have revealed that a significant fraction of N-regulated genes (~81%) require the incorporation of inorganic nitrogen to organic nitrogen, strongly suggesting that plants possess sensory mechanisms for organic N (Gutierrez *et al.* 2008). AA, formed as the result of the assimilation of inorganic N, are considered the prime candidate for organic N signals in plants. Evidence demonstrates that AA levels affect the activities

of key players in the nitrogen assimilation pathway through transcriptional and post-transcriptional processes. For example, gene expression of both cytosolic and plastidic glutamine synthetases GLN1 and GLN2 are regulated by the levels of amino acids in *Arabidopsis* and tobacco (Oliveira *et al.* 2001, Taira *et al.* 2004, Fritz *et al.* 2006, Sulieman *et al.* 2010). The non-protein amino acid GABA (γ-amino-butyric acid), when supplied to plant growth medium, is capable of modulating not only the activity of key enzymes in nitrogen assimilation, but also the uptake of nitrate itself (Barbosa *et al.* 2010). Amino acids also were demonstrated to modulate the uptake of inorganic and organic nitrogen through membrane transporters (Nazoa 2003, Hirner *et al.* 2006).

In addition to gene regulation at the transcriptional level, amino acids have been shown to trigger rapid responses when supplied externally to plant cells: exogenous application of amino acids to plants causes a transient cytosolic calcium increase and membrane depolarization (Dennison and Spalding 2000, Dubos *et al.* 2003, Demidchik *et al.* 2004, Qi *et al.* 2006, Stephens *et al.* 2008). Further, GABA and D-Ser also have been shown to trigger transient changes in cytosolic [Ca^{2+}] in pollen grains (Michard *et al.* 2011). These studies illustrate that plants have endogenous mechanisms of monitoring the concentration of amino acid levels, enabling modulation of nitrogen metabolism.

Metabolic pathways associated with amino acid ana- and catabolism play integral roles in plant defence. Amino acid metabolic pathways can directly provide stress signals such as the Met-derived hormone ethylene and the systemic acquired resistance regulator pipecolic acid (Lys catabolite). Further, they can produce natural products exerting harmful activity to pathogenic microbes or herbivorous insects. Some AA-derivatives have vital roles in reactive oxygen species generation, redox processes, hormone crosstalk, metabolic conversion (Zeier 2013). Also, exogenous AA are to act as damage-associated molecular patterns and regulate various processes e.g stomatal closure (Forde and Roberts 2014, Zeier 2013) Thus, evidence emerges that AA are also exploited as endogenous signalling molecules. This aspect will be discussed in context of glutamate in section 1.2.5.

1.2.2 L-Glutamate and L-Asparagine metabolism/catabolism

Every amino acid (except glycine) can occur in two isomeric forms, because of the possibility of forming two different enantiomers (stereoisomers) around the central carbon atom. Only L-amino acids are manufactured in prokaryotic cells and incorporated into proteins. L-glutamate is an extraordinary abundant

AA in living organisms (reviewed in Young and Ajami 1998). Glu foremost is a precursor in the synthesis of proteins. Glu also is a common precursor of organic compounds as: other protein amino acids (glutamine, proline, arginine and histidine), non-protein amino acid (g-aminobutyric acid, GABA), antioxidant tripeptide (glutathione, GSH), heme, chlorophyll, and so forth (Brosnan and Brosnan 2013). Glu has the following features that probably contributed to its role as a proteinaceous amino acid: (i) it is chemically stable, (ii) Glu may be metabolically produced and removed readily by virtue of its interconversion with a-ketoglutarate, a Krebs cycle intermediate, and (iii) it is negatively charged (at physiological pH value), due to its two carboxyl groups (α-and γ-carboxyl) and one amino group (**Fig 1.5**) (Brosnan and Brosnan 2013, Qiu *et al.* 2020).

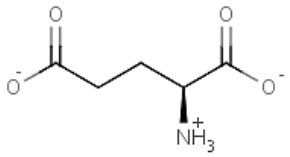

Fig 1.5. Structure of L-Glutamate in ionized form in physiological pH (credit: https://www.uniprot.org)

In plants, Glu can be principally synthesized in the chloroplasts of photosynthetic tissue and plastids in non-photosynthetic tissues *via* glutamine synthetase (GS)/Glu synthase (also known as Gln-a-ketoglutarate aminotransferase, GOGAT) cycle and catabolized in mitochondria or cytoplasm *via* Glu dehydrogenase (GDH). These proteins regulate the homeostasis of Glu, Gln, 2-oxoglutarate (GO), and ammonia (NH_3) in plant cells. In addition, plants also can produce Glu by Pro/pyrroline 5-carboxylate (P5C) cycle and transamination, which are alternative pathways (Davenport 2002, Brosnan and Brosnan 2013, Seifi *et al.* 2013,). Glutamine synthetase is the key enzyme in ammonia assimilation and catalyzes the ATP- dependent condensation of NH_3 with glutamate to produce glutamine (Ortega *et al.* 1999, Haroun *et al.* 2010). These pathways not only ensure the timely supply of Glu from nitrate reduction, but also maintain ammonia homeostasis in plant cells, which prevents from the toxic action of ammonia.

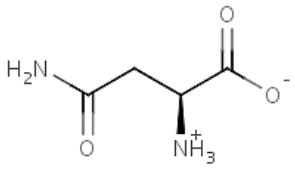

Fig 1.6. Structure of L-Asparagine in ionized form in physiological pH (credit: https://www.uniprot.org)

Asparagine is derivative of aspartic acid, it possesses an amide functional group in the carbon distal from the α carbon (**Fig 1.6**). Unlike its acidic analogue, the side chain of asparagine has no electric charge; thus it is polar at physiological pH. Asparagine (Asn) has one of the highest C/N ratios (4:2), thus it plays a primary role in nitrogen recycling,

storage and transport (Gaufichon *et al.* 2015). Asparagine is a substrate for only a few enzymatic reactions in the soluble form and has little net charge under physiological conditions. It therefore forms an ideal storage compound. Similarly, it is a major transported form of nitrogen, particularly in leguminous plants (Lea *et al.* 2007).

The major route of asparagine synthesis involves the initial assimilation of ammonia to the amide position of glutamine (Lea and Miflin, 2003), followed by the transfer to form the amide position of asparagine (Ta and Joy 1986). The enzyme AS (asparagine synthase) catalyses the adenosine triphosphate (ATP)-dependent transfer of the amino group of glutamine to a molecule of aspartate to generate glutamate and asparagine (Lea *et at*. 2007).

Asparagine can be catabolized mainly through two enzymatic pathways in higher plants. The first route involves the hydrolysis of asparagine by asparaginase (ASPG) that releases the amide nitrogen as ammonium and aspartate in the cytosol (Gabriel *et al.* 2012). The second route occurs via the transamination of the α-amino group of asparagine to the 2-oxo-acid acceptor, producing 2-oxosuccinamate which can be deamidated to ammonium and oxaloacetate. Also, 2-oxosuccinamate can be rapidly reduced to 2-hydroxysuccinamate which is deaminated to ammonium and malate. Released ammonium is reassimilated by the GS/GOGAT pathway into glutamine and glutamate (reviewed in Gaufichon *et al.* 2016). Glutamine, glutamate, asparagine and aspartate thus are utilized for the biosynthesis of all nitrogenous compounds.

1.2.3 Environmental AA and their distribution in plant

Besides metabolic synthesis, AA can also be taken up directly by the roots, and then distributed among tissues and organs through xylem and phloem. Amino acids are rather common in both soil (Young and Ajami 2000) and aquatic sediments (Yao *et al.* 2012, Feng *et al.* 2019). Amino acids represent the largest fraction of dissolved low molecular weight organic nitrogen in the soil and aqueous habitats, yet concentrations of individual amino acids in the bulk soil solution are reported to be in the 0,01– 10 μM range. However, it is reported that AA concentration in soil may be heightened upon decomposition of organic matter (up to mM concentrations) (Jones *et al.* 2005). The soil amino acid pool was reported to be dominated by Glu, Ala together with Asn, glutamine, aspartic acid and histidine irrespective of the successional stage of forest (Werdin-Pfisterer *et al.* 2009). AA composition of ectopic lakes' sediments is dominated by Gly, Lys, Ala and Glu, depend on depth and reach up to 38,2 μmol g^{-1} with Glu up to 4,6 μmol g^{-1} (Yao *et al.* 2012).

In general, the redistribution of AA inside a plant can be achieved by transporters located in the plasma membrane. In *Arabidopsis*, the AA and Glu transporters are: cationic amino acid transporters (CAT) family (amino acid-polyamine-choline facilitator, g-aminobutyric acid (GABA) permease-related family (APC superfamily), and amino acid transporter family (ATF superfamily) (Fischer *et al.* 1998). AA redistribution can alter plant growth and development, which in turn can improve the resistance of plants to adverse environments (Yang *et al.* 2014).

In tissues, organs, and subcellular organelles, Glu is maintained in different concentrations. In *Arabidopsis thaliana* leaves, the amount of Glu remains about 1 mmol g^{-1} fresh weight, but in phloem cells Glu content reaches 50 mM (Forde and Lea 2007). In vascular plants, apoplastic Glu content is ~1 mM (Lohaus and Heltd 1997), while in symplast it can exceed 10 mM (Sandström and Pettersson 1994). Glu content does vary in plant species, yet Glu concentration gradient among of phloem cells, symplast and extracellular spaces is thought to be the basis of Glu signalling in plants (Qiu *et al.* 2019).

Regarding Characeaen internal amino acid content, it was reported that *Nitellopsis obtusa* total concentration of AA in the cell sap was ~5,5 mM with dominating glutamate/glutamine (~1 mM) and asparagine/aspartate (~1,2 mM) (Wayne and Staves 1991). In *Chara australis* it is characterized that about 90% percent of the amino acids are located in the cytoplasm whose volume is only about 5% of the total cell volume, thus the concentration of amino acids in the cytoplasm is estimated to be about 50 mM (about one hundred times higher than that in the vacuole). This gradient is thought to be maintained by the H^+/amino acid symport (Amino and Tazawa 1989). In brackish water Charophyte *Lamprothamnium* the major free amino acids in the cytoplasm of internodal cells were reported to be Glu, Asp, I-Asn, Gln, Pro with Glu concentration being ~50 mM (Okazaki *et al.* 1987). Thus AA distribution gradient stands also in Characeaen. The internal Glu concentration is comparable to vascular plants (Forde and Lea 2007).

Recently, Glu emerged as a novel signalling molecule in plants, linked to a series of physiological processes. Therefore, Glu is a multifunctional amino acid, acting both as a metabolite and as a signalling molecule (Qiu *et al.* 2019).

1.2.4 Signalling of Glu and Asn

Most straight-forward Glu signalling mechanism lies in the root-soil interface. It is well described that externally applied Glu elicits specific changes in root system architecture. In *Arabidopsis*, where these effects have been studied in most detail, Glu inhibited primary root growth while at the same time

stimulating the outgrowth of lateral roots near the primary root tip, producing a shorter and more branched root system (Walch-Liu *et al.* 2006). Exogenous AA can regulate germination of seeds and growth of pollen. Application of L-Glu alleviates salt-induced inhibition of seed germination by mediating ethylene production (Cheng *et al.* 2010). Application of AA enhanced the $[Ca^{2+}]_{cyt}$ gradient toward subapical zone in pollen tubes, leading to an inhibition of pollen tube growth (Michard *et al.* 2011). In rice *via* transcriptome analysis Kan *et al.* (2017) revealed that Glu irrigation within 30 min could upregulate the expression of at least 122 genes.

In addition to root architecture, seed germination, and pollen tube growth mentioned above, Glu as a signalling molecule is also involved in the response and adaptation to salt, cold, heat, drought, pathogen, and wound stress (Qiu *et al.* 2019). In *Arabidopsis* Glu is proposed to act as DAMP (damage-associated molecular pattern) – tissue wounding could be indicated by Glu passively leaking or being actively released. Increased apoplastic Glu elicits propagating systemic defense signal through altered $[Ca^{2+}]_{cyt}$ (Vatsa *et al.* 2011, Toyota *et al.* 2018). In addition, Glu can act as a long-distance signalling transducer among cells, tissues, organs, and even the whole plants by the crosstalk with Ca^{2+}, ROS, and electrical signalling (Mousavi *et al.* 2013, Nguyen *et al.* 2018, Toyota *et al.* 2018).

Plant response to exogenous asparagine is mostly related to growth and nitrogen assimilation. For example, in French bean (*Phaseolus vulgaris*) exogenous asparagine (1 and 2 mM) induces an increase in general ion content (K^+, Na^+, Ca^{2+} and Mg^{2+}), enhances synthesis of chlorophylls, glucose, sucrose. Also, protein and total nitrogen contents are heightened (while the ammonia, peptide and total soluble nitrogen decrease). Exogenous Asn raises levels of growth promoters (auxins, gibberellins and cytokinins), followed by increase in vegetative length, fresh and dry weights. Nitrogen assimilation enzymes are regulated accordingly (Haroun *et al.* 2010). It is noteworthy that higher concentrations than 2 mM induced a reversed action. Similar pattern of adaptations to exogenous Asn was reported in soybean (Shetty *et al.* 1992) maize, spring barley and field beans (Geisler 1985). Thus regulations of these house-holding functions are extensively dose-dependent.

To date, a vast pool of genomic and pharmacological studies has indicated that Glu and other AA usually exert signalling role by binding to receptors, that is, glutamate receptors (GLRs), the homologs of animal iGluRs (Lam *et al.* 1998).

1.3 GLR receptors

1.3.1 General features and stucture

Discovery of plant glutamate receptor-like channels (GLR) genes in *Arabidopsis* (Lam *et al.* 1998, Lacombe *et al.* 2001) shed new light on AA signalling in plants. Also, GLRs were confirmed to take an essential part in calcium signalling. Generally, channels permeable to calcium in plants are: voltage-gated tonoplast channels (two-pore channels, TPC), mechanosensitive channels (mechanosensitive channels of small (MscS) conductance-like channels – MSL; mid1-complementing activity channels – MCA; hyperosmolality-induced $[Ca^{2+}]_{cyt}$ channels – OSCA), annexins and two ligand-gated ion channel families: Ca^{2+}-permeable channels activated by cyclic nucleotides (CNGC) and glutamate receptor-like channels, GLR (Mousavi *et al.* 2013, Demidchik *et al.* 2018, Medvedev 2019). Latter ones received broad interest on the ground of striking similarity with their animal counterparts - ionotropic glutamate receptors (iGluRs).

iGluRs are a highly conserved family of ligand-gated ion channels with homologs present in animals, plants, and bacteria. Between themselves iGluRs share the structural and some functional features (reviewed in Croset *et al.* 2010).

In mammals iGluRs are cation channels activated by the neurotransmitters Glu, Gly, and D-serine released in the synaptic space. They have been extensively studied for their central role in neurotransmission, learning, and memory (Traynelis *et al.* 2010). iGluRs (NMDA type) permeate cations including calcium, predicating signal transduction in neurons. iGluRs can be segregated into three subtypes according to their sensitivity to the synthetic agonists AMPA, kainate (a structural analogue of glutamate) and NMDA; or in two groups as NMDA and non-NMDA type iGluRs. NMDA-type iGluRs physiologically are gated by Glu and Gly (co-agonists). Non-NMDA type receptors are gated by Glu. NMDA-type iGluR competitive antagonists are AP-5 and AP-7, non-NMDA – DNQX and CNQX (reviewed in Rousseaux 2008).

Plant GLR genes are closely related to the mammalian iGluRs (Price *et al.* 2012). The stoichiometry and architecture of plant GLRs are believed to be similar to animal iGluRs, yet there are substantial differences (Wudick *et al.* 2018). Plant GLRs are gated by a broad spectrum of agonists and have mostly non-selective cation permeability. To date best described GLRs are *Arabidopsis* GLRs – *At*GLRs – a total of 20 genes, divided into three clades (Lacombe *et al.* 2001, Chiu *et al.* 2002). Each *Arabidopsis* gene clade

potentially has an individual agonist profile and a wide range of ion selectivity from non-selective cation to highly selective Ca^{2+} permeability (Tapken and Hollmann 2008, Vincil *et al.* 2012).

All known iGluRs and their homologs are homo-or hetero-tetrameric proteins (**Fig 1.7**). Each out of its four subunits hosts an extracellular amino-terminal domain (ATD), an extracellular ligand-binding domain (LBD) composed of segments S1 and S2, 4 transmembrane helices (M1 to M4; M2 is not fully transmembrane). M3 contain the 'gate' motif – in iGluRs, it is highly conserved and is represented by a 'SYTANLAA' amino acid motif (Traynelis *et al.* 2010). The last part of each subunit is a cytoplasmic tail (carboxyl- terminal domain - CTD).

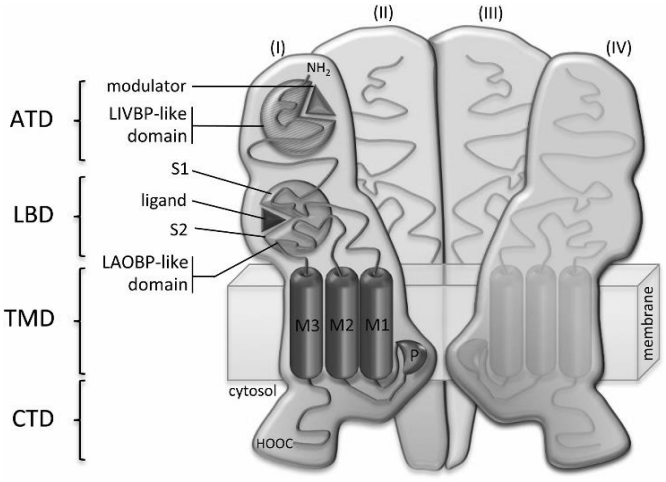

Fig. 1.7 Putative tetrameric membrane structure of *Arabidopsis* GLRs based on the structure of animal iGluRs. Schematic membrane structure of four *At*GLR subunits (I–IV). As exemplified in (I), each subunit consists of:

- **ATD** - amino- terminal domain, that forms a clamshell-shaped binding site for modulators with homology to bacterial leucine/isoleucine/valine-binding protein (LIVBP) domains.
- **LBD** - ligand-binding domain, which has a similar structure to ATD, but the two lobes are composed of segments S1 and S2, that bear a lysine/arginine/ornithine-binding protein (LAOBP)-like domain with homology to the periplasmic binding protein- like II superfamily.
- **TMD**- the transmembrane domain with three membrane-spanning helices - **M1**–**M3** - and a membrane re-entrant loop, forming the pore region (**P**) of the channel
- **CTD -** the cytosolic carboxy-terminal domain.

After Shepherd and Huganir (2007). Not drawn to scale (Wudick *et al.* 2018).

The similarity between GLR and iGluRs ranges from 16% to 63% within the ligand binding domains S1 and S2 and the transmembrane domains M1 to M4 when compared with NMDA receptors in animals. A part of the pore-forming M3 domain features the highest level of identity (Lam *et al.* 1998, Chiu *et al.* 1999).

The LBD domain among iGluRs has a conserved clamshell architecture with segments S1 and S2. In vertebrates, the binding of a ligand/agonist induces a variable degree of closure of the clamshell that pulls the transmembrane segments and opens the channel pore. After ligand binding and opening, channel spontaneously closes in a ligand-independent manner and transiently stays ligand insensitive. This desensitization is ATD region-dependant. Desensitization has not so far been unequivocally described for plant GLRs at the electrophysiological level, and there are no data indicating that the conformational changes in iGluRs are identical to those of plant GLRs (Wudick 2018). Unlike animal iGluRs, plant GLRs contain two different ligand-binding regions: one ligand-binding domain is composed of the two putative ligand-binding sites S1 and S2 - these sites form a lysine/arginine/ornithine-binding protein (LAOBP)-like domain with a homology to the periplasmic binding protein-like II superfamily (Acher and Bertrand 2005). The LAOBP-like domain can be found also in iGluRs and it is supposed to bind glutamate. The second ligand-binding domain is located in ATB and exhibits a similarity to a leucine/isoleucine/valine-binding protein (LIVBP) domain. This second domain could fulfil a modulating function of the receptor complex by binding a second molecule. Potential additional ligands are either other amino acids or completely different agents (Acher and Bertrand 2005). Studies revealed that plant GLRs seem to respond to a wide range of amino acids including non-conventional ones (Michard *et al.* 2011, Weiland *et al.* 2016).

The pore region of *At*GLR exhibits poor conservation between animal and plant glutamate receptors which makes it impossible to derive information on GLR selectivity (De Bortoli *et al.* 2016). The gating of *At*GLRs is still not well characterized as well as its selectivity and regulation mechanisms. However, gating of plant GLRs was initially assessed by employing pharmacological agents used for iGluRs, also major part of physiological functions in plants were described indirectly, based on inhibition.

1.3.2 Gating and function of GLR channels

Such AA as Glu, Ala, Asn, Cys, Gly, Ser and Met have been reported to trigger depolarization of MP and increase in $[Ca^{2+}]_{cyt}$ in *Arabidopsis* root cells (Qi *et*

al. 2006) by activating Ca^{2+}-permeable channels (Vincill *et al.* 2012, Tapken *et al.* 2013), probably GLRs. Later it was confirmed that GLRs mediate an AA-induced calcium-based signalling, a striking similarity to animal counterparts.

Each *Arabidopsis* gene clade (*At*GLR1/2/3) is supposed to possess individual agonist profile and wide range of ion selectivity. Selectivity of few GLRs was directly described in heterogenous expression systems. Glu activated non-selective cation currents were recorded of *At*GLR1.1 and *At*GLR1.4 (pore regions of these channels were inserted in animal iGluR gene in heterogenic *Xenopus* expression system) (Tapken and Hollmann 2008), while GLR3.4 expressed in human embryonic kidney cells exhibited highly selective Ca^{2+} permeability (Vincil *et al.* 2012). In *Arabidopsis* GLRs were reported to localize in both the plasma membrane and the chloroplast envelope (Teardo *et al.* 2011, Tapken *et al.* 2013).

In contrast to iGluRs, GLRs can be gated by at least 12 proteinogenic amino acids (Met, Trp, Phe, Leu, Tyr, Asn, Thr, Ala, Cys, Glu, Gly, Ser) as well as by an unknown number of small molecules and peptides such as glutathione (GSH) and γ-aminobutyric acid - GABA (Forde and Roberts 2014). In studies using T-DNA insertion mutants of *At*GLR3.3 and 3.4 it was directly demonstrated that Ala, Cys, Asn, Glu, Ser, Gly can induce membrane depolarization in glr3.3 mutants, while glr3.4 mutants responded only to a subset of amino acids (Stephens *et al.* 2008). Other *At*GLRs might have different agonist profiles, as suggested by the sequence diversity within the LBD as well as by experimental studies (Tapken *et al.* 2013 Demidchik *et al.* 2018).

To this date it has been demonstrated that Asn gates three types of *Arabidopsis* GLRs: GLR3.4. (Vincill *et al.* 2013), GLR3.3 (Stephens *et al.* 2008), GLR1.4. (Tapken *et al.* 2013), while Glu activates GLR3.3 (Dubos *et al.* 2003, Qi *et al.* 2006, Stephens *et al.* 2008). *At*GLR3.4 is also gated by L-Glu (Dennison and Spalding 2000, Meyerhoff *et al.* 2005, Michard *et al.* 2011, Vincill *et al.* 2012) (reviewed in Weiland *et al.* 2016, Wudick *et al.* 2018).

All documented physiological implications of *At*GLRs so far are linked to their capability to permeate Ca^{2+}. GLR channels have various physiological functions:

- AA sensing (Kang et al. 2003, Baluska and Mancuso 2013),
- light signal transduction (Lam et al. 1998),
- regulation of root branching and root growth (Cho et al. 2009, Vincill et al. 2013, Kong et al. 2016, Singh et al. 2016),
- aluminium toxicity (Sivaguru et al. 2003),
- regulation of stomatal aperture (Yoshida et al. 2016),

- pollen tube growth (Michard et al. 2011),
- hypocotyl elongation (Dubos et al. 2003),
- seed germination (Cheng et al. 2018), and others.

These physiological functions are concurrent with calcium signalling mediated by GLRs (reviewed by Weiland et al. 2016, Wudick *et al.* 2018).

One of the most important discoveries following GLR research was demonstration that GLRs are directly involved in propagation of electrical signals. It was shown that in *Arabidopsis* GLRs are crucial to evoke and propagate an electrical signal along the phloem in response to a herbivory attack. The mutations in *At*GLR3.1, 3.2, 3.3, and 3.6 caused reduced duration of surface potential changes in *Arabidopsis* leaves after caterpillar-induced wounding. Strikingly, the propagation of the electrical signal to neighbouring leaves was dependent on *At*GLR3.3 and 3.6, showing the implication of those genes in conveying the electrical signal over a long distance. Propagating membrane depolarization upon wounding is necessary for stimulation of the accumulation of jasmonic acid (JA) - the potent lipidic regulator of defence response (Vatsa *et al.* 2011, Mousavi *et al.* 2013, Nguyen *et al.* 2018, Toyota et. 2018)

Thus mounting data on GLR genes' and proteins' functions point the integrity of AA signalling in plant physiology, yet questions remain, e.g. it is not entirely understood how sensitivity is maintained during GLR-mediated signalling so far. The multiplicity of GLR genes combined with their overlapping patterns of expression means that an ability to co-assemble as heteromeric complexes would potentially generate a huge diversity of GLR receptors distributed in most, if not all, cell types throughout the plant. Taking together what is known about related glutamate receptors in other species and research conducted on plant GLRs, it would be unexpected to find GLRs as static ion channels instead of highly regulated members of signalling pathways (Weiland *et al.* 2016, Wudick *et al.* 2018).

1.3.3 Inhibition of GLR channels

The use of appropriate antagonists is essential to cross-validate the effects exerted by glutamate and other ligands on GLRs. Some common iGluR antagonists are fully functioning in plants - the most extensively used agents are DNQX and AP-5.

The inhibiting effect of DNQX on all *At*GLRs is supposed to rely on the attachment inside of the ligand-binding sites in LBD. In *Arabidopsis* DNQX inhibited light-induced hypocotyl shortening and the reduction of chlorophyll

accumulation (Lam *et al.* 1998, Oliveira *et al.* 2001). Also DNQX was able to block glutamate- (and glycine-) mediated increases in cytosolic [Ca^{2+}] in cotyledons (Dubos *et al.* 2003). However, it seems that DNQX has a unique inhibition mechanism: using heterologous expression in *Xenopus* oocytes it was demonstrated that *At*GLR1.4 is most effectively activated by methionine and the addition of DNQX (and CNQX) inhibited methionine-induced currents. Yet, the extent of inhibition was the same when the methionine concentration was 100 mM or 1 mM indicating that DNQX (and CNQX) were not functioning as competitive antagonists and thus act differently on *At*GLR1.4 than on animal iGluRs (Tapken *et al.* 2013).

On the other hand, AP-5 is probably competing with the natural ligand at the L-glutamate binding site (Dubos *et al.* 2003). AP-5 inhibits glutamate-activated production of nitrogen oxide (Vatsa *et al.* 2011). Also, AP-5 completely prevents glutamate (together with Al^{3+}) induced depolarisation of the plasma membrane as well as microtubules' depolymerisation (Sivaguru *et al.* 2003). In latter study microtubules' depolymerisation was also induced by NMDA and blocked by AP-5. AP-5 also inhibits D-serine- or glycine-activated dose-dependent growth of pollen tube of *Arabidopsis*, also the increase in frequency of Ca^{2+} oscillations at the tip of the pollen tube (Michard *et al.* 2011). Summarizing, in *Arabidopsis* the effects of glutamate, glycine and NMDA are inhibited by AP-5 (Weiland *et al.* 2016).

Other commonly used antagonists and iGluR blockers include dizocilpine (MK-801), memantine, 5,7-dinitro-1,4-dihydro-2,3-quinoxalinedione (MNQX) and CNQX (Meyerhoff *et al.* 2005, Vatsa *et al.* 2011). GLRs are susceptible to unspecific ion channel blockers such as La^{3+} or Gd^{3+} (Meyerhoff *et al.* 2005). The use of non-specific ion channel blockers can be helpful to verify Ca^{2+} involvement but bears a lack of specificity since almost all important ion fluxes across membranes are impeded (Weiland *et al.* 2016).

1.3.4 NMDA research

There are three different groups of mammalian iGluRs (AMPA, NMDA and Kainate receptors), which are based on their pharmacological properties and structural similarities (Armstrong *et al.* 1998). A unique feature of NMDA-type iGluR receptors within the glutamate receptor family is their requirement for both glutamate and the co-agonist glycine for efficient gating (Hirai *et al.* 1996). NMDA is a water-soluble D-alpha-amino acid, a synthetic NMDA-type iGluR agonist binding the glycine binding site. However, effect of NMDA as an active substance in plants has been highly debatable since some

studies reported no discernible effect of NMDA on GLRs (Dennison and Spalding 2000, Qi *et al.* 2006). In literature NMDA is most often regarded as a none-active agonist (Forde and Roberts 2014).

NMDA as an active compound in plants was revealed only in few investigations. In *Conocephalum* NMDA application induced APs (as did Glu and Gly), this effect was blocked by AP-5 in all three cases (Krol *et al.* 2007). In *Arabidopsis* seedling roots both NMDA and Glu depolymerized microtubules and depolarized plasma membrane, Glu effect was suppressed by AP-5 (Sivaguru *et al.* 2003).

NMDA excitatory effect and inhibition by both AP-5 and DNQX in Characeaen *Nitellopsis obtusa* is reported in this study.

2. MATERIALS AND METHODS

2.1 Object

Internodal cells of mature freshwater algae Starry stonewort *Nitellopsis obtusa* (Devs.) J. Gr. (*Characeae*) were used in experiments (**Fig 2.1**).

Fig 2.1 Starry stonewort *Nitellopsis obtusa* internodal cell (lower) and a segment of stem (upper) containing two internodal cells and connective nodes (indicated by arrows) with branchlets.

Nitellopsis obtusa constitutes a single-species genus *Nitellopsis* (McCourt *et al.* 1999) in the family *Characeae*. It grows in brackish and fresh water bodies (Beilby and Casanova 2014), and is native to Eurasia (Soulié-Märsche *et al.* 2002).The Characeaen thallus consists of long multinucleate single cells interrupted by multicellular nodes (**Fig. 2.1**) from which lateral whorls of branchlets grow. The thallus is anchored in the soil with colorless rhizoids. Instead of nodes, large rhizoid cells are connected by star-shaped bulbils, which are full of starch grains. Characeaen internodal cell is extraordinary in the terms of cell size (up to 30 cm length and ~0,5 mm diameter), this enables various electrophysiological approaches. Structure of internodal cell is common to that of typical plant cells. The coenocytic cells are surrounded by a cell wall composed mainly of cellulose which protects the cell from inherent high turgor (5-7 atms) and external pressure. Most of the cell interior (up to 95%) is composed of a large central vacuole surrounded by the tonoplast, with streaming (up to 100 μm/s) endoplasm layer of 10 μm (Beilby and Casanova 2014).

Nitellopsis obtusa thalli were collected from fresh-water lake Stanka (Lithuania, Vilnius district) using gaffed anchor from a depth of 4 – 8 m. The species is distinguishable by the smooth stem and characteristic star-shaped bulbils growing between transparent rhizoids at the base of algae. Full-grown *Nitellopsis* were harvested in September – November, transported in lake water. Few weeks after collecting, stems were transferred to fresh dechlorinated tap water every other day to minimize natural contamination by microorganisms. Afterwards, intact stems were maintained in glass aquariums at room temperature (20±1 °C) under daylight conditions (95±0,19 μmol m^{-2} s^{-1}) of light/dark photo regime of 12/12 h in dechlorinated tap water.

Prior to the experiments, second or third internodal cells below the thallus tip were cut from neighboring internodal cells near the node. Separated cells were kept overnight in APW (artificial pond water) under daylight conditions.

2.2 Microelectrode technique arrangement

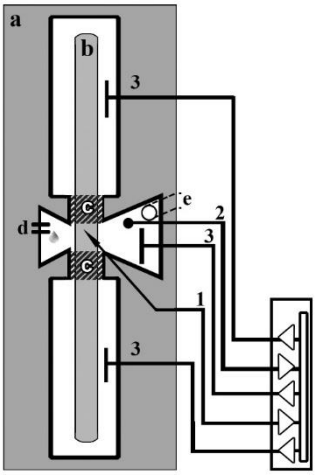

Fig 2.2 Principal parts of registration chamber and placement of electrodes:
a – plexiglass chamber
b – internodal cell
c – vaseline isolation of central compartment (5 mm)
d,e - perfusion
1 – intracellular glass electrode
2 - reference glass electrode
3 – extracellular Ag/AgCl electrodes

Two-pair current/voltage clamp intracellular glass electrode technique was used for the registration of single cell electrical signalling. Principal arrangement of this method is presented in **Fig 2.2**. Intracellular glass microelectrodes were made from borosilicate glass capillaries (inner Ø 0,84 mm, World Precision Instruments) with a tip diameter of 1-3 μm (8 – 20 MΩ) and filled with 3 M KCl. The reference electrode (immersed in the vicinity of the cell) was filled with 3M KCl in agar-agar (2,5%) with a tip diameter of ~100 μm. Calomel (Hg_2Cl_2) half-cells saturated with KCl were used in our experiments. Current (direct current, DC) was injected by separate circuit

through extracellular Ag/AgCl electrodes placed in each compartment of the chamber. The employed computer I/O and data acquisition system: voltage/current clamp amplifier TEC-10CX (NPI Electronic), digitizer Digidata 1440A, data acquisition software pCLAMP 10.2 (Molecular Devices). The used signal gain was 10×, discretisation frequency – 100-1000 Hz. Solution surrounding a cell in the central compartment of the chamber was perfused in the rate of ~1 ml/min using a programmable perfusion system and vacuum waste kit (Scientifica PPS).

APs of giant Characeaen cell exhibit relatively consistent characteristics in comparison to tissue APs and variation potentials (VPs) of vascular plants. (Kisnieriene *et al.* 2018, Sukhov *et al.* 2019). Because of the vacuole volume (~95% of the cell, Beilby and Casanova 2014), when the microelectrode is inserted into a Characeaen cell, the tip is generally located in the vacuole. Therefore, the potential difference measured between the extracellular electrode and the microelectrode represents the sum of the membranes' (plasmalemma's and tonoplast's) potentials (Shimmen *et al.* 1994). Thus in our study reported APs represent superposition of APs of both membranes. Unlike other Characeaen cells, *Nitellopsis* AP peak is usually positive and reversal potential of anion efflux is around 100 mV (Kisnieriene *et al.* 2016). Another important note is that for DC excitation, ramped current was used in this study, this allows precise determination of excitation threshold MP – in contrast to over-threshold current stimulus often used in previous experiments with Characeaen (Beilby and Casanova 2014).

2.3 Experimental procedure

Recordings were performed as described in Kisnieriene *et al.* 2018; Lapeikaite *et al.* 2019. The cell was placed in the borosilicate chamber and the central compartment of 5 mm length was tightly isolated from adjacent compartments with vaseline. The chamber then was filled with APW, its central compartment set under perfusion. The intracellular electrode was impaled to the vacuole using micromanipulator (PatchMan, Eppendorf) while the cell was monitored using a binocular (7× magnification).

Experiments were conducted in room temperature (20±1 °C), during the daytime, under constant illumination (95±0,19 μmol m^{-2} s^{-1}). Microelectrode impalement was followed by at least 1 h resting period, which is usually sufficient for stabilization of cell MP. *Nitellopsis obtusa* cells are highly variable in their resting potential. In standard conditions maintained in our experiments (7,2 pH, $[K^+]_{out}$ 0,1 mM) most of the cells are found in

hyperpolarized pump state (Beilby 1986), thus only cells maintaining more negative than -175 mV RP were examined. Electrophysiological procedures were conducted in the following order (**Fig 2.3**): first in current-clamp (CC) mode 3 APs were evoked by direct current increasing in 0,02 μA/s ramp rate from zero. Once AP E_{th} was reached, stimulating current was ceased manually (**Fig. 2.4**). After 30 min resting period, a voltage-clamp (VC) mode was applied. MP in the central compartment (5 mm) was clamped at -180 mV, and rectangular depolarization current pulses (10 s) every 20 or 10 mV voltage steps from the holding potential in the voltage interval from –140 to +80 mV were applied in 5 min intervals. Voltage clamp experiments were followed by 30 min resting period, then the solution in the central compartment was changed to a solution of interest (under constant perfusion). After 30 min exposure the whole procedure was repeated.

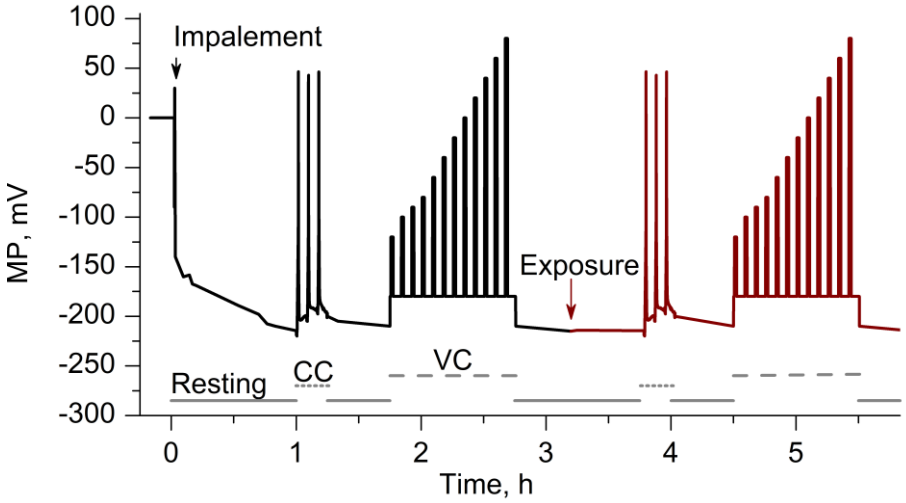

Fig 2.3 Protocol for the investigation of *Nitellopsis obtusa* internodal cell electrical excitability. One set consists of AP excitation by direct current in current-clamp mode (CC), excitation in voltage-clamp (VC) mode and rest periods in-between. During VC MP was clamped at -180 mV and depolarised for 10 s every 5 min in 10-20 mV steps. Red trace indicates exposure to a solution of interest and repeated measurement set.

Exposure effect was tested of these compounds:

- Putative GLR agonists:
  - L-Glu (0,1 mM and 1 mM),
  - L-Asn (0,1 mM and 1 mM),
  - NMDA (0,01; 0,1 and 1 mM),
  - L-Glu + NMDA (0,1 mM each);
- NMDA type receptor antagonist AP-5 (0,1 mM);

- Non-NMDA type receptor antagonist DNQX (0,1 mM).

To evaluate the possible inhibitory effect of AP-5 and DNQX cells were pre-treated with antagonists, then agonists were applied together with an antagonists: APW → APW + antagonist → APW + antagonist + agonist.

Co-treatment experiments were caried out with NMDA and AP-5 (0,1 mM each) as well as Glu and AP-5 (0,1 mM each). In all combinations of compounds, the same measurement protocol was performed.

2.4 Solutions

The control solutions: APW (0,1 mM KCl, 1,0 mM NaCl, 0,1 mM $CaCl_2$, and 3 mM TRIS, adjusted to a pH 7,2 by HEPES). APW' (APW supplemented with 1 mM HCl, adjusted to pH 7,2) was used to establish control for 1 mM Glu-Cl treatment. Agonist/antagonist solutions were APW-based, maintained in pH and ion concentrations as corresponding control conditions. Asn (L-asparagine monohydrate), Glu (potassium L-glutamate, or L-Glutamic acid hydrochloride); NMDA (N-Methyl-D-aspartic acid), AP-5 (DL-2-Amino-5-phosphonopentanoic acid), DNQX (6,7-Dinitroquinoxaline-2,3(1H,4H)-dione) were procured from Sigma Aldrich.

2.5 Electrophysiological parameters

Following parameters were evaluated as described in Kisnieriene *et al.* (2018) and Lapeikaite *et al.* (2019). In CC mode (**Fig 2.4**):

- RP was evaluated prior to AP excitation, also before and after exposure to presented compounds by 2 s hyperpolarizing current pulses.
- Membrane resistance was evaluated by passing several hyperpolarizing current impulses of 1 s duration prior to AP excitation, also before and after 30 min exposure to presented compounds. Membrane resistance calculated in Ω/m^2 following:

$$R = \frac{\Delta U}{I \pi d l}$$

  Where ΔU - MP difference (V), I - applied current (A), *l* - cell length in central compartment (0,005 m); d - cell diameter (m).

- E_{th} - AP excitation threshold - determined as the MP when the depolarization rate exceeded 60 mV/s.
- AP peak.

- AP amplitude - determined from E_{th} to the AP peak potential.
- Repolarization duration was evaluated as time span of 100 mV repolarization from peak potential.

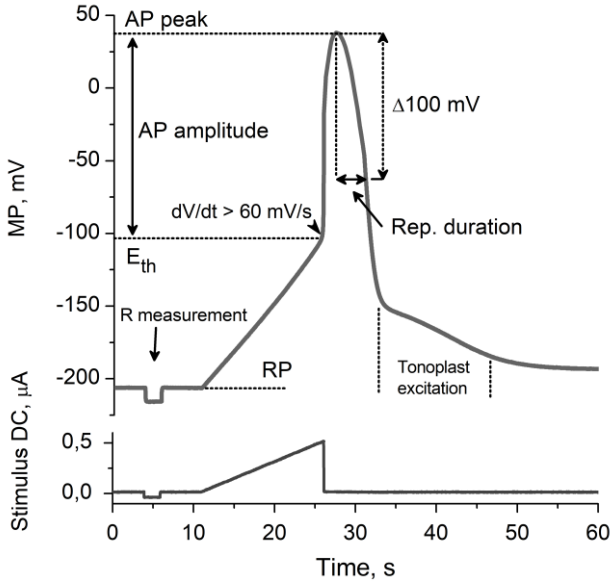

Fig 2.4 Example of DC elicited AP and evaluated parameters in CC. E_{th} - MP potential with depolarization exceeding 60 mV/s. AP amplitude – the MP interval from E_{th} to the peak potential. Repolarization duration – the time span of 100 mV repolarization from the peak. R (resistance) measurement – rectangular hyperpolarizing DC impulses.

In VC mode, Cl^- efflux amplitude was assessed. In *Nitellopsis obtusa* high amplitude efflux during excitation, following Ca^{2+} influx, was attributed to Cl^- efflux by Lunevsky *et al.* (1983). Both of these currents have inward direction thus Ca^{2+} influx component might overlap with Cl^- efflux component especially near excitation threshold (Lunevsky *et al.* 1983, Berestovsky and Kataev 2005). Distinguishing these currents in voltage-clamp recordings is based on temporal properties of Ca^{2+} influx. Lunevsky (1983) in intact *Nitellopsis* with chloride channels blocked by ethacrynic acid recorded low-amplitude calcium current reaching peak in ~0,3 s (Lunevsky *et al.* 1983 Fig. 7 therein), and inactivating in ~1 s from the stimulus onset. In this study Cl^- efflux onset is evaluated based on flux dispatch per membrane area ($dI/dt < -5\ \mu Acm^{-2}s^{-1}$), this value is reached in 0,3-1 s from the onset of rectangular stimulus and the chloride efflux peak is reached in ~1,4 s from Cl^- efflux onset. It is not dismissible that our evaluated inward current overlaps with calcium, yet, considering previously described data and presented I-V curves with

reversal potential characteristic for E_{cl} in results, described inward current is referred as chloride efflux.

In VC recordings, it was observed that AA effect also influences temporal dynamics of Cl^- efflux. Thus, two novel parameters - activation and inactivation durations $t_{act.}$ and $t_{inact.}$ - were introduced. (**Fig 2.5**). In voltage-clamp mode evaluated parameters:

- I_{max} - maximum Cl^- current transient amplitude, measured from abrupt increase of inward current to its maximum. Onset of the Cl^- efflux was determined by transmembrane current derivative (dI/dt value exceeding -5 μA cm^{-2} s^{-1}).
- I_{-90} - Cl^- current transient amplitude at -90 mV clamped MP, measured in the same manner as I_{max}.
- $t_{act.}$ - current transient activation duration - period from abrupt efflux to its maximum value.
- t_{inact} - current transient inactivation duration - period during which maximum current amplitude decreased by 63%.

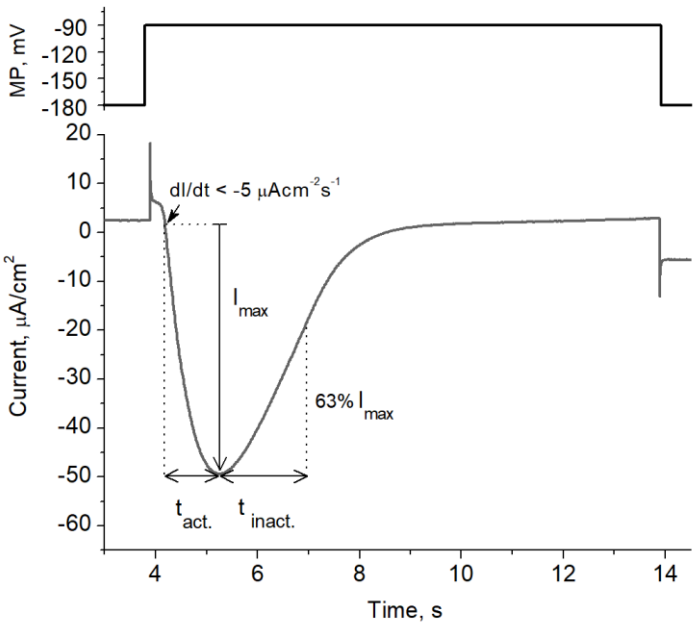

Fig 2.5 Example of Cl^- efflux at -90 mV and evaluated parameters. $t_{act.}$ - efflux activation duration. $t_{inact.}$ - inactivation duration - evaluated as a time of 63% decrease of current amplitude.

Parameter alterations (Δ – difference between values in control solution and solution of interest) upon exposure to different concentrations of agonists were approximated with Michaelis-Menten kinetics as follows:

$$\Delta = \frac{\Delta_{max} \cdot [X]}{K_M + [X]}$$

where Δ_{max} is a saturating difference of a parameter, $[X]$ - concentration of an agonist solution. K_M - Michaelis-Menten constant, equal to concentration $[X]$ in which parameter's difference becomes half-saturating. ($\Delta_{max}/2$).

2.6 Statistics

Due to inherent variation of electrical signalling patterns (e.g., RP, E_{th}, AP amplitude), each parameter's value under the influence of a specific substance was compared to its value in the control solution of the same cell. Between concentrations, differences of values from values in control solution were compared. For each treatment cycle measurements were repeated in 3-9 individual cells and are presented as mean values ± standard error (SE) (unless noted otherwise). In CC mode the first AP was evaluated. Shapiro–Wilk test was used to confirm normality of samples. Two-tailed paired Student's t-test was used for testing differences for individual cells and independent t-test for differences between concentrations/groups of compounds. Differences with $p<0,05$ were considered significant – indicated by asterisks in the results section. Correlations between parameters was tested using the Pearson correlation coefficient for normal distribution samples, otherwise – Spearman's correlation coefficient was used. Data analysis was carried out using software:

- Clampfit (Molecular Devices Corporation),
- Excel (Microsoft Office Corporation),
- OriginPro (OriginLab Corporation),
- *R* programming language (R Core Team),
- Statistica (TIBCO Software).

3. RESULTS

3.1 Temporal control and control solutions

Temporal control experiments were performed to validate the above-described protocol and confirm the stability of electrophysiological parameters of *Nitellopsis*. A full-length experiment - 3 measurement sets with identical protocol – was performed under stable conditions in the APW solution (n=5). Data of the first measurement set were compared to the last (5,5 h in-between). AP parameters remained stable during experiments in both free running MP and clamped MP potentials.

Initial average RP in first measurement set was -209±5 mV, membrane resistance – 1,8±0,1 **Ω**/m^2, E_{th} -104±5 mV, AP peak potential – 34±5 mV, giving the AP of 138±6 mV amplitude with repolarization duration of 3,2±0,3 s. In the last measurement set average RP was -205±4 mV (p=0,6 in comparison to values in first set), membrane resistance – 1,7 **Ω**/m^2 (p=0,7), E_{th} -102±5 mV (p=0,2), AP peak potential 35±5 mV (p=0,6), AP amplitude -136±6 mV (p=0,3), AP repolarization duration – 3,3±0,3 s (p=0,5) (**Fig 3.1 a**, **b** and **Fig S3a** in the Supplementary Data section). Parameters evaluated in VC mode likewise remained stable. Initial I_{max} (at ~100 mV MP) was -51±3 μA/cm^2 and remained stable in the last measurement set (-53±4 μA/cm^2, p=0,6) (**Fig 3.1 c**). Cl^- efflux at -90 mV was also unaltered: I_{-90} was -44±4 μA/cm^2 in the first set, while in the last – -43±5 μA/cm^2 (p=0,9). Temporal parameters of this current transient: $t_{act.}$ – efflux activation duration and $t_{inact.}$ –

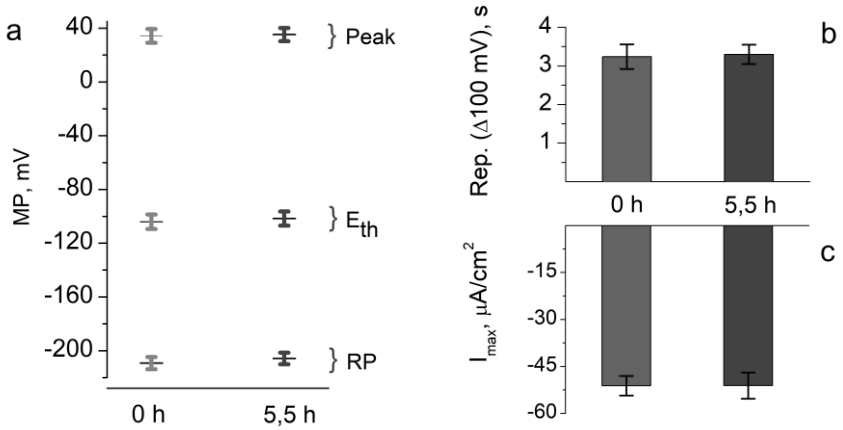

Fig 3.1 Average E_{th}, peak and RP values during repeated measurements in control solution (APW) (a). Average AP repolarization duration (Δ100 mV) (b) and maximum Cl^- efflux values (c) during repeated measurements in APW, n=5.

efflux inactivation duration at -90 mV MP also persisted during repeated excitation (supplementary S3a and S3b). In first measurement set $t_{act.}$ lasted 1,3±0,1 s, while $t_{inact.}$- 2,0±0,1 s. In the last measurement set $t_{act.}$ duration was 1,3±0,1 s (p=0,6), $t_{inact.}$- 2,1±0,1 (p=0,5).

With no significant changes among parameters it was concluded that established resting periods between measurements sets (30 min) are sufficient for stabilization of the cell state. Consequently, *Nitellopsis obtusa* does not exhibit intrinsic circadian drift of electrophysiological parameters at least up to 8 h during daytime.

Control solutions

APW solution as a control was used in all experiments except the investigation of 1 mM of L-Glutamate (L-Glutamic acid hydrochloride). Since AA chloride salt was used, proper control conditions were established, using APW supplemented with additional 1 mM of HCl ($[Cl^-]_o$ of 2,3 mM instead of 1,3 mM) as a control solution for 1 mM glutamate treatment. pH and other ion concentrations were adjusted to basic APW. This arrangement allows dismissing the possible effect of increased extracellular Cl^- concentration when investigating exposure to Glu. Thus, prior to exposure to 1 mM of Glutamate, double control was performed, APW→APW' (APW+1 mM HCl).

Effect of 1 mM HCl on electrophysiological parameters was investigated after 0,5-1 h exposure. 1 mM of HCl did not alter membrane RP (from -197±7 to -206±4 mV (p=0,7)) or resistance (from 1,9±02 Ω/m^2 to 1,7±0,1 Ω/m^2 (p=0,2)). AP E_{th} (from -91±4 mV to -93±5 mV (p=0,7), peak value (from 34±5

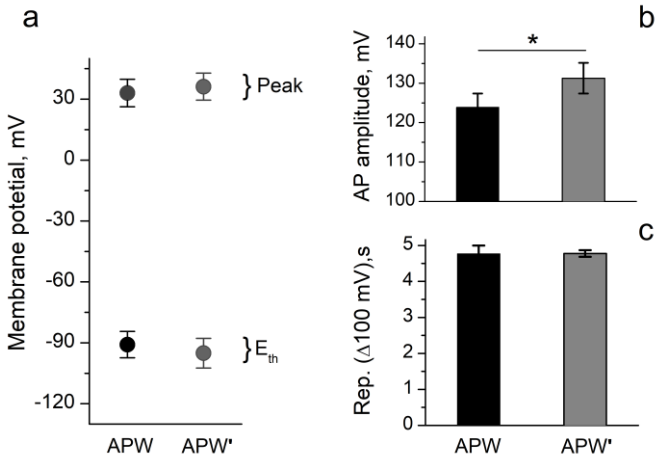

Fig 3.2 Average AP E_{th}, peak (a); AP amplitude (b) and repolarization duration (c) values after exposure to APW'(APW+1 mM HCl), n=9.

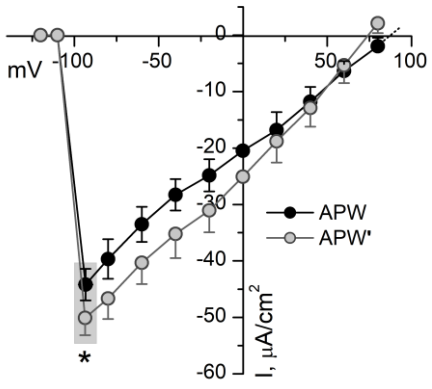

Fig 3.3 Cl^- efflux dependence on membrane voltage in control solution (APW) and after exposure to an additional 1 mM of HCl (APW'), n=9.

mV to 38±5 mV (p=0,1)) and repolarization duration (from 4,8±0,2 s to 4,7±0,1 s (p=0,9) remained stable, yet 1 mM HCl slightly but statistically significantly increased AP amplitude (by 6,7±1,6 mV from 125±4 mV to -132±4 mV (p=0,01)) (**Fig 3.2**).

VC experiments revealed no significant changes in Cl^- efflux activation and inactivation durations (supplementary figure **Fig S3c**). $t_{act.}$ at -90 mV in APW was 1,4±0,1 s, while $t_{inact.}$ – 2,1±0,1 s. These parameters remained unchanged ($t_{act.}$ of 1,5±0,1 s, $t_{inact.}$ -2,1±0,1 s, p=0,8 and 0,9 respectively). However maximum Cl^- efflux was statistically significantly increased from -44±3 µA/cm^2 (at -90 mV in this data set) to -50±3 µA/cm^2 (Δ6±2 µA/cm^2, 15±5%, p=0,02) (**Fig 3.3**).

As depicted in I-V characteristics (**Fig 3.3**) the reversal potential of chloride is slightly pulled to negative MPs upon exposure to HCl (from ~88±6 mV in APW to ~74±7 mV in APW'). In APW, given that $[Cl^-]_o$ equals to 1,3 mM, and Nernst potential for Cl^- is ~90 mV, $[Cl^-]_{cyt}$ results in ~45 mM - a physiological range for *Nitellopsis* (Katsuhara and Tazawa 1988). Reversal potential shift indicated after 1 HCl exposure is proportional to that of heightened $[Cl]_o$ to 2,3 mM. Thus, with stable $[Cl^-]_{cyt}$ the mechanism of increased Cl^- efflux upon heightened $[Cl]_o$ is hitherto unclear. Still, shifts in AP amplitude (5±1%) and maximum Cl^- efflux (14±4%) are tangible, thus double control for Glu-Cl investigation is advisable.

3.2 Electrophysiological parameters in control solution

Described experiments were performed with a total of 93 cells (including temporal control). Evaluated mean electrophysiological parameters' values in control conditions of full set are presented in **table 3.1**. All parameters' data sets followed a normal (Shapiro–Wilk test, p>0,05) distribution, except the distribution of peak values. Correlations (Pearson Corr. or Spearman Corr.) between all independent parameters were estimated in free-running MP. Independent parameters exhibited no correlation. Neither E_{th}, AP amplitude,

Table 3.1 Electrophysiological parameters of *Nitelopsis obtusa* in control solution (APW) of all investigated cells, mean ± standard deviation, n=93.

Parameter	Mean ± SD
RP, mV	-211 ± 17
E_{th}, mV	-97 ± 13
AP peak, mV	30 ± 14
AP amplitude, mV	128 ± 19
Rep. (Δ100 mV), s	3,8 ± 1
I_{max}, μA/cm^2	-48 ± 11
I_{-90}, μA/cm^2	-41 ± 10
$t_{act.}$ (at -90 mV), s	1,43 ± 0,2
$t_{inact.}$ (at -90 mV), s	2,2 ± 0,4
R, Ω/m^2	1,8 ± 0,4

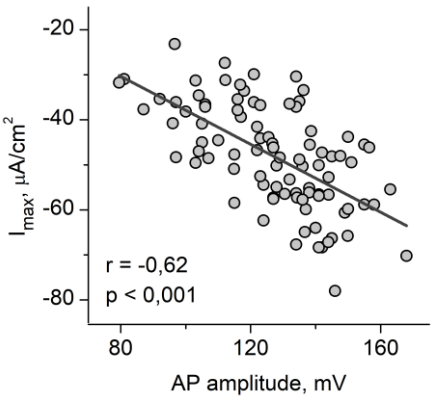

Fig 3.4 Correlation between maximum Cl^- efflux values and corresponding AP amplitudes of each cell in control solution (APW), n=93.

nor repolarization duration in investigated cells set correlated with RP (e.g. E_{th} vs RP r=0,001, p=0,99, for others p>0,4), or with each other. Even though RPs are highly variable among cells, such lack of correlations indicates that RP variability has no effect on excitation parameters. Also, evaluated parameters (RP, E_{th}, AP peak, rep. duration) are proved to be independent and reflect different attributes of ion channel activity. RPs and corresponding AP amplitude values are plotted in supplementary **Fig S3d**. As assumed, AP amplitude did correlate with maximum Cl^- efflux (r=-0,62, p<0,001, **Fig 3.4**).

Temporal Cl^- transient parameters – activation and inactivation durations ($t_{act.}$ and $t_{inact.}$) – are a novel, thus their relation to each other and efflux amplitude was to be determined. It was concluded that efflux $t_{act.}$ and $t_{inact.}$ at -90 mV do not correlate with I_{-90} (r=-0,07, p=0,5 and r=0,04, p=0,7, respectively, **Fig 3.5**, **Fig S3e**, **Fig 3.6**); thus, temporal parameters reflect different attributes of channel activity and are evaluated separately. $t_{act.}$ correlated with the corresponding $t_{inact.}$ -90 mV (r=0,39 p<0,001, **Fig 3.6**). Since $t_{act.}$ and $t_{inact.}$ exhibit different voltage dependance, they are evaluated independently. Concluding, investigated AP parameters may be modulated independently (e.g. AP amplitude and repolarization duration), as do chloride efflux characteristics; thus, analysis of separate excitation parameters allows indication of specific effect pattern.

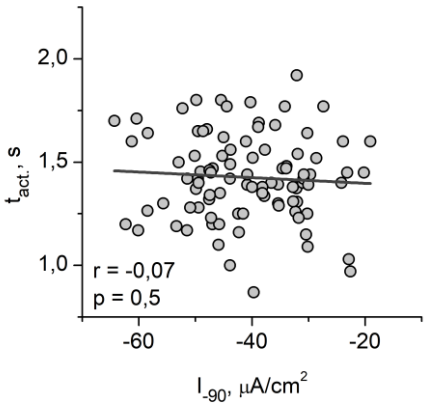

Fig 3.5 Correlation between Cl^- efflux values at -90 mV MP and corresponding activation durations of each cell in control solution (APW), n=93.

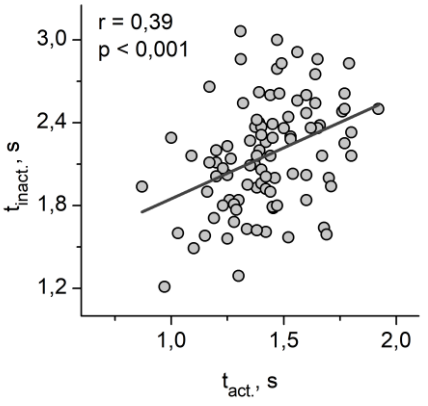

Fig 3.6 Correlation between Cl^- efflux activation and corresponding inactivation durations of each cell at -90 mV MP in control solution (APW), n=93.

3.3 Effect of natural GLR agonists on excitation parameters

AP parameters of *Nitellopsis obtusa* internodal cell were investigated and compared to values in control solution after exposure to two natural GLR agonists – L-glutamate, L-Asparagine, and a synthetic iGluR agonist – NMDA. The cell surface of 0,5 cm was exposed for 30 min to APW-based, buffered solutions of: 0,1 mM and 1 mM Asn, 0,1 mM and 1 mM Glu, 0,01 mM, 0,1 mM and 1 mM NMDA.

AP parameters were investigated in CC and VC modes, as described in segment 2.5. with identical protocols in control solutions and after/during exposure.

3.3.1 Asparagine effect on excitation parameters

The effect of 0,1 mM (n=7) and 1 mM (n=7) Asn was investigated as described in section 2.3. Since one of the primary plant cell responses to AA is membrane depolarization (Stephens *et al.* 2008) RP during exposure was monitored. Although general tendency of both 0,1 mM and 1 mM Asn to slightly depolarize membrane potential was observed (about 15±12 mV and 9±16 mV respectively), it was not consistent and was statistically insignificant due to high variation. During this period, membrane resistance was also not altered (1,8±0,1 Ω/m^2 in APW; after 0,1 Asn – 1,9±0,4 Ω/m^2; after 1 mM Asn – 2,0±0,2 Ω/m^2; p>0,5 in both cases).

AP amplitude

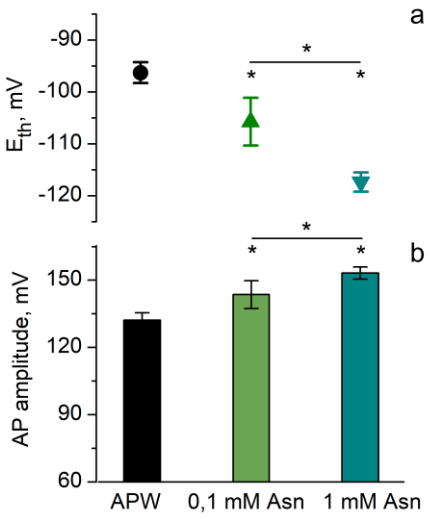

Fig 3.7 Mean values of AP excitation threshold potential (E_{th}) in control solution (APW) and after exposure to 0,1 and 1 mM Asn (a), corresponding AP amplitudes determined from E_{th} to AP peak (b), n=7.

Statistically significant hyperpolarization of E_{th} after exposure to Asn was observed after both applied concentrations. 0,1 mM Asn hyperpolarised E_{th} by -9±3 mV (10±4%) and 1 mM of Asn by -21±3 mV (22±5%) resulting in E_{th} of -106±4 mV and -117±1 mV respectively. Results indicate dose-dependency since hyperpolarisation of AP E_{th} between Asn concentrations differs significantly (**Fig 3.7 a**). AP peak values did not differ between control and asparagine solutions: 36±5 mV in APW, 37±3 mV in 0,1 mM Asn and 36±2 mV in 1 mM Asn. Given the hyperpolarized E_{th} and unchanged AP peaks, APs after Asn application featured heightened amplitudes (**Fig. 3.7 b**). In APW average AP amplitude was 132±6mV, after 0,1 mM Asn application 143±6 mV (9±3% higher) and 153±3 mV (16±3% higher) after 1mM of Asn. Given data imply that APs after exposure Asn retain typical peak values, but exhibit hyperpolarized E_{th} and higher amplitude.

AP repolarization

In control solution average repolarization duration in Asn data set was 3±0,3 s. After 0,1 mM and 1 mM Asn treatment - 3,7±0,4 s and 5,1±0,6 s respectively. Thus, prolongations differed significantly from control values by 0,9±0,2 s (32±11%) and 2,2±0,5 s (74±16%). An overview of mean E_{th}, AP peaks and repolarization durations is presented in **Fig 3.8**. Summarizing given data it was concluded that in cells treated with 0,1 mM and 1 mM Asn electrically induced APs are prolonged, exhibiting heightened amplitudes and hyperpolarized E_{th}.

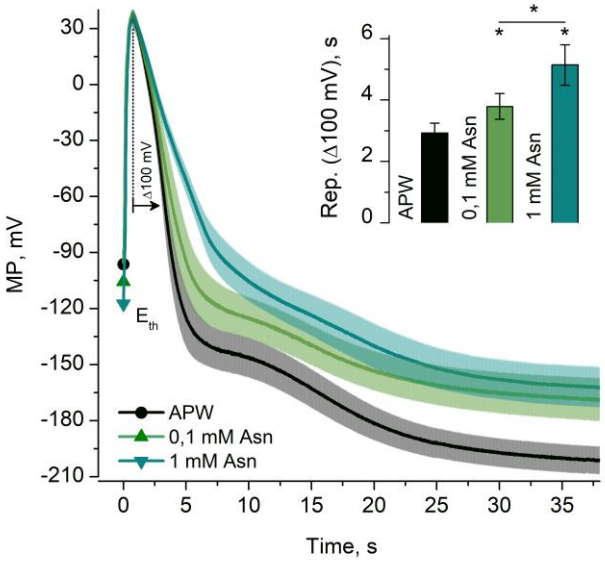

Fig 3.8 Averaged AP repolarization phases in control solution (APW) and after exposure to Asn. Solid lines represent mean MP with transparent SE values. Note the differences of AP threshold and stable values of APs peaks. Dot line and arrow indicate evaluated repolarization duration of Δ100 mV (represented in insert) compared to APW, n=7.

Asn effect on Cl^- efflux during excitation

First, the Cl^- efflux amplitudes in all clamped MPs, as described in section 2.5, were evaluated. In VC mode, the first excitation elicited efflux is usually of highest amplitude (I_{max}), with clamped potential close to E_{th} in free-running MP. I-V relations are presented as flux across clamped membrane area (0,5 cm in the central chamber compartment) (**Fig 3.9**). Maximum chloride efflux in control solution was -53±2 μA/cm^2 (at MP of ~-100 mV). After 0,1 mM and 1 mM Asn treatment, efflux excitation voltage tended to hyperpolarize (<-100 mV and <-110 mV respectively) with maximum values of -62±4 μA/cm^2 and -76±9 μA/cm^2 respectively (**Fig. 3.9** insert), giving efflux percentage increase from the control of 17±6% and 41±16%. Although Cl^- efflux increased in all voltages after Asn treatment, it did not differ in voltages after first excitation. I_{-90} in APW was -45±3 μA/cm^2, after 0,1 mM Asn -51±5 μA/cm^2 (p=0,5), after 1 mM Asn - -59±9 μA/cm^2 (p=0,1). Also, reversal potentials of efflux retained at values ~100 mV.

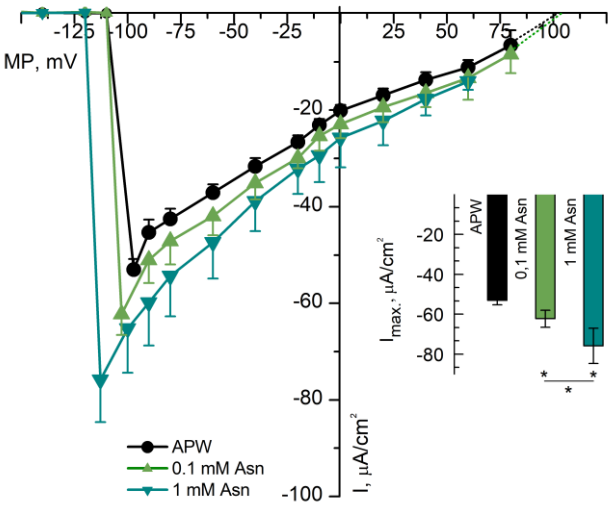

Fig 3.9 Cl^- efflux dependence on membrane voltage in control solution (APW) and after exposure to Asn. MP was clamped at –180 mV. The current data were obtained by injecting rectangular depolarization current pulses (10 s) every 20 or 10 mV steps from the holding potential. Maximum amplitudes of Cl^- current were considered for the statistical analysis presented in the insert, n=7.

Cl^- efflux activation and inactivation durations

During experiments, it was noticed that exposure to Asn results in prolonged efflux in all clamped voltages; thus, activation ($t_{act.}$) and inactivation durations ($t_{inact.}$) were analysed. Since they do not share the same relation to clamped MP (shape), these parameters were analyzed separately. Interestingly, efflux activation duration $t_{act.}$ relation to clamped membrane voltage has a unique form: activation durations are slowest near E_{th} (-110 mv - -80 mV) (**Fig 3.10**). After Asn application, this inherent form becomes more prominent with maximum retained at -90 mV and decreased durations closer to 0 mV. $t_{act.}$ at -90 mV are highlighted in **Fig 3.10** by grey background and presented in the insert. In APW Cl^- efflux activation lasted 1,4±0,1 s; after 0,1 mM Asn - 1,7±0,1 s (Δ0,3±0,1 s, 18±5%) and after 1 mM Asn treatment – 2±0,1 s (Δ0,7±0,2 s, 48±11%). Both concentrations increased $t_{act.}$ significantly, also prolonged $t_{act.}$ significantly differed between concentrations of Asn.

Relation of current inactivation duration $t_{inact.}$ to clamped MP potential had a different shape with maximum duration around -10 mV in APW, -20 mV after 0,1 mM Asn and -40 mV after 1 mM Asn. Since the voltage of maximum and minimum $t_{inact.}$ differed, the same clamped potential as in $t_{act.}$ was evaluated (in **Fig 3.11** indicated by grey background).

In APW Cl^- inactivation lasted 2±0,1 s, after Asn – 2,6±0,1 and 3,4±0,2 s respectively for both concentrations (**Fig 3.11** insert), giving absolute increase of 0,5±0,1 s (28±5%) and 1,3±0,1 s (67±10%) from values in control solution. As in $t_{act.}$ case, Asn impact on $t_{inact.}$ was dose-dependent. After Asn application typical $t_{inact.}$ relation to clamped MP became more expressed as t_{inact} grew considerably from initial $t_{inac.}$ at -90 mV to the maximum at about -40 mV.

Altogether, absolute Cl^- efflux amplitude was altered at the first excitation event (voltage); however, it was not significantly altered in all clamped MP rage, including -90 mV, where $t_{act.}$ was the most prominently prolonged by Asn. General duration of Cl^- efflux was prolonged, both in Cl^- activation and inactivation stages and do not necessarily correspond to the increase of maximum efflux amplitude as indicated by Cl^- efflux and corresponding $t_{act.}$ discorrelation (**Fig 3.5**).

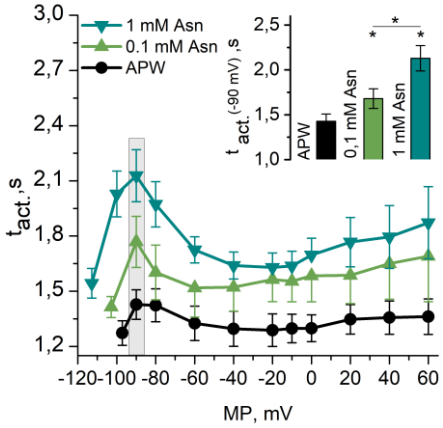

Fig 3.10 Cl^- efflux activation time $t_{act.}$ dependence on clamped MP in control solution (APW) and after exposure to Asn solution. $t_{act.}$ at -90 mV (indicated by the grey background) was used for the statistical analysis presented in the insert, n=7.

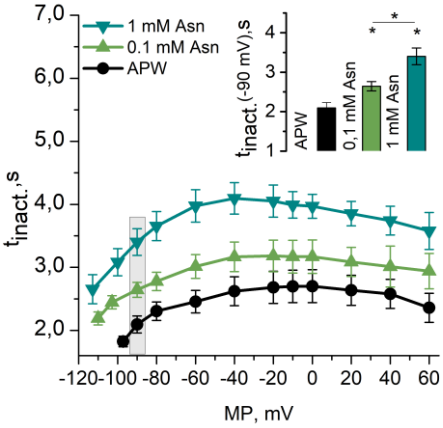

Fig 3.11 Cl^- efflux inactivation time $t_{inact.}$ dependence on clamped MP in control solution (APW) and after exposure to Asn solution. $t_{inact.}$ at -90 mV (indicated by the grey background) was used for the statistical analysis presented in the insert, n=7.

Summarizing VC and CC experiments it is evident, that *Nitellopsis obtusa* internodal cells are sensitive to L-Asn and the effect of AA is reflected in parameters of electrical signalling. Exposure of a small surface area (0,5 cm) to 0,1-1 mM of Asn for 30 min:

a) hyperpolarizes electrically stimulated AP excitation threshold (E_{th}),
b) increases AP amplitude,
c) prolongs AP repolarization phase,

d) prolongs Cl^- efflux activation and inactivation durations,
e) increases maximum Cl^- efflux at E_{th}.

All parameters are altered in a dose-dependent manner. Above described set of alterations is termed as a pattern of effect.

3.3.2 Glutamate effect on excitation parameters

Glu effect (0,1 mM (n=9) and 1 mM (n=8) of L-Glu) was investigated in the same manner as Asn. APW was used as the control solution prior to exposure to 0,1 mM Glu and APW' prior to 1 mM Glu(Cl). The parameters upon exposure were compared respectively. 0,1 mM Glu did not altered RP or membrane resistance. 1 mM Glu however significantly depolarized RP (from -219±5 mV to -193±9 mV: Δ26±4 mV, 12±2%), but did not alter membrane resistance.

AP amplitude

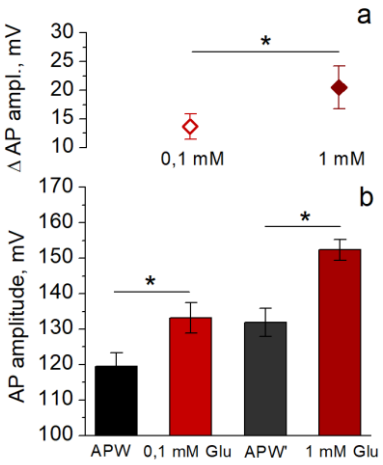

Fig 3.12 Mean values of AP amplitude in control solutions (APW/ APW') and after exposure to 0,1 and 1 mM Glu (b), corresponding increases from values in control solutions (a), n=8-9.

Under Glu AP peaks also remained stable; thus AP amplitudes were increased mainly by hyperpolarization of E_{th}. E_{th} was significantly hyperpolarized by 0,1 mM Glu from -89±2 mV to -101±2 mV (Δ12±2 mV, 14±2%) and by 1 mM of Glu – from -93±5 mV to -114±6 mV (Δ21±5 mV, 23±6%). Corresponding amplitudes in control solutions (APW/APW') and after Glu exposure are presented in **Fig 3.12**. Increase of amplitude from values in control solutions are presented in **Fig 3.12(a)**. 0,1 mM Glu increased AP amplitude from 120±4 mV to 133±4 mV (Δ14±2 mV, 11±1%), 1 mM from 132±4 mV to 152±3 mV (Δ21±4 mV, 16±3%). As in Asn case, AP amplitude increase depended on Glu concentration.

AP repolarization

Averaged repolarisation phases of APs after exposure to Glu are presented in **Fig 3.13**. Absolute values of Δ100 mV repolarization duration are displayed in the insert. 0,1 mM Glu prolonged repolarization from 3,4±0,2 s to 4,2±0,3 s (Δ 0,8±0,2 s, 25±6%).1 mM Glu prolonged this parameter from 4,7±0,1 s to 6,9±0,4 s (Δ 2,1±0,4 s, 45±8%). Prolongations caused by both concentrations significantly differed. Thus AP parameters in the free-running MP are altered in the same manner as by Asn.

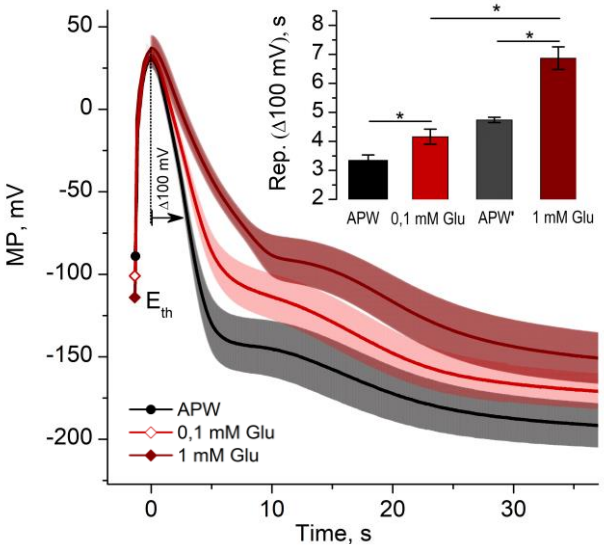

Fig 3.13 Averaged AP repolarization phases after exposure to 0,1 and 1 mM of Glu. Solid lines represent mean MP with transparent SE values. Dot line and arrow indicate evaluated repolarization duration of Δ100 mV presented in insert: both concentrations significantly prolonged repolarizations, increases from control (APW/APW') differ significantly, n=8.

Glu effect on Cl^- efflux during excitation

Similarly to Asn effect, Glu increased maximum efflux amplitude at E_{th}. I-V characteristic is displayed in **Fig 3.14**. Maximum effluxes are depicted in the insert. I_{max} in control solution occurred around -90 mV, upon 0,1 mM Glu - around -100 mV of MP and upon 1 mM Glu - around -120 mV. 0,1 mM significantly enlarged the maximum Cl^- efflux from -45±3 μA/cm^2 to -56±3 μA/cm^2 (Δ 11±2 μA/cm^2, 25±5%). 1 mM of Glu – from -50±3 μA/cm^2 to -73±6 μA/cm^2 (Δ 23±4 μA/cm^2, 45±7%). Increase from control values after 1 mM Glu exposure was significantly higher than one after exposure to 0,1 mM of Glu. Like in Cl^- transients' alterations upon exposure to Asn, I_{-90} was not significantly increased by Glu. In APW I_{-90} was -45±3 μA/cm^2, after 0,1 mM

Glu - 52±4 μA/cm^2 (p=0,1). In APW' I_{-90} was -50±3 μA/cm^2, after 1 mM Glu treatment - -58±5 μA/cm^2 (p=0,2). Reversal potential upon 0,1 mM Glu retained at values ~100 mV, and upon 1 mM Glu at ~80 mV (characteristic for APW').

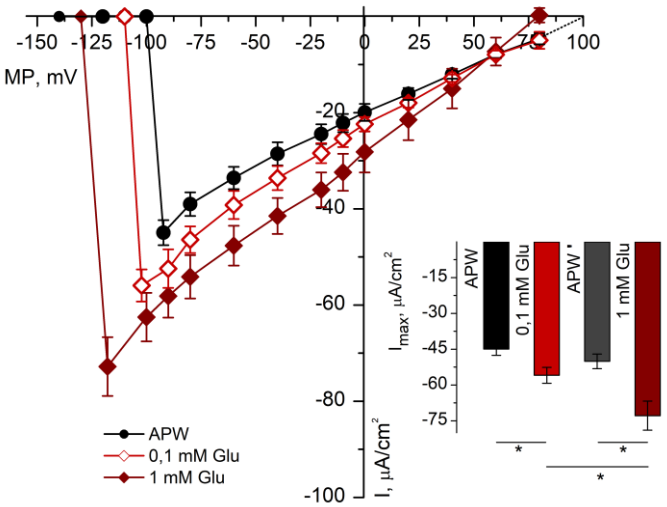

Fig 3.14 Cl^- efflux dependence on membrane voltage in control solution (APW) and after exposure to Glu. MP was clamped at –180 mV. The current data were obtained by injecting rectangular depolarization current pulses (10 s) every 20 or 10 mV voltage steps from the holding potential. Maximum amplitudes of Cl^- current were considered for the statistical analysis presented in the insert, n=8-9.

Cl^- efflux activation and inactivation durations

Glu exposure resulted in a similar to Asn $t_{act.}$ dependance on clamped MP shape, with maximum exhibited at -90 mV in both concentrations (**Fig 3.15**). 0,1 mM Glu prolonged $t_{act.}$ at -90 mV MP from 1,4±0,1 s to 1,8±0,1 s (Δ 0,4±0,1 s, 27±3%). 1 mM Glu – from 1,5±0,1 s (APW') to 2,1±0,1 s (Δ 0,7±0,1 s, 51±13%). Efflux inactivation duration was also altered in the same fashion as by Asn – in all voltage range with longest durations at -40 - -20 mV. At -90 mV $t_{inact.}$ were extended from 2,2±0,1 s to 2,8±0,1 s (Δ 0,6±0,1 s, 30±5%) by 0,1 mM Glu and from 2,1±0,1 s to 3,1±0,2 s (Δ 1,1±0,2 s, 56±10%) by 1 mM Glu (**Fig 3.16**).

Glu and Asn effect was comparable, however effect of Glu surpassed that of Asn in all parameters except repolarization duration. A detailed comparison between effects of GLR agonists is presented in section 3.5.

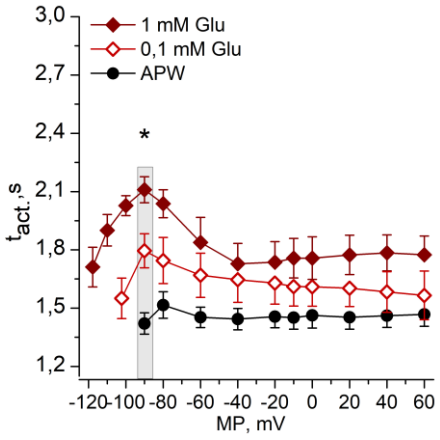

Fig 3.15 Cl^- efflux activation time $t_{act.}$ dependence on clamped MP in control solution (APW) and after exposure to Glu. $t_{act.}$ at -90 mV is indicated by a grey background. Prolongations from the control values differ significantly, n=8-9.

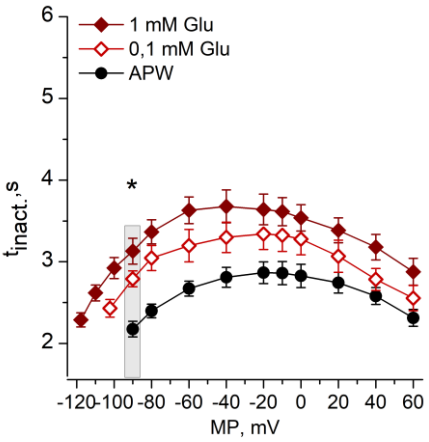

Fig 3.16 Cl^- efflux inactivation time $t_{inact.}$ dependence on clamped MP in control solution (APW) and after exposure to Glu. $t_{inact.}$ at -90 mV is indicated by a grey background. Prolongations from the control values differ significantly, n=8-9.

3.4 NMDA effect on excitation parameters

0,1 mM NMDA (n=8) effect was investigated and compared to already established alterations of electrical signalling by Glu.

Exposure to 0,1 mM NMDA did not elicited prominent depolarization of RP or alteration of membrane resistance. Yet NMDA effect was prominent once APs were elicited. 0,1 mM of NMDA significantly hyperpolarized E_{th} and prolonged AP repolarization duration with NMDA effect significantly exceeding effect of 0,1 mM Glu (**Fig 3.17**). As in natural GLR agonist exposure outcome, peak value of AP was not significantly altered.

0,1 mM of NMDA hyperpolarized E_{th} from -89±3 mV to -109±3 mV (Δ20±3 mV, 23±4%) (**Fig. 3.17** upper insert). This alteration is significantly higher than that caused by 0,1 mM Glu (Δ12±2 mV, 13±2%).

AP repolarization phase duration was prolonged by 0,1 mM NMDA from 4,2±0,4 s to 7,3±0,8 s (Δ 3,0±1 s, 72±13%), also significantly longer both in absolute values (**Fig 3.17** lower insert) and increase compared to APW (0,1 mM Glu prolonged repolarisation by 0,8±0,2 s, 25±6%).

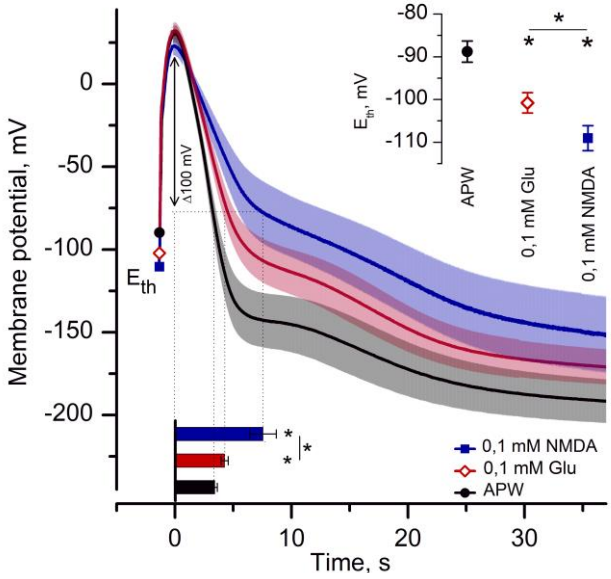

Fig 3.17 Averaged APs after exposure to 0,1 mM Glu or 0,1 mM NMDA. Solid lines represent mean MP with transparent SE values. Note the differences of AP threshold (E_{th}) and relatively unchanged values of peaks. Dot lines and arrow indicate evaluated repolarization duration (presented in the lower insert). Corresponding E_{th} values are presented in the upper insert. E_{th} did not differed in control solutions of the sets thus represented as sigle data point, n=8-9.

Voltamperic characteristics of Cl^- efflux in control solution and after 30 min exposure to 0,1 mM Glu and 0,1 NMDA as well as corresponding $t_{act.}$ and $t_{inact.}$ in all clamped voltages are presented in **Fig. 3.18**. I_{max} was observed at -90 mV in control solution, upon 0,1 Glu around -100 mV, and upon 0,1 NMDA – around -110 mV. Increase of maximum Cl^- efflux surpassed that of 0,1 mM Glu: 0,1 mM NMDA increased efflux by 25±5 μA/cm^2 (64±17%), while the same concentration of Glu caused 11±2 μA/cm^2 increase (25±5%). Also, unlike applied Glu concentrations, 0,1 mM NMDA significantly increased I_{-90} which was enhanced from -44±6 μA/cm^2, to -62±7 μA/cm^2 (Δ17±5 μA/cm^2, 40±13%, p=0,01).

Prolongations of $t_{act.}$ and $t_{inact.}$ at -90 mV upon 0,1 mM NMDA also surpassed ones of 0,1 mM Glu. 0,1 mM NMDA increased $t_{act.}$ from 1,4±0,1 s to 2,2±0,2 s (Δ0,8±0,1s, 53±9%). $t_{inact.}$ – from 2,1±0,2 s to 3,3±0,3s (Δ1,2±0,2 s, 58±12%). The characteristic shape of $t_{act.}$ vs voltage became more

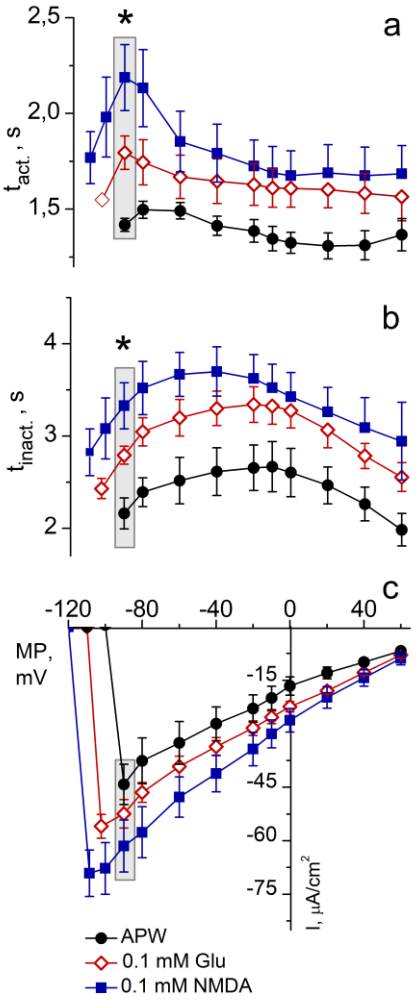

Fig 3.18 Cl^- efflux dependence on clamped MP in control solution (APW) and after exposure to 0,1 mM Glu or 0,1 mM NMDA (c), corresponding efflux activation $t_{act.}$ (a) and inactivation $t_{inact.}$ (b) durations are presented above . $t_{act.}$ and $t_{inact.}$ at -90 mV (grey background) was used for statistical analysis. Asterisks indicate statistically significant difference between effect of Glu and NMDA, n=8-9 for each treatment set.

emphasised upon exposure to 0,1 mM of NDMA. Summarizing giving data, it was concluded that NMDA alters excitation parameters in the same pattern as Glu and Asn, yet NMDA effect surpasses both.

To establish dose-dependency of NMDA additional experiments using 0,01 mM (n=9) and 1 mM of NMDA (n=3) were performed. 0,01 mM of NMDA was an effective concentration, exhibiting same effect pattern as Glu, and Asn. 1 mM NMDA effect statistically did not surpass 0,1 mM in any of the parameters.

0,01 mM NMDA significantly hyperpolarized E_{th} from -94±4 mV to -105±4 mV (Δ10±2 mV, 10±2%), while 0,1 mM of NMDA hyperpolarized E_{th} by Δ20±3 mV, (23±4%). 1 mM NMDA hyperpolarized E_{th} from -89±1 mV to -113±6 mV (Δ24±7 mV, 27±7%). E_{th} changes upon 0,01 mM and 0,1 mM NMDA differed significantly, yet 1 mM induced E_{th} hyperpolarization did not exceed that of 0,1 mM. As in Glu and Asn results, AP peak values remained unchanged in all NMDA concentrations, thus increase in AP amplitude was dominated by hyperpolarization of the threshold potential. 0,01 mM increased AP amplitude by 10±3 mV, 0,1 mM - 24±4 mV and 1 mM - 27±8 mV. Again, effect of 0,01 mM and 0,1 mM differed significantly, and 1 mM NMDA effect did not exceed that of 0,1 mM.

Repolarization durations were affected in the same manner. 0,01 mM NMDA prolonged repolarization duration by 0,8±0,3 s (26±9%). 0,1 mM by 3,0±0,7 s (72±13%), and 1 mM – by 3,2±0,7 s (83±20% - comparing to prolongation caused by 0,1 mM not significantly different). An overview of average repolarization durations in all NMDA concentrations and increases of AP amplitude are presented in **Fig 3.19**.

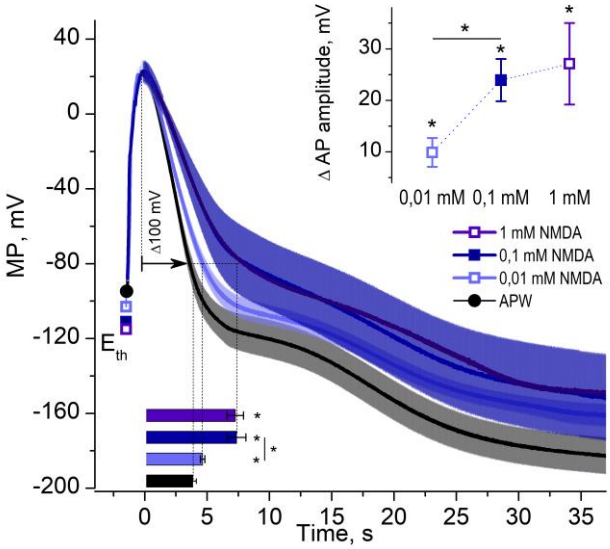

Fig 3.19 Averaged APs after exposure to NMDA. Solid lines represent mean MP with transparent SE values. Rep. durations after 0,1 mM and 1 mM exposure did not differ. Only negative SE of 0,1 mM and positive SE of 1 mM are depicted – average repolarizations of these concentrations overlap (insert). Note the differences of AP threshold (E_{th}) and unchanged values of peaks. Dot lines and arrow indicate evaluated repolarization durations presented in the lower insert. Increase of AP amplitude from control values presented in the upper insert. Asterisks indicate significant difference from the control and between concentrations, n=3-9.

Average I-V curves after NMDA treatments are presented in **Fig. 3.20**. As with AP parameters in free running MP, 0,01 mM NMDA did elicit significant increase in maximum chloride efflux and alterations between 0,01 mM and 0,1 mM differed significantly. In control solution I_{max} was observed around -90 mV, upon 0,01 mM NMDA around -100 mV, upon 0,1 mM around -110 mV and upon 1 mM around -120 mV. Reversal potentials of efflux as in other treatments retained at values ~100 mV. 0,01 mM NMDA increased maximum chloride efflux from -44±5 μA/cm^2 to -55±8 μA/cm^2 (Δ11±5 μA/cm^2, 22±13%), 0,1 mM NMDA increased I_{max} from -45±3 μA/cm^2 to -70±6

μA/cm^2 (Δ25±6 μA/cm^2, 57±15%,), and 1 mM from -45±3 μA/cm^2 to -73±8 (Δ28±5 μA/cm^2, 64±11%). 1 mM NMDA effect did not surpass 0,1 mM.

However I_{-90} remained unaltered by 0,01 mM NMDA. I_{-90} in APW was -41±5 μA/cm^2, after 0,01 NMDA -47±6 μA/cm^2 (p=0,2). 0,1 mM NMDA increased I_{-90} by Δ17±5 μA/cm^2 (40±13%,). 1 mM NMDA enlarged I_{-90} from -44±3 μA/cm^2 to -66±4 μA/cm^2 (Δ21±2 μA/cm^2, 48±6% - not significantly different from 0,1 mM NDMA). Thus, among all tested putative agonists, only NMDA in 0,1 mM or higher concentration altered I_{-90}. Similarly to Asn and Glu data, reversal potentials of efflux were not altered (~100 mV).

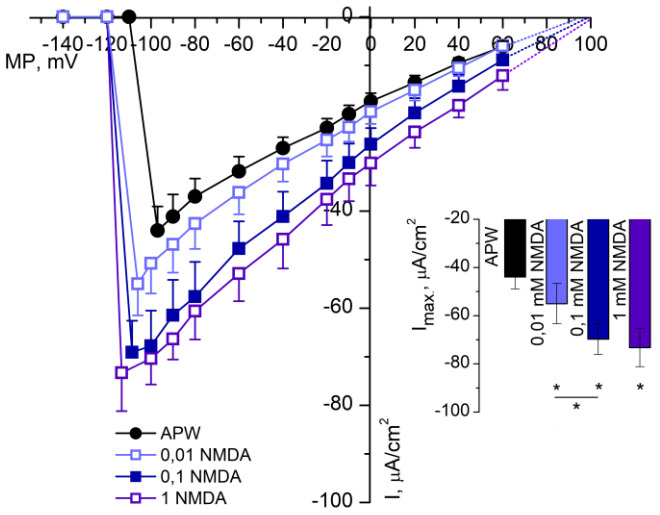

Fig 3.20 Cl^- efflux dependence on membrane voltage in standard conditions (APW) and after exposure to NMDA. Maximum amplitudes of Cl^- current were considered for the statistical analysis presented in the insert. Asterisks indicate significant difference from the control and between concentrations 1 mM NMDA effect did not differ from 0,1 mM, n=3-9.

All tested NMDA concentrations significantly altered both $t_{act.}$ and $t_{inact.}$ at -90 mV clamped MP. As in other parameters, 0,01 and 0,1 mM effect differed significantly. $t_{act.}$ duration expanded from 1,4±0,1 s to 1,6±0,1 s (Δ0,2±0,1 s, 13±4%) upon 0,01 mM NMDA, to 2,2±0,2 s (Δ0,8±0,1 s, 53±9%) upon 0,1 mM, and to 2,5±0,3 s (Δ1±0,1 s, 7411%) upon 1 mM NMDA. Prolongation caused by 1 mM did not significantly surpass 0,1 mM effect (**Fig. 3.21**). $t_{inact.}$ was prolonged from 2,2±0,2 s to 2,5±0,1 (Δ0,3±0,1 s, 16±6%) upon 0,01 mM exposure, to 3,3±0,3 s (Δ1,2±0,2 s, 58±12%) upon 0,1 mM exposure, and to 4±0,4 s (Δ 1,6±0,3 s, 66±10%) upon 1 mM (no significant difference between 0,1 and 1 mM) (**Fig. 3.22**).

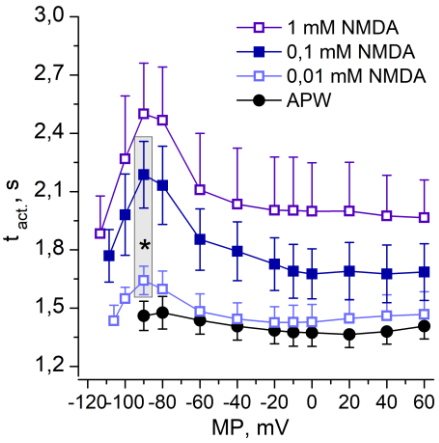

Fig 3.21 Cl^- efflux activation time $t_{act.}$ dependence on MP in control solution (APW) and after exposure to NMDA. $t_{act.}$ at -90 mV is indicated by a grey background. Prolongations from the control values differ significantly, n=3-9.

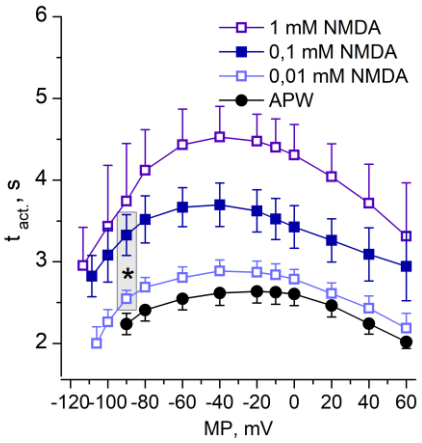

Fig 3.22 Cl^- efflux inactivation time $t_{inact.}$ dependence on MP in control solution (APW) and after exposure to NMDA. $t_{inact.}$ at -90 mV is indicated by a grey background. Prolongations from the control values differ significantly, n=3-9.

It was concluded that 0,01 mM of NMDA - ten times lesser than the active concentration of both investigated AA - is effective. Electrical signalling response to NMDA is dose-dependant. Concentrations above 0,1 mM are saturating.

3.5 Comparison of dose-dependance of GLR agonists

Changes of excitation parameters from the values in control solution were compared between all investigated GLR agonists. Differences' dependences on the concentration of agonists were approximated with Michaelis-Menten kinetics, as described in section 2.5. All below presented changes (Δ) were significant in comparison with control solution, asterisks in the figures represent statistically significant differences between Δ.

AP shape upon exposure to putative GLR agonists is altered *via* E_{th}, amplitude, and repolarizarion duration. As mentioned earlier, AP amplitude increase is dominated by hyperpolarization of E_{th}. E_{th} alterations upon all excitatory compounds are plotted in **Fig S3f**. Corresponding increases of AP amplitude after exposure to Asn, Glu and NMDA are depicted in Fig **3.23**. K_M of amplitude increase upon Glu and Asn is ~0,1 mM, while upon NMDA ~0,02 mM (**Fig S3g**). 0,1 mM of NMDA effect was significantly higher than

the effect of the same concentration of both Asn and Glu while 1 mM effects did not differ between agonists.

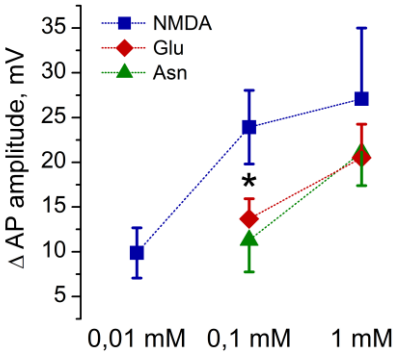

Fig 3.23 Average AP amplitude increase after exposure to various concentration of Glu, Asn and NMDA. The asterisk indicates significant differences between the effects of AA and the effect of NMDA, n=3-9.

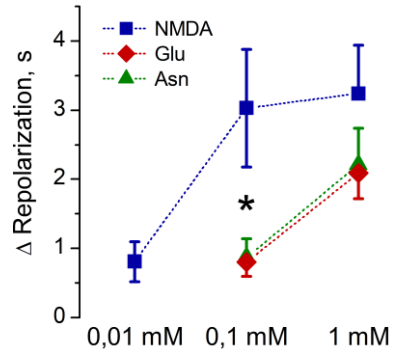

Fig 3.24 Average repolarization prolongations after exposure to various concentration of Glu, Asn and NMDA. The asterisk indicates significant differences between the effects of AA and the effect of NMDA, n=3-9.

1 mM of NMDA saturating effect likewise was prominent in observed prolonged AP repolarizations (**Fig 3.24**). Asn and Glu had very similar strength of the effect. Glu and Asn K_M for this parameter is 0,2 mM, while NMDA - 0,03 mM.

Maximum chloride efflux dose-dependency is plotted in **Fig 3.25**. K_M for I_{max} of NMDA was 0,02 mM, while for Asn 0,2 mM and Glu - 0,14 mM. $t_{act.}$ and t_{inact} prolongations are plotted in **Fig 3.26**. For $t_{act.}$ NMDA K_M was 0,05 mM, Asn – 0,11 mM, Glu -0,09 mM. $t_{inac.}$ half saturating effect was calculated to be reached by 0,04 mM of NMDA, by 0,18 mM of Asn and by 0,09 mM of Glu

Excitation parameters in clamped MP had analogous dose-dependency between agonists. 0,01 mM of NMDA had a comparable impact to 0,1 mM of Asn or Glu. Effect of 0,1 mM NMDA exceeded the effect of the same concentration of Asn or Glu for all evaluated chloride efflux parameters. 1 mM NMDA exposure did not result in a more pronounced effect than 0,1 mM NMDA. Thus as in AP parameters, 1 mM of NMDA was concluded to be saturating.

Calculated K_M values for each electrophysiological parameter are listed in table 3.2. Applied Michaelis-Menten approximations are plotted in supplementary data (**Fig S3g**).

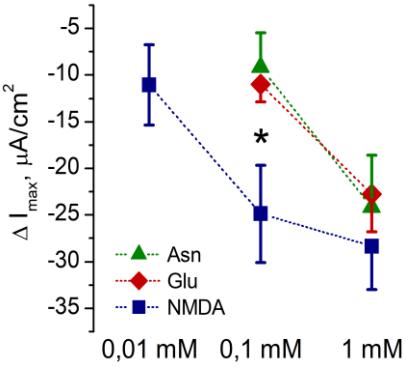

Fig 3.25 Maximum Cl^- current amplitude increase after exposure to various concentration of Glu, Asn and NMDA. The asterisk indicates significant differences between the effects of AA and the effect of NMDA, n=3-9.

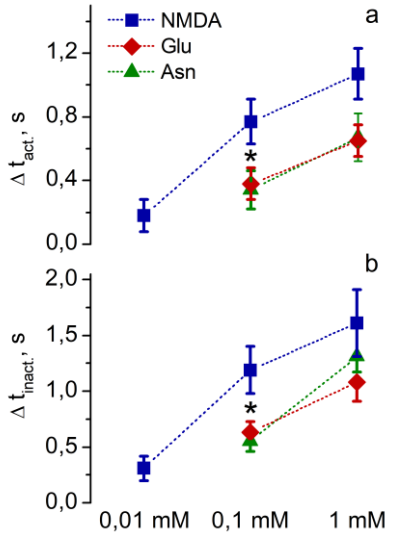

Fig 3.26 Cl^- current activation $t_{act.}$ (a) and inactivation $t_{inact.}$ (b) duration prolongations at -90 mV after exposure to various concentration of Glu, Asn and NMDA. The asterisk indicates significant differences between the effects of AA and the effect of NMDA, n=3-9.

It was concluded that all agonists induced a similar effect pattern. The effect of all three substances exhibited dose-dependancy. Effects of Asn and Glu are of comparable strength, while effect of NMDA is more potent.

3.6 Effect of application of NMDA together with Glu

Since it was demonstrated that Gly and Gu act synergically to modulate $[Ca^{2+}]_{cyt}$ (Dubos *et al.* 2003) and a mixture of these AA (0,1 mM each) triggered APs in *Conocephalum conicum* while the administration of either amino acid alone held no effect (Krol *et al.* 2007), the possible synergetic effect of NMDA and Glu was tested. A mixture of NMDA and Glu (0,1 mM+0,1 mM, n=6) did not elicit APs, nor did it depolarize MP or alter membrane resistance.

Electrophysiological parameters alterations upon NMDA/Glu mixture had an identical effect pattern as exposure to single agonist solutions. 0,1 mM Glu+0,1 mM NMDA effect on each parameter was not significantly higher than caused by 0,1 mM NMDA (presented in supplementary **Fig S3g**). The mixture of NMDA and Glu hyperpolarized E_{th} by 23±3 mV (25±4%), did not alter AP peak value, the resulted AP amplitude increase was 32±4 mV (31±5%). AP repolarization was prolonged by 3,9±0,2 s (89±6%). I_{max}

Table 3.2 K_M values of evaluated electrophysiological parameters (Michaelis-Menten approximations).

Parameter	K_M, mM		
	Asn	Glu	NMDA
E_{th}	0,16	0,095	0,016
AP ampl.	0,107	0,07	0,018
Rep.	0,209	0,22	0,025
I_{max}	0,221	0,135	0,016
$t_{act.}$	0,119	0,092	0,048
$t_{inact.}$	0,182	0,086	0,042

was increased by -30±5 μA/cm2 (75±18%), $t_{act.}$ prolonged by 1,0±0,1 s (70±10%), $t_{inact.}$ by 1,5±0,1 s (42±3%).

Concluding - NMDA did not exhibit synergetic action with Glu, nor was its effect additive.

3.7 Inhibition of the excitatory agonists' effect

3.7.1 NMDA effect inhibition by AP-5 and DNQX – pre-treatment

Before investigating the possible inhibitory effect of both NMDA- and non-NMDA-type receptors antagonists – AP-5 and DNQX, their possible interaction with electrical signalling was tested.

Cells were exposed to antagonists alone for 30 min. 0,1 mM AP-5 (n=8) and 0,1 mM DNQX (n=8) did not have a significant effect on RP, membrane resistance or excitation parameters. After measurements upon exposure to AP-5 or DNQX, 0,1 mM of NMDA together with an antagonist was applied on the same pre-treated cell for 30 min.

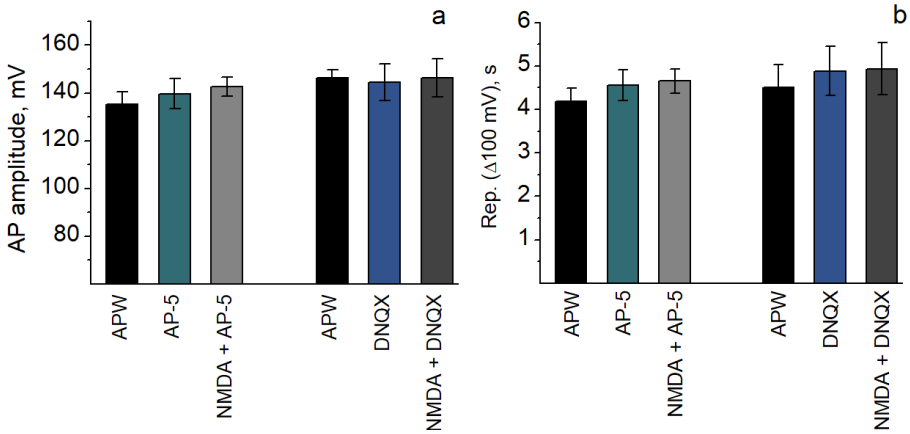

Fig 3.27 Average AP amplitude (a) and repolarization durations (b) in control solution (APW), 0,1 mM AP-5 or 0,1 mM DNQX pretreatment, then coexposure to 0,1 mM NMDA and the inhibitor, n=8. No significant differences were observed.

Average AP amplitude and repolarization duration values during the described experiment course are presented in **Fig 3.27**. In the AP-5 data set, the average E_{th} in control solution was -107±5 mV and corresponding AP amplitude 135±5 mV with repolarization duration of 4,2±0,2 s. After AP-5 treatment, E_{th} was -111±6 mV (p=0,4 comparing with values in APW), AP amplitude - 139±6 mV (p=0,3) with repolarization of 4,5±0,3 s (p=0,2). After exposure to NMDA together with AP-5, AP E_{th} remained at -111±5 mV (p=0,9 compared to values under AP-5) and amplitude was 142±4mV (p=0,6) with repolarization duration of 4,7±0,3 (p=0,6).

In DNQX data set under APW average E_{th} was -109±3 mV, AP amplitude was 146±3 mV, with average repolarization of 4,5± 0,5 s. After DNQX treatment E_{th} was -105±4 (p=0,3 in comparison to APW values). Corresponding AP amplitude was 144±8 mV (p=0,5) with repolarization of 4,8±0,6 s (p=0,4). NMDA+DNQX treatment resulted in E_{th} of -102±3 mV (p=0,6 compared to values under DNXQ), with AP amplitude of 146±8 mV (p=0,6) with repolarization lasting 4,9±0,6 (p=0,6).

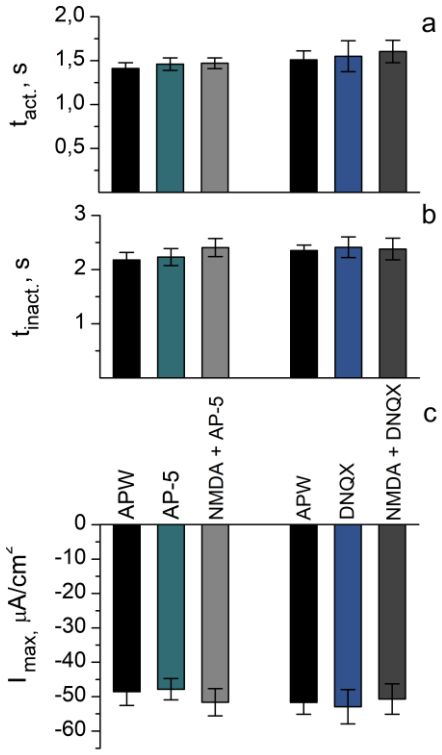

Fig 3.28 Average maximum Cl^- efflux values (c), activation $t_{act.}$ (a) and inactivation $t_{inact.}$ (b) durations at -90 mV MP in control solution (APW), 0,1 mM AP-5/DNQX pretreatment and sequent exposute to 0,1 mM NMDA together with AP-5 or DNQX, n=8 for each set. No significant differences were observed.

Voltage-clamp measurements also did not reveal significant changes in Cl^- efflux amplitude or activation/in-activation durations (**Fig 3.28**). Maximum chloride efflux in APW was -48±4 µA/cm^2, after AP-5 treatment -48±2 µA/cm^2 (p=0,8). Following NMDA+AP-5 exposure resulted in maximum efflux of - 52±4 µA/cm^2 (p=0,3). I_{max} in all cases occurred at around -100 mV of clamped MP.

In DNQX treatment set, average I_{max} in APW was -52±3 µA/cm^2, after DNQX - 55±7 µA/cm^2 (p=0,7), following NMDA+DNQX treatment resulted in I_{max} of -51±4 µA/cm^2 (p=0,2), also at around -100 mV. Cl^- efflux activation durations at -90 mV MP in control solution was 1,4±0,1 s,

after AP-5 treatment – 1,5±0,1 s (p=0,8) and after NMDA+AP-5 treatment 1,5±0,1 s (p=0,9). During same experiments' sets including DNQX, $t_{act.}$ was 1,5±0,1 s in APW, after DNQX – 1,5±0,1 s (p=0,8) and after NMDA+DNQX – 1,5±0,1 s (p=0,5) (**Fig 3.28**).

It was concluded that neither AP-5 nor DNQX by themselves interfere with electrical signalling parameters. Both AP-5 and DNQX suppress NMDA excitatory effect in a pre-treatment setup.

3.7.2 NMDA and Glu effect inhibition by AP-5 – co-treatment

Additional experiments were performed in a co-treatment manner. Cells were exposed to 0,1 mM NMDA together with 0,1 mM AP-5 (n=9). In control solution AP amplitude was 143±5 mV with repolarization lasting 4,5±0,3 s, after co-treatment AP amplitude was -149±4 mV (p=0,3 in comparison to APW), with 4,8±0,3 s repolarization (p=0,2). In this set up I_{max} in APW was -49±4 μA/cm^2 (at ~-100 mV), after NMDA/AP-5 co-treatment - 50±5 μA/cm^2 (p=0,9) (also at ~-100 mV),. $t_{act.}$ in APW was 1,5±0,1 s, after co-treatment – 1,5±0,1 s (p=0,4). $t_{inact.}$ initially lasted 2,3±0,1 s, after NMDA application together with AP-5 – 2,4±0,1 s (p=0,4). With no significant changes occurring among parameters, it was concluded that AP-5 prevents excitatory action of NMDA on *Nitellopsis obtusa* internodal cells when applied simultaneously.

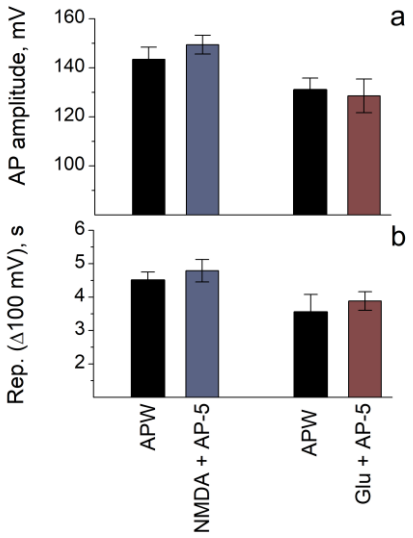

Fig 3.29 Average AP amplitude (a) and repolarization durations (b) in control solution (APW) and after 0,1 mM Glu and 0,1 mM NMDA co-treatment with 0,1 mM AP-5 (n=5, n=9 resp.). No significant differences were observed.

Since in animal ionotropic glutamate receptors AP-5 competitively prevents glutamate binding site of NMDA receptors, possible AP-5 inhibitory effect on Glu action reported above was tested in co-treatment experimental setup. Cells were co-treated with 0,1 mM Glu together with 0,1 mM AP-5 for 30 min (n=5). In APW AP amplitude was 131±5 mV, after treatment – 129±7 mV (p=0,6). AP repolarization in APW lasted 3,6±0,5 s, after co-treatment 3,9±0,3 s (p=0,3). I_{max} in control solution was -49±5 μA/cm^2 (at ~-100 mV), after co-treatment - 52±5 μA/cm^2 (p=0,4) also at -100

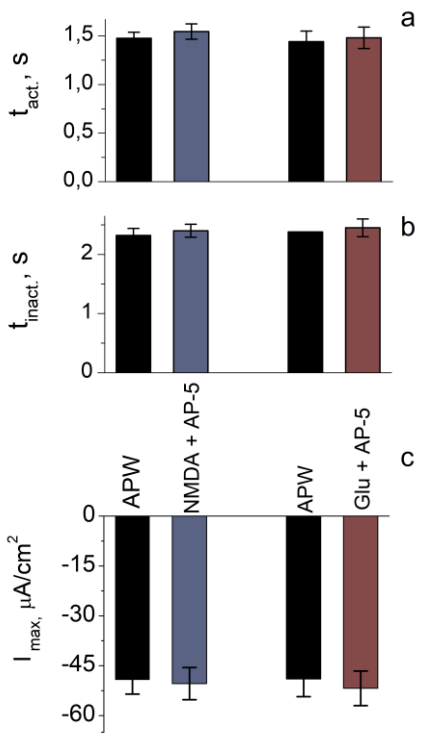

Fig 30 Average maximum Cl^- efflux values (c), activation $t_{act.}$ (a) and inactivation $t_{inact.}$ (b) durations at -90 mV MP in control solution (APW), after 0,1 mM Glu and 0,1 mM NMDA co-treatment with 0,1 mM AP-5 (n=5, n=9 resp.). No significant differences were observed.

mV. Cl^- efflux activation and inactivation durations at -90 mV were also unaltered ($t_{act.}$ 1,4±0,1 s in APW, after co-exposure - 1,5±0,1 s, p=0,6; $t_{inact.}$ 2,4±0,1 s in APW and 2,5±0,2 after co-treatment, p=0,7). With no significant changes of parameters upon Glu aplied together with AP-5 it was concluded that glutamate effect is prevented by AP-5. Co-treatment experiments results are summarized in **Fig 3.29** (CC) and **Fig 3.30** (VC).

Summarizing, AP-5 suppresses both NMDA and Glu modulatory effect.

3.8 Reversibility of putative GLR agonist effect

To investigate whether Asn, Glu and NMDA excitatory effects are reversible, cells after exposure to agonist were washed with control solution (APW). The general observation is that all electrophysiological parameters drifted towards initial values in APW during the time and usually stabilized in 1,5 h. Here the results of 1 h washing after 0,1 mM agonist treatment (n=5 for each agonist) are presented. Values in APW before the treatment with agonist, and values after APW perfusing were compared in each cell.

AP amplitude together with repolarization duration, was restored to initial values after exposure to all tested agonists. In Asn data set average AP amplitude in APW before exposure was 128±3 mV with repolarization of 3,1±0,2 s, after perfusing with APW, AP amplitude was 133±6 mV (p=0,3) with repolarization of 3,4±0,4 s (p=0,4).

In Glu data set initial AP amplitude was 120±4 mV with rep. of 3,3±0,2 s, after 0,1 Glu treatment and perfusing with APW - 125±4 mV (p=0,2) with rep. of 3,4±0,3 s (p=0,8).

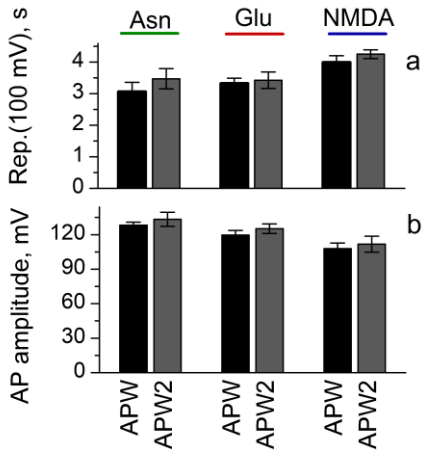

Fig 3.31 AP amplitude (b) and repolarization durations (a) in control solution before and after (APW/ APW2) exposure to 0,1 mM Glu, Asn, and NMDA, n=5 for each set. No significant differences were observed.

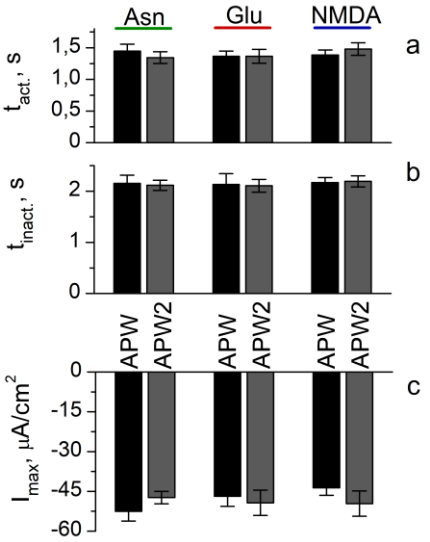

Fig 3.32 Average maximum Cl^- efflux values (c), activation $t_{act.}$ (a) and inactivation $t_{inact.}$ (b). durations at -90 mV MP in control solution before and after (APW/ APW2) exposure to 0,1 mM Glu, Asn, and NMDA, n=5 for each set. No significant differences were observed.

In NMDA data set initial amplitude in APW was 108±5 mV, rep. duration of 4±0,2 s. After perfusion, these parameters returned to initial values even after intense NMDA effect (AP amplitude after exposure 0,1 mM NMDA was 132±5 mV, rep. lasted 7,3±0,8 s). After perfusion AP amplitude declined to 112±7 mV (p=0,6) with 4,3±0,1 s rep. duration (p=0,4) (**Fig 3.31**)

Maximum chloride efflux parameters and excitation voltage also returned to initial values during perfusion with APW. Before exposure to 0,1 mM Asn, maximum efflux in APW was -53±4 µA/cm^2 (at ~-100 mV). $t_{act.}$ at -90 mV MP lasted 1,5±0,1 s, $t_{inact.}$- 2,2±0,2. After exposure and perfusion with APW I_{max} decreased to -48±2 µA/cm^2 (p=0,2) and was observed around -100 mV. $t_{act.}$ resulted in 1,3±0,1 s (p=0,4), $t_{inact.}$ – in 2,2±0,1 s (p=0,9).

In Glu data set initial average I_{max} value was -47±4 µA/cm^2 (at ~-90 mV), $t_{act.}$ lasted 1,4±0,1 s, $t_{inact.}$ - 2,1±0,2 s. After 0,1 mM Glu treatment and perfusion with APW I_{max} was -49±5 µA/cm^2 (p=0,6) (also at ~-90 mV), $t_{act.}$ - 1,4±0,1 s (p=0,9), $t_{inact.}$ - 2,2±0,1 s (p=0,7).

Before exposure to 0,1 mM NMDA I_{max} in control solution was -44±3 µA/cm^2 (at ~-90 mV), $t_{act.}$ lasted 1,4±0,1 s, $t_{iact.}$ – 2,2±0,1 s. After exposure and perfusion I_{max} attained -50±5 µA/cm^2 (p=0,2) (also at ~-90 mV), $t_{act.}$ 1,5±0,1 s (p=0,8) and $t_{inact.}$

returned to 2,2±0,1 s (p=0,4) (**Fig 3.32).**

It was concluded that alterations of electrophysiological parameters upon Asn, Glu, and NMDA are reversible. Parameters upon washing return to initial values after short-term (2,5 h) exposure to the agonist.

4. DISCUSSION

4.1 Excitation parameters in control solution

Since the alterations of temporal properties of Cl^- efflux upon excitation modifying compounds had been undocumented yet, it was set to characterize relationships between Cl^- current and its $t_{act.}$ and $t_{inact.}$ durations. The main observation is that $t_{act.}$ and $t_{inact.}$ do not correlate with the amplitude of the efflux, suggesting a separate mechanism of regulation, yet to be determined. As presumed $t_{act.}$ and $t_{inact.}$ correlate positively. Relation of AP amplitude (from E_{th} to peak) to other excitation parameters had not been described yet. To elucidate this aspect of excitation, correlations between all investigated parameters (n=93) were calculated concluding, that electrically elicited AP amplitude positively correlates with maximum Cl^- current, while other excitation parameters do not correlate in *Nitellopsis* cells in pump state. These observations are consistent with reported results: upon exposure to all tested excitatory compounds, both AP amplitude and maximum Cl^- efflux are altered with comparable K_M values (Table 3.2). Also both parameters were increased upon enhanced $[Cl^-]_o$ in control solution.

4.2 Increased Cl^- efflux upon heightened $[Cl^-]_o$

In the 3.1 section, it is described how additional 1 mM of HCl alters excitation parameters: increases AP amplitude and I_{max}, but not temporal dynamics of chloride efflux.

In early experiments regarding *Nitellopsis obtusa* electrical signalling, it was determined that increase (ten-fold) in extracellular chloride has little effect on the peak of the action potential, but occasionally produces prolongation of it (Findlay 1970). In presented study the prolongation of AP was not observed. However, it is contra-intuitive that heightened extracellular chloride concentration would increase Cl^- efflux since chloride electrochemical gradient is directed out of the cell. There are reports that increase in the medium $[Cl^-]_o$ is followed by an increase in $[Cl^-]_{cyt}$ by H^+/Cl^- symporter as described in *Sinapis alba* root hair cells by ion-selective electrodes (Felle 1994). $2H^+/Cl^-$ symporter active upon chloride starvation is described in Characeaen (Beilby and Walker 1981) and preliminary mathematical modelling of the salt-tolerant charophyte *Lamprothamnium* response to salinity stress (Beilby and Shepherd 2001) demonstrated, that an increase in $[Cl^-]_{cyt}$ would increase the Cl^- efflux through Ca^{2+}-activated Cl^- channels. This mechanism was attributed to the observed hypersensitivity of *Chara corallina* to mechanical stimulation upon salinity stress (Shepherd *et*

al. 2008). However, *Nitellopsis obtusa* research indicates that upon salinity stress (1 h of 100 mM NaCl) cytoplasmic and vacuolar [Cl^-] do not change (Katsuhara and Tazawa 1986). The estimated chloride cytoplasmic concentration (according to reversal potential of Cl^- efflux) in our experiments also remained unchanged upon 1 mM HCl (Section 3.1). There are reports that outward rectifying anion channel activity in plants may have an inverse dependence on extracellular Cl^- concentration - as described by patch-clamp studies of GCACl (voltage-dependent anion channel) in *Vicia faba* guard cells, where peak amplitude of anion currents increased as the extracellular chloride concentration was raised from 0 up to 300 mM (Hedrich 1994). Thus, a similar mechanism could regulate chloride channels responsible for AP depolarization. Altogether, the mechanism of Cl^- efflux increase upon heightened $[Cl^-]_o$ is unclear. Range of Cl^- in natural habitats of *Nitellopsis* is variable. *Nitellopsis* maintains permanent populations in brackish water with salinity up to ~50 mM NaCl and Cl^- concentration even in oligohaline lakes can reach ~15 mM (Winter *et al.* 1999). Thus adaptational mechanisms including electrical signalling are expected and appropriate control conditions for investigation of AA salts are advisable.

4.3 Alterations of excitation upon AA and NMDA

In our study application of Glu, Asn and NMDA did not elicit prominent depolarization of resting potential (except 1 mM Glu), spontaneous activity or alterations of membrane resistance. MP depolarization upon AA was reported in various GLR related studies (Weiland *et al.* 2016), also some degree of depolarization of MP could be attributed to a separate mechanism – AA uptake via proton symport (Ortiz-Lopez *et al.* 2000). *Nitellopsis obtusa* cells' RP reaches up to -255 mV and is composed of two components - passive diffusion potential and active potential generated by an electrogenic proton pump maintaining highly negative RP (Tsutsui *et al.* 1987). Since all assessed cells' RP was lower than -180 mV, putative depolarizing AA effect could be concealed by pump activity. Depolarizing effect of AA on Characeaen cells could be prominent in more depolarized potassium-state (Beilby, 2007). It is not dismissible that alterations of patterns of electrical signalling could differ among cell states.

Spontaneous activity in our case occurred in a few cells, but with no consistency, thus it is not considered a characteristic response of *Nitellopsis* to AA or NMDA in the pump state, where RP is hyperpolarized and far from the excitation threshold. Spontaneous APs are a possible feature of *Nitellopsis* response to electrical signalling modifying compounds, e.g. exposure of the

same cell surface to 5 mM of acetylcholine led to depolarization of MP and spontaneous generation of APs (Kisnieriene *et al.* 2012). In plants Glu-elicited spontaneous APs were recorded in barley - leaf immersion in 1 mM of Glu was sufficient for APs generation (Felle and Zimmermann 2007). In *Conocephalum conicum* exogenously applied 5 mM Glu/Gly elicited APs (Krol *et al.* 2007). In sunflower injection of 5 mM Glu into the stem also elicited propagating APs (Stolarz and Dziubinska 2017). Lack of spontaneous APs upon Glu, Asn and NMDA in *Nitellopisis* could be due to relatively small exposure surface (<5% of cell surface), insufficient concentration, or depend on cell state - proton pump activity could compensate possible depolarizing currents (e.g. Ca^{2+}) needed to reach E_{th}.

Effect of exposure to Glu, Asn and NMDA was prominent once APs were elicited. In the presented study, it was demonstrated that 0,1- 1 mM of AA and 0,01-1 mM of NMDA alter electrically-induced AP parameters in *Nitellopsis obtusa* internodal cell: hyperpolarize AP E_{th}, increase AP amplitude, repolarization duration as well as Cl^- efflux together with its activation ($t_{act.}$) and inactivation ($t_{inact.}$) durations in a dose-dependent manner. Effect pattern upon exposure to glutamatergic compounds (AP amplitude increase together with prolonged repolarization) described here is comparable to one reported by Krol *et al.* (2007) where Glu/Gly-triggered APs and voltage transients had significantly increased half-time duration (up to 3-fold), while the presence of Glu/Gly heightened amplitude of APs elicited by other stimuli (~1,5 fold). In our experiments, 1 mM of Glu prolonged repolarization by 2 s (44%), 1 mM of NMDA by 3 s (66%). AP amplitude was increased by 16% upon 1 mM of Glu, and 26% upon 1 mM of NMDA. Detailed investigation revealed that the leading cause of AP amplitude increase in *Nitellopsis* is attributed to hyperpolarization of E_{th}.

Hyperpolarization of E_{th}

AP excitation threshold (E_{th}) is one of the primary physiological parameters that determines cell electrical excitability - ability to react to stimuli (Stolarz *et al.* 2010). Thus a precise evaluation of cell E_{th} is crucial since it is a critical point of intact cell electrical excitation in natural conditions. Only when the membrane potential is depolarized sufficiently to exceed the threshold potential, an action potential is generated and consequently physiological reaction is initiated. E_{th} is variable between individual cells and depends on cytoplasmic calcium content, calcium permeable transport systems' activation (Beilby, 2007) and chloride channels voltage dependency (Thiel *et al.* 1997). The regulation of transient $[Ca^{2+}]_{cyt}$ increase during AP is very precise and

occurs according to the all-or-none mechanism (Wacke *et al.* 2003). The changes in Ca^{2+} homeostasis are reflected in AP generation (Beilby and Al Khazaaly 2016) which is not entirely based on the time- and voltage-dependent activation properties of plasma membrane ion channels but on a complex signal transduction cascade. These interlinks still need to be elucidated. Cl^- efflux during excitation is directly related to $[Ca^{2+}]_{cyt}$: it was demonstrated that the amplitude of depolarizing Cl^- current is proportional to the square of the cytoplasmic Ca^{2+} concentration in Characeaen (Berestovsky and Kataev 2005). It could be suggested that recorded increase of AP amplitude by hyperpolarization of AP E_{th} after Glu, Asn and NMDA treatment (**Fig 3.17**, **Fig 3.23**) in *Nitellopsis* could be assigned to activation of Ca^{2+} permeable channels leading to elevated $[Ca^{2+}]_{cyt}$/transmembrane calcium gradient as suggested in *Dionaea muscipula* (Krol *et al.* 2006). Approach of this study does not regard this question directly, still, increased $[Ca^{2+}]_{cyt}$ would lead to increase of Cl^- efflux, resulting in higher AP amplitude and relatively stable peak values as reported in results (**Fig 3.8**, **Fig 3.13**, **Fig 3.19**). Possibility of increased $[Ca^{2+}]_{cyt}$ is also supported by unchanged reversal potentials of Cl^- efflux. Contrary to Krol (2007) where the amplitude of the action potentials was not related to amino acid concentration in *Conocephalum*, cell response of *Nitellopsis* to Glu, Asn and NMDA shows clear dose-dependency. This could rise from lower concentrations of Asn (0,1 mM vs. 5 mM used on *Conocephalum*) reflecting non saturating response. Common AP amplitude evaluation from resting potential to peak value could lead to different results because the nature of varying resting potential in plants depends on transport systems different from those active during excitation. When AP amplitude is measured from the E_{th}, variable RP component is eliminated.

Another possible explanation of the observed results would be a Glu/Asn/NMDA modulation of the second messenger activity. In Characeaen, the short transient inflow of calcium during excitation could depend on two pathways: from outside, through TRP-like channels, and simultaneously via second messenger (IP_3, inositol 1,4,5-trisphosphate or IP_6) activated channels from the internal stores. Higher plants lack IP_3 receptors, yet mathematical modelling strongly supports the existence of second messengers that could also imply the all-or-none nature of AP (Wacke *et al.* 2003, Munnik and Vermeer 2010, Beilby and Al Khazaaly 2016, Kisnieriene *et al.* 2019). If AA could indeed increase second messenger levels in plants, upon excitation it would enhance calcium flux to the cytoplasm from internal stores, leading to an observed increase in AP amplitude, decreased E_{th} and prolonged

repolarization besides possible involvement of plasmalemma ion transport systems.

Prolongation of AP repolarization

Besides the effect on E_{th}, Glu, Asn and NMDA prolongs AP repolarization phase (**Fig 3.8**, **Fig 3.13š**, **Fig 3.19**). Similar effect of AA on AP duration was observed in *Conocephalum conicum* AP: Glu and Gly substantially prolonged repolarization of AP and voltage transients (Krol *et al.* 2007). In addition, ACh (acetylcholine) in *Nitellopsis obtusa* cells induced significant prolongation of AP (Kisnierienė *et al.* 2009). Although prolonged repolarization recorded in our study is no more than 66%, it is dose-dependent. Mechanism by which AP repolarization is lagged can be attributed to several ion transporters.

First, AP prolongation could be caused by decelerated sequestration of Ca^{2+} from cytoplasm during AP as suggested by (Krol *et al.* 2007). Impaired removal of calcium from cytoplasm could explain both prolonged AP and Cl^- efflux duration in voltage-clamp measurements: it is postulated that Cl^- channels inactivate as $[Ca^{2+}]_{cyt}$ decreases (Berestovsky and Kataev 2005). Decrease in Cl^- conductance is a crucial factor in the repolarization phase of the AP (Beilby 2007). Prolonged Cl^- efflux duration and increased maximum current indicated in this study by voltage-clamp experiments could be a result of altered calcium sequestration and explain longer repolarization in free running MP measurements. Prolongation of *Chara australis* APs under salinity stress is also reported to be determined by prolonged opening of the Ca^{2+}-activated Cl^- channels (Shepherd *et al.* 2008). Recent mathematical modelling (Thiel-Beilby model) of APs of salinity-stressed Characeaen *Nitellopsis obtusa* and *Chara australis* cells revealed that *Nitellopsis'* intrinsically slower AP repolarization should be contributed to differences in the Ca^{2+} pump activity which sequestrates Ca^{2+} into internal stores during AP repolarization (Kisnieriene *et al.* 2019).

Since the target of the AA effect is unclear, it is possible that prolongation of AP repolarization could be contributed to K^+_{out} channels' modulation. K^+_{out} channels are the main transport system conditioning process of repolarization in Characeaen (Thiel *et al.* 1997). As in Ca^{2+}-activated Cl^- channels' dynamics, K_{out}^+ channels' activation/inactivation is demonstrated to be dependent on $[Ca^{2+}]_{cyt}$ (Katsuhara and Tazawa 1992, Homann and Thiel 1994, Thiel *et al.* 1997).

Another possibility is allosteric K^+_{out} modulation by an unknown mechanism. It has been revealed that in *Arabidopsis* AP shape is highly modulated by GORK (outward-rectifying potassium-selective ion channels).

Decreased GORK channel activity (knock-out mutant) not only prolongs the duration of an AP but also increases AP amplitude by altering its peak (Cuin *et al.* 2018). Thus calcium-independent regulation of K^+ channels is a viable prospect.

Increase and prolongation of Cl^- efflux

Increase of Cl^- efflux amplitude together with activation and inactivation durations by Glu, Asn and NMDA coincides with possible elevation of cytoplasmic Ca^{2+} or sequestration lagging concept since Cl^- efflux directly depends on cytoplasmic Ca^{2+} concentration (Berestovsky and Kataev 2005).

However, Cl^- efflux regulation via second messenger cascade is possible. Experiments with *Chara corallina* cells have shown that inhibitor neomycin (phosphoinositide-specific phospholipase C inhibitor, interferes with IP_3 production) caused a delay and a suppression of the electrically stimulated elevation of the Cl^- conductance, i.e., the conductance that causes the depolarization in an AP (Biskup *et al.* 1999). Yet IP_3 involvement in plant excitation is debatable (Tazawa and Kikuyama 2003). The mathematical model applied to Biskup results revealed that delay of Cl^- peak current together with decreased amplitude is due to the decrease of the rate constant of IP_3-induced Ca^{2+} release from internal stores. This could explain the prolongation of $t_{act.}$ reported in our study, given that upon AA and NMDA most prominent effect occurs near excitation threshold (-90 mV, **Fig 3.10**, **Fig 3.15**, **Fig 3.18**). Yet this approach does not account a simultaneous prolongation and increase of Cl^- current. Since I_{max} is increased upon AA and NMDA, one should expect increased probability of Cl^- channels opening or increased permeability by allosteric regulation. Alteration of $[Cl^-]_o$ is not the case since reversal potentials remain stable upon AA and NMDA.

A separate mechanism of the prolongation of activation duration is plausible – a temporally dispersed activation of Cl^- channels populations by delayed quantum releases of calcium from internal stores as one could speculate from Thiel and co-workers observations (Biskup *et al.* 1999). To date neither experimental data nor mathematical modelling suggest causation for both increased and prolonged Cl^- efflux.

Dose-dependency

AA and NMDA act dose-dependently and in a similar manner, with 0,1 mM NMDA effect significantly surpassing that of Glu and Asn in all tested parameters. Also determined K_M of Glu are at least twice as high as those of NMDA. Employment of Michaelis–Menten kinetics described here is rather

orentational due to few data points, yet the described dose-dependency of Glu in *Nitellopsis* is comparable to dependency of Glu-induced cation currents in the plasma membrane of *Arabidopsis* root cells, where half-maximal activation was seen at 0,2–0,5 mM glutamate (Demidchik *et al.* 2004). It is possible that Glu, Asn and NMDA act on the same ion transport systems involved in excitability – plausibly GLR channels. However, despite the direct evolutionary relation between Charophytes and land plants (Lewis and McCourt 2004), homologs of GLRs were not identified in *Chara braunii*, the only Characean family representative with a sequenced genome (Nishiyama *et al.* 2018). This by itself is surprising, since homolog genes of iGluRs were found in both brown and green algae (De Bortoli *et al.* 2016), liverworts and mosses (Qrtiz-Ramírez *et al*. 2017, Wudick *et al.* 2018). Based on their sequence homology and the analyzed sequence region, plant GLRs were shown to be similar to both NMDA and non-NMDA iGluRs, suggesting a divergence of iGluRs/GLRs prior to their clade differentiation (Weiland *et al.* 2016).

Thus it was concluded that NMDA is an active compound in *Niteloppsis*. For a few decades (e.g. Dennison and Spalding 2000) NMDA has been regarded as non-active agonist of plant GLRs since it did not have any significant effect on L-Glutamate-induced cytoplasmic calcium increase in *Arabidopsis*. Thus, NMDA has been excluded from further investigations. However, this compound was reported to be electrogenically-active in liverwort *Conocephalum* (Krol *et al.* 2007). In *Nitellopsis*, NMDA was also revealed as a modulator of electrical signalling. Curiously, Characeaen algae differ from land plants by both lacking any characterized homologues of iGluRs and exhibiting NMDA-induced alterations of electrical signalling, which indicates yet unknown molecular targets of glutamatergic compounds. Since NMDA applied together with Glu did not cause a higher effect than that elicited by above-K_M NMDA concentration (0,1 mM), it is plausible that these compounds act on the same binding site.

4.4 Inhibition of NMDA effect by iGluRs antagonists

Since treatment with 0,1 mM DNQX or 0,1 mM AP-5 did not have any distinguishable effect on membrane potential or AP parameters, it seems that these compounds do not interfere with the main ion transport systems involved in electrical signalling. No effect of AP-5/DNQX was recorded in *Arabidopsis* root hair Glu-induced (200 μM) growth inhibition (Walch-Liu *et al.* 2006). AP-5 and DNQX at 1 mM applied alone did not elicit any effect on embryo

axis elongation in *Medicago truncatula* compared to control conditions (Philippe *et al.* 2019).

Glutamate effect inhibition by AP-5 is common in *Arabidopsis* (Sivaguru *et al.* 2003, Walch-Liu *et al.* 2006, Vatsa *et al.* 2011), and was demonstrated in *Conocephalum* where AP-5 also inhibited NMDA (Krol *et al.* 2007). NMDA inhibition in higher plants is uncharted since its action was reported only indirectly on microtubules' organization (Sivaguru *et al.* 2003) and NMDA is generally assumed to be inactive in *Arabidopsis* (reviewed in Weiland *et al.* 2015). It was demonstrated that in *Nitellopsis* – in contrary to both *Arabidopsis* and *Conocephalum* – NMDA effect was suppressed by Kainate-type iGluRs antagonist – DNQX. DNQX inhibitory effect on Glu was not tested in this study since it was repeatedly described among Glu induced alterations of electrical signalling (Section 2.3.3), e.g. pre-treatment with DNQX inhibits Glu induced APs in *Conocephalum* (Krol *et al.* 2007) and prevents Glu (and Gly) caused Ca^{2+} fluxes in *Arabidopsis* (Dubos *et al.* 2003).

4.5 General speculations

The reversibility of alterations upon exposure to AA and NMDA are in accordance with the effect being imposed through a receptor. Since the excitatory effect is observed throughout the extended period, desensitization is not probable as described in *At*GLR. In hypocotyl cells of *Arabidopsis* exposure to Glu desensitized a cell to a second application, even though the ligand had been removed by a 2-min washout period (Stephens *et al.* 2008). In our study, the effect was sustained upon exposure to agonist, reversibility of the effect also indicates no lasting changes of electrical signalling after removal of AA and NMDA.

While NMDA is a synthetic compound, amino acids (AA) are rather common in both soil (Young and Ajami 2000) and aquatic sediments (Yao *et al.* 2012, Feng *et al.* 2019). Effect of exposure to these compounds in Characeaen cells include modulation of electrical signal shape. Modulation of electrical signalling patterns upon environmental or internal stimuli may be a relevant feature of plant cells as plants do not possess differentiated cells for electrical signalling (Fromm and Lautner 2007). Information within the transmitted AP may be encoded by the shape of a single AP determined by the relative contribution of the ionic conductances or by the frequency of AP generation (Fromm and Lautner 2007). Increased calcium concentration could be a cellular signal itself, but combined with additionally exhibited electrical signals (caused by other environmental factors) it could have completely different physiological significance, as it was demonstrated in stimulus-

dependant frequeancies of spontaneous APs of *Helianthus* (Stolarz and Dziubinska 2017). Calcium signatures are highly variable signals in amplitude, frequency, and localization; their spatiotemporal characteristics may serve as a selective trigger for a plethora of cell responses (McAinsh and Pittman 2009, Medvedev 2018). Similarly, APs with varying amplitude, duration and firing frequency may bear information by their spatiotemporal properties.

Amino acids' regulatory function on various physiological processes in different plants and tissues (root branching, response to light, membrane depolarization) (Sivaguru *et al.* 2003, Vincill *et al.* 2013, Forde and Roberts 2014, Weiland *et al.* 2016, Yoshida *et al.* 2016) stress the signalling role of AA. Yet, none of these systemic responses can be directly assigned to a single plant cell serving as the main structural element of Characeaen. According to our data AA and NMDA affect electrical signalling in stimulus strength related manner. Given that land plants are evolutionarily closely related to Characean algae, exploring the basics of electrical events in a single plant cell may give valuable insights into complexity of the whole cell responses in *Plantae*.

4.6 Limitations of the approach and future prospects

The presented set of results reflects responses of cells found in hyperpolarized (pump) state. To expand effect pattern of the AA and NMDA, it should be described in all physiological cell states of Characeaen.

Mechanism by which AP threshold is hyperpolarized and chloride efflux increased cannot be resolved directly by presented electrophysiological approach, although it clearly demonstrates that properties of ion channels involved in AP generation are altered by AA and NMDA. Cytoplasmic calcium imaging recording coupled with excitation recordings would expand the interpretation of the data.

Besides that, described results represent excitations of both plasma membrane and tonoplast. This overlapping registration could conceal some vital effects or specific alterations of tonoplast excitation. Thus, separate examination of electrophysiological parameters of plasma membrane and tonoplast excitation would be preferable. This could be obtained by using two pairs of electrodes and impaling one electrode tip to the cytoplasm and the other to the vacuole. It is demonstrated that this approach is viable in *Nitellopsis* (Kikuyama 1986, Kisnieriene *et al*. 2019)

In this study only a short-term exposure effect was investigated. Future electrophysiological experiments should aim to determine both short- and

long-term responses to AA and NMDA. Real-time voltage-clamp recordings upon exposure to AA would be preferable. Another vital angle - AP transduction between cells in Characeaen. Hyperpolarization of E_{th} could likely have a prominent effect on the transmission of AP in long distances. Also, the question of both AA and NMDA targets remain unanswered. The effect pattern, dose-dependency and inhibition of NMDA suggest the existence of GLR-like receptors. Presented results point the importance of multi-scale quantitative characterization of electrical signalling, which by itself demands standardization of electrophysiological parameters.

CONCLUSIONS

1. Exposure to glutamate, asparagine and NMDA alters *Nitellopsis obtusa* cell electrical signalling and excitability in similar pattern: hyperpolarizes the action potential excitation threshold, prolongs action potential repolarization, increases maximum Cl^- efflux amplitude and prolongs both current activation and inactivation durations.

2. Effect of glutamate, asparagine and NMDA is dose-dependant and reversible; NMDA effect surpasses that of amino acids.

3. The effect of NMDA is prevented by pre-treatment and co-treatment with both NMDA and non-NMDA type ionotropic glutamate receptors – AP-5 and DNQX – neither of whom *per se* interfere with the electrical signalling of *Nitellopsis obtusa*.

REFERENCES

Acher FC, Bertrand HO (2005) Amino acid recognition by *Venus flytrap* domains is encoded in an 8-residue motif. *Biopolymers* 80, 357–66.

Amino S, Tazawa M (1989) Dependence of Tonoplast Transport of Amino Acids on Vacuolar pH in *Chara* Cells. *Proc Jpn Acad Ser B Phys Biol Sci* 65, 34–37.

Armstrong N, Sun Y, Chen GQ, Gouaux E (1998) Structural of a glutamate-receptor ligand-binding core in complex with kainate. *Nature* 395, 913–917.

Azimov RR, Geletyuk VI, Berestovskii GN (1987) Single potential dependent K^+ channel of the cells of the alga *Nitellopsis obtusa*. *Biophysics* 32, 82-88.

Baluska F, Mancuso S (2013) Root apex transition zone as oscillatory zone. *Front Plant Sci* 4, 354.

Barbosa JM, Singh NK, Cherry JH, Locy RD (2010) Nitrate uptake and utilization is modulated by exogenous gamma-aminobutyric acid in *Arabidopsis thaliana* seedlings. *Plant Physiol Biochem* 48, 443–450.

Beilby MJ (1986) Potassium channels and different states of Chara plasmalemma. *J Membr Biol* 89, 241–249.

Beilby MJ (2007) Action potential in charophytes. *Int Rev Cytol* 257, 43–82.

Beilby MJ, Al Khazaaly S (2016) Re-modeling *Chara* action potential: I. from Thiel model of Ca^{2+} transient to action potential form. *AIMS Biophys* 3, 431–449.

Beilby MJ, Al Khazaaly S (2017). Re-modeling *Chara* action potential: II. The action potential form under salinity stress. *AIMS Biophys* 4, 298-315.

Beilby MJ, Casanova MT (2014) *The Physiology of Characean Cells*.

Beilby MJ, Coster HGJ (1976a) The Action Potential in *Chara corallina*: Effect of Temperature. *Funct Plant Biol* 3, 275–289.

Beilby MJ, Coster HGL (1976b). Effect of Temperature on Punchthrough in Electrical Characteristics of the Plasmalemma of *Chara corallina*. *Funct Plant Biol* 3, 819-826.

Beilby MJ, Shepherd VA (2001) Modeling the current–voltage characteristics of charophyte membranes: II. the effect of salinity on membranes of *Lamprothamnium papulosum*. *J Membr Biol* 181, 77–89.

Beilby MJ, Walker NA (1981) Chloride transport in *Chara*. I Kinetics and current–voltage curves for a probable proton symport. *J Exp Bot* 32, 43–54.

Berecki G, Eijken M, Van Iren F, Van Duijn B (2001) Tonoplast anion channel activity modulation by pH in *Chara corallina*. *J Membr Biol* 184, 131–141.

Berestovskii GN, Zherelova OM, Kataev AA (1987) Ionic channels in Characean algal cells. *Biophysics* 32, 1101–1120.

Berestovsky GN, Kataev AA (2005) Voltage-gated calcium and Ca^{2+}-activated chloride channels and Ca^{2+} transients: voltage-clamp studies of perfused and intact cells of *Chara*. *Eur Biophys J* 34, 973–986.

Biskup B, Gradmann D, Thiel G (1999) Calcium release from InsP3-sensitive internal stores initiates action potential in *Chara*. *FEBS Lett* 453, 72–76.

Bisson MA, Walker NA (1981). The hyperpolarization of the *Chara* membrane at high pH: Effects of external potassium, internal pH, and DCCD. *J Exp Bot* 32, 951-971.

Blinks LR, Harris ES, Osterhout WJV (1929). Studies on Stimulation in *Nitella*. *Proc Soc Exp Biol Med* 26, 836–838.

Brosnan JT, Brosnan ME (2013) Glutamate: A truly functional amino acid. *Amino Acids* 45, 413–418.

Bulychev AA, Kamzolkina NA, Luengviriya J, Rubin AB, Müller SC (2004) Effect of a single excitation stimulus on photosynthetic activity and light-dependent pH banding in *Chara* cells. *J Memb Biol* 202, 11–19.

Bulychev AA, Krupenina NA (2010) Inactivation of plasmalemma conductance in alkaline zones of *Chara corallina* after generation of action potential. *Biochem (Mosc) Suppl Ser A Membr Cell Biol* 4, 232–239.

Cheng Y, Tian Q, Zhang W-H (2016) Glutamate receptors are involved in mitigating effects of amino acids on seed germination of Arabidopsis thaliana under salt stress. *Environ Exp Bot* 130, 68–78.

Cheng Y, Zhang X, Sun T, Tian Q, Zhang WH (2018) Glutamate Receptor Homolog3.4 is Involved in Regulation of Seed Germination under Salt Stress in Arabidopsis. *Plant Cell Physiol* 59, 978–988.

Chiu J, DeSalle R, Lam HM, Meisel L, Coruzzi G (1999) Molecular evolution of glutamate receptors: A primitive signaling mechanism that existed before plants and animals diverged. *Mol Biol Evol* 16, 826–838.

Chiu JC, Brenner ED, DeSalle R, Nitabach MN, Holmes TC, Coruzzi GM (2002) Phylogenetic and expression analysis of the glutamate-receptor-like gene family in *Arabidopsis thaliana*. *Mol Biol Evol* 19, 1066–1082.

Cho D, Kim SA, Murata Y, Lee S, Jae SK, Nam HG, Kwak JM (2009) De-regulated expression of the plant glutamate receptor homolog *At*GLR3.1 impairs long-term Ca^{2+}-programmed stomatal closure. *Plant J* 58, 437–449.

Choi W, Miller G, Wallace I, Harper J, Mittler R, Gilroy S (2017) Orchestrating rapid long-distance signaling in plants with Ca^{2+}, ROS and electrical signals. *Plant J* 90, 698–707.

Croset V, Rytz R, Cummins SF, Budd A, Brawand D, Kaessmann H, Gibson TJ, Benton R (2010) Ancient protostome origin of chemosensory ionotropic glutamate receptors and the evolution of insect taste and olfaction. *PLoS Genetics* 6.

Cuin TA, Dreyer I, Michard E (2018) The role of potassium channels in *Arabidopsis thaliana* long distance electrical signalling: AKT2 modulates tissue excitability while GORK shapes action potentials. *Int J Mol Sci* 19, 1–17.

Davenport R (2002) Glutamate Receptors in Plants. *Ann Bot* 90, 549–557.

De Bortoli S, Teardo E, Szabò I, Morosinotto T, Alboresi A (2016) Evolutionary insight into the ionotropic glutamate receptor superfamily of photosynthetic organisms. *Biophysical Chemistry* 218, 14–26.

Demidchik V (2018) ROS-activated ion channels in plants: Biophysical characteristics, physiological functions and molecular nature. *Int J Mol Sci* 19, 17–21.

Demidchik V, Essah PA, Tester M (2004) Glutamate activates cation currents in the plasma membrane of *Arabidopsis* root cells. *Planta* 219, 167–75.

Demidchik V, Maathuis FJM (2007) Physiological roles of nonselective cation channels in plants: From salt stress to signalling and development. *New Phytol* 175, 387–404.

Demidchik V, Shabala S, Isayenkov S, Cuin TA, Pottosin I (2018) Calcium transport across plant membranes: mechanisms and functions. *New Phytol* 220, 49–69.

Dennison KL, Spalding EP (2000) Glutamate-Gated Calcium Fluxes in Arabidopsis. *Plant Physiol* 124, 1511–1514.

Dubos C, Huggins D, Grant GH, Knight MR, Campbell MM (2003) A role for glycine in the gating of plant NMDA-like receptors. *Plant J* 35, 800–810.

Dziubińska H (2003) Ways of signal transmission and physiological role of electrical potentials in plants. *Acta Soc Bot Pol* 72, 309–318.

Dziubinska H, Trebacz K, Zawadzki T (1989) The effect of excitation on the rate of respiration in the liverwort *Conocephalum conicum*. *Physiol Plant* 75, 417–423.

Favre P, Agosti DR (2007) Voltage-dependent action potentials in *Arabidopsis thaliana*. *Physiol Plant* 131, 263-272.

Favre P, Krol E, Stolarz M, Szarek I, Greppini H, Trebacz K, Agostii RD (1999) Action potentials elicited in the liverwort *Conocephalum conicum* (*Hepaticae*) with different stimuli. *Archives Des Sciences Journal* 52, 175–185.

Felle HH (1994) The H^+/Cl^- symporter in root-hair cells of *Sinapis alba*. An electrophysiological study using ion-selective microelectrodes. *Plant Physiol* 106, 1131–1136.

Felle HH, Zimmermann MR (2007) Systemic signalling in barley through action potentials. *Planta* 226, 203–214.

Feng W, Liu S, Li C, Li X, Song F, Wang B, Chen H, Wu F (2019) Algal uptake of hydrophilic and hydrophobic dissolved organic nitrogen in the eutrophic lakes. *Chemosphere* 214, 295–302.

Findlay GP (1970) Membrane electrical behaviour in *Nitellopsis obtusa*. *Aust J Biol Sci* 23, 1033–1046.

Findlay GP, Hope AB (1964). Ionic Relations of Cells of *Chara australis* VII. The Separate Electrical Characteristics of the Plasmalemma and Tonoplast. *Aust J Biol Sci* 17, 62-77.

Fisahn J, Herde O, Willmitzer L, Peña-Cortés H (2004) Analysis of the transient increase in cytosolic Ca^{2+} during the action potential of higher plants with high temporal resolution: Requirement of Ca^{2+} transients for induction of jasmonic acid biosynthesis and PINII gene expression. *Plant Cell Physiol* 45, 456–459.

Fischer WN, André B, Rentsch D, Krolkiewicz S, Tegeder M, Breitkreuz K, Frommer WB (1998) Amino acid transport in plants. *Trends Plant Sci* 3, 188–195.

Forde BG, Lea PJ (2007) Glutamate in plants: Metabolism, regulation, and signalling. *J Exp Bot* 58, 2339–2358.

Forde BG, Roberts MR (2014) Glutamate receptor-like channels in plants: a role as amino acid sensors in plant defence? *F1000prime reports* 6, 37–43.

Fritz C, Mueller C, Matt P, Feil R, Stitt M (2006) Impact of the C-N status on the amino acid profile in tobacco source leaves. *Plant Cell Environ* 29, 2055–2076.

Fromm J, Bauer T (1994). Action potentials in maize sieve tubes change phloem translocation. *J Exp Bot* 45, 463–469.

Fromm J, Lautner S (2007) Electrical signals and their physiological significance in plants. *Plant Cell Environ* 30, 249–257.

Gabriel M, Telmer PG, Marsolais F (2012) Role of asparaginase variable loop at the carboxyl terminal of the alpha subunit in the de- termination of substrate preference in plants. *Planta* 235, 1013–1022.

Gaufichon L, Rothstein SJ, Suzuki A (2016) Asparagine metabolic pathways in *Arabidopsis*. *Plant Cell Physiol* 57, 675–689.

Geisler G (1985) Investigation into the effect of nitrogen on the morphology, dry matter formation and uptake efficiency of the root systems of maize, spring barley and field bean varieties, taking temperature into consideration. *J Agro and Crop Sci* 154, 25–37.

Gilroy S, Read ND, Trewavas AJ (1990) Elevation of cytoplasmic calcium by caged calcium or caged inositol trisphosphate initiates stomatal closure. *Nature* 346, 769–771.

Gong XQ, Bisson MA (2002) Acetylcholine-activated Cl^- Channel in the *Chara* Tonoplast. *J Membr Biol* 188, 107–113.

Gutiérrez RA, Stokes TL, Thum K, Xu X, Obertello M, Katari MS, Tanurdzic M, Dean A, Nero DC, McClung CR, Coruzzi GM (2008) Systems approach identifies an organic nitrogen-responsive gene network that is regulated by the master clock control gene CCA1. *Proc Natl Acad Sci USA* 105, 4939–4944.

Haroun SA, Shukry WM, El-Sawy O (2010) Effect of asparagine or glutamine on growth and metabolic changes in *Phaseolus vulgaris* under in vitro conditions. *Bioscience Research* 7, 1–21.

Hayama T, Tazawa M (1980) Ca^{2+} reversibly inhibits active rotation of chloroplasts in isolated cytoplasmic droplets of *Chara*. *Protoplasma* 102, 1-9.

Hedrich R (1994) Voltage-Dependent Chloride Channels in Plant Cells: Identification, Characterization, and Regulation of a Guard Cell Anion Channel. *Current Topics in Membranes* 42, 1–33.

Hedrich R, Salvador-Recatalà V, Dreyer I (2016) Electrical wiring and long-distance plant communication. *Trends Plant Sci* 21, 376–387.

Hetherington AM, Brownlee C (2004) The generation of Ca^{2+} signals in plants. *Annu Rev Plant Biol* 55, 401–427.

Hirai H, Kirsch J, Laube B, Betz H, Kuhse J (1996) The glycine binding site of the N-methyl-D-aspartate receptor subunit NR1: Identification of novel

determinants of co-agonist potentiation in the extracellular M3-M4 loop region (glutamate receptor/bacterial amino acid-binding protein/transmembrane topolo. *Proc Natl Acad Sci USA* 93, 6031–6036.

Hirner A, Ladwig F, Stransky H, Okumoto S, Keinath M, Harms A, Frommer WB, Koch W (2006) *Arabidopsis* LHT1 is a high-affinity transporter for cellular amino acid uptake in both root epidermis and leaf mesophyll. *Plant Cell* 18, 1931–1946.

Homann U, Thiel G (1994) Cl^- and K^+ channel currents during the action potential in *Chara*. Simultaneous recording of membrane voltage and patch currents. *J Membr Biol* 141, 297–309.

Huber AE, Bauerle TL (2016) Long-distance plant signaling pathways in response to multiple stressors: The gap in knowledge. *J Exp Bot* 67, 2063–2079.

Iijima T, Sibaoka T (1985) Membrane potentials in excitable cells of *Aldrovanda vesiculosa* trap-lobes. *Plant Cell Physiol* 26, 1–13.

Jones DL, Shannon D, Junvee-Fortune T, Farrar JF (2005) Plant capture of free amino acids is maximized under high soil amino acid concentrations. *Soil Biol Biochem* 37, 179–181.

Kan CC, Chung TY, Wu HY, Juo YA, Hsieh MH (2017) Exogenous glutamate rapidly induces the expression of genes involved in metabolism and defense responses in rice roots. *BMC Genomics* 18, 1–17.

Kang J, Mehta S, Turano FJ (2004) The putative glutamate receptor 1.1 (AtGLR1.1) in *Arabidopsis thaliana* regulates abscisic acid biosynthesis and signaling to control development and water loss. *Plant Cell Physiol*, 45, 1380-1389.

Kang J, Turano FJ (2003) The putative glutamate receptor 1.1 (AtGLR1.1) functions as a regulator of carbon and nitrogen metabolism in *Arabidopsis thaliana*. *Proc Natl Acad Sci USA* 10011, 6872-6877.

Kataev AA, Zherelova OM, Berestovsky GN (1984) Ca^{2+}-induced activation and irreversible inactivation of chloride channels in the perfused plasmalemma of *Nitellopsis obtusa*. *Gen Physiol Biophys* 3, 447–462.

Katsuhara M, Tazawa M (1986) Salt tolerance in *Nitellopsis obtusa*. *Protoplasma* 135, 155–161.

Katsuhara M, Tazawa M (1988) Changes in sodium and potassium in *Nitellopsis* cells treated with transient salt stress. *Plant Cell Environ* 11, 71–74.

Katsuhara M, Tazawa M (1992) Calcium-Regulated Channels and their Bearing on Physiological Activities in Characean Cells. *Philosophical Transactions of the Royal Society B: Biological Sciences* 338, 19–29.

Kikuyama M (1986) Tonoplast Action Potential of Characeae. *Plant Cell Physiol* 27, 1461–1468.

Kikuyama M, Shimada K, Hiramoto Y (1993) Cessation of cytoplasmic streaming follows an increase of cytoplasmic Ca^{2+} during action potential in *Nitella*. *Protoplasma* 174, 142–146.

Kikuyama, M, Tazawa M (1983) Transient increase of intracellular Ca^{2+} during excitation of tonoplast-free Chara cells. *Protoplasma* 117, 62-67.

Kishimoto U (1968). Response of *Chara* internodes to mechanical stimulation. *Ann Rep Biol Works Fac Sci Osaka Univ* 16, 213–218.

Kisnieriene V, Ditchenko TI, Kudryashov AP, Sakalauskas V, Yurin VM, Ruksenas O (2012) The effect of acetylcholine on Characeae K^+ channels at rest and during action potential generation. *Cent Eur J Biol* 7, 1066–1075.

Kisnieriene V, Lapeikaite I, Pupkis V (2018) Electrical signalling in *Nitellopsis obtusa*: Potential biomarkers of biologically active compounds. *Funct Plant Biol* 45, 132-142.

Kisnieriene V, Lapeikaite I, Pupkis V, Beilby MJ (2019) Modeling the Action Potential in Characeae *Nitellopsis obtusa*: Effect of Saline Stress. *Front Plant Sci* 10, 1–15.

Kisnieriene V, Lapeikaite I, Sevriukova O, Ruksenas O (2016) The effects of Ni^{2+} on electrical signaling of *Nitellopsis obtusa* cells. *J Plant Res* 129, 551–558.

Kisnieriene V, Sakalauskas V (2005) Al^{3+} induced membrane potential changes in *Nitellopsis obtusa* cells. *Biologija* 1, 31-34.

Kisnieriene V, Sakalauskas V, Pleskačiauskas A, Yurin V, Rukšenas O (2009) The combined effect of Cd^{2+} and ACh on action potentials of *Nitellopsis obtusa* cells. *Cent Eur J Biol* 4, 343–350.

Kong D, Hu HC, Okuma E, Lee Y, Lee HS, Munemasa S, Cho D, Ju C, Pedoeim L, Rodriguez B, Wang J, Im W, Murata Y, Pei ZM, Kwak JM (2016) L-Met Activates *Arabidopsis* GLR Ca^{2+} Channels Upstream of ROS Production and Regulates Stomatal Movement. *Cell Rep* 17, 2553–2561.

Kong D, Ju C, Parihar A, Kim S, Cho D, Kwak JM (2015) Arabidopsis Glutamate Receptor Homolog3.5 Modulates Cytosolic Ca^{2+} Level to Counteract Effect of Abscisic Acid in Seed Germination. *Plant Physiol*, 167, 1630-1642.

Koziolek C, Grams TEE, Schreiber U, Matyssek R, Fromm J (2004) Transient Knockout of Photosynthesis Mediated by Electrical Signals, *New Phytol* 161, 715–722.

Krol E, Dziubinska H, Stolarz M, Trebacz K (2006) Effects of ion channel inhibitors on cold- and electrically-induced action potentials in *Dionaea muscipula*. *Biol Plant* 50, 411–416.

Król E, Dziubińska H, Trebacz K (2010) What do plants need action potentials for? *Action potential: biophysical and cellular context, initiation, phases and propagation* 1–26.

Krol E, Dziubinska H, Trebacz K, Koselski M, Stolarz M (2007) The influence of glutamic and aminoacetic acids on the excitability of the liverwort *Conocephalum conicum*. *J Plant Physiol* 164, 773–784.

Kwaaitaal M, Huisman R, Maintz J, Reinstadler A, Panstruga R (2011) Ionotropic glutamate receptor (iGluR)-like channels mediate MAMP-induced calcium influx in *Arabidopsis thaliana*. *Biochem J* 440, 355–373.

Lacombe B, Becker D, Hedrich R, DeSalle R, Hollmann M, Kwak JM, Schroeder JI, Le Novère N, Nam HG, Spalding EP, Tester M (2001) The Identity of Plant Glutamate Receptors. *Science* 292, 1486 – 1487.

Lam HM, Chiu J, Hsieh MH, Meisel L, Oliveira IC, Shin M, Coruzzi G (1998) Glutamate-receptor genes in plants. *Nature* 396, 125–126.

Lapeikaite I, Dragunaite U, Pupkis V, Ruksenas O, Kisnieriene V (2019) Asparagine alters action potential parameters in single plant cell. *Protoplasma* 256, 511–519.

Laver DR, Walker NA (1991) Activation by Ca^{2+} and block by divalent ions of the K^+ channel in the membrane of cytoplasmic drops from *Chara australis*. *J Membr Biol* 120, 131–139.

Lea PJ, Miflin BJ (2003) Glutamate synthase and the synthesis of glutamate in plants. *Plant Physiol Biochem* 41, 555–564.

Lea PJ, Sodek L, Parry MAJ, Shewry PR, Halford NG (2007) Asparagine in plants. *Ann Appl Biol* 150, 1–26.

Lewis LA, McCourt RM (2004) Green algae and the origin of land plants. *Am J Bot* 91, 1535–1556.

Lohaus G, Heldt H-W (1997) Assimilation of gaseous ammonia and the transport of its products in barley and spinach leaves. *J Exp Bot* 48, 1779–1786.

Lunevsky VZ, Zherelova OM, Vostrikov IY, Berestovsky GN (1983) Excitation of Characeae cell membranes as a result of activation of calcium and chloride channels. *J Membr Biol* 72, 43–58.

McAinsh MR, Pittman JK (2009) Shaping the calcium signature. *New Phytol* 1816 275-294

McCourt RM, Casanova MT, Karol KG, Feist M (1999) Monophyly of genera and species of Characeae based on rbcL sequences, with special reference to Australian and European *Lychnothamnus barbatus* (Characeae: Charophyceae). *Aust J Bot* 47, 361–369.

Medvedev SS (2018) Principles of Calcium Signal Generation and Transduction in Plant Cells. *Russ J Plant Physiol* 65, 771–783.

Meyerhoff O, Müller K, Roelfsema MRG, Latz A, Lacombe B, Hedrich R, Dietrich P, Becker D (2005) AtGLR3.4, a glutamate receptor channel-like gene is sensitive to touch and cold. *Planta* 222, 418–427.

Michard E, Lima PT, Borges F, Silva AC, Portes MT, Carvalho JE, Gilliham M, Liu LH, Obermeyer G, Feijó JA (2011) Glutamate receptor-like genes form Ca^{2+} channels in pollen tubes and are regulated by pistil D-serine. *Science* 332, 434–437.

Miller AJ, Fan X, Shen Q, Smith SJ (2008) Amino acids and nitrate as signals for the regulation of nitrogen acquisition. *J Exp Bot* 59, 111–119.

Mimura T, Tazawa M (1983). Effect of intracellular Ca^{2+} on membrane potential and membrane resistance in tonoplast-free cells of *Nitellopsis obtusa*. *Protoplasma* 118, 49-55.

Mousavi SAR, Chauvin A, Pascaud F, Kellenberger S, Farmer EE (2013) GLUTAMATE RECEPTOR-LIKE genes mediate leaf-to-leaf wound signalling. *Nature* 500, 422–426.

Munnik T, Vermeer JE (2010) Osmotic stress-induced phosphoinositide and inositol phosphate signalling in plants. *Plant Cell Environ* 33, 655-669.

Nazoa P, Vidmar JJ, Tranbarger TJ, Mouline K, Damiani I, Tillard P, Zhuo D, Glass AD, Touraine B (2003) Regulation of the nitrate transporter gene AtNRT2.1 in *Arabidopsis thaliana*: responses to nitrate, amino acids and developmental stage. *Plant Mol Biol* 52, 689–703.

Nguyen CT, Kurenda A, Stolz S, Chételat A, Farmer EE (2018) Identification of cell populations necessary for leaf-to-leaf electrical signaling in a wounded plant. *Proc Natl Acad Sci USA* 115, 10178–10183.

Nishiyama T, Sakayama H, de Vries J, Buschmann H, Saint-Marcoux D, Ullrich KK, Haas FB, Vanderstraeten L, Becker D, Lang D, Vosolsobě S, Rombauts S, Wilhelmsson PKI, Janitza P, Kern R, Heyl A, Rümpler F, Villalobos LIAC, Clay JM, Skokan R, Toyoda A, Suzuki Y, Kagoshima H, Schijlen E, Tajeshwar N, Catarino B, Hetherington AJ, Saltykova A, Bonnot C, Breuninger H, Symeonidi A, Radhakrishnan G V., Van Nieuwerburgh F, Deforce D, Chang C, Karol KG, Hedrich R, Ulvskov P,

Glöckner G, Delwiche CF, Petrášek J, Van de Peer Y, Friml J, Beilby M, Dolan L, Kohara Y, Sugano S, Fujiyama A, Delaux PM, Quint M, Theißen G, Hagemann M, Harholt J, Dunand C, Zachgo S, Langdale J, Maumus F, Van Der Straeten D, Gould SB, Rensing SA (2018) The Chara Genome: Secondary Complexity and Implications for Plant Terrestrialization. *Cell* 174, 448–464.

Okazaki Y, Sakano K, Tazawa M (1987) Turgor Regulation in a Brackish Water Charophyte, *Lamprothamnium succinctum* III. Changes in Cytoplasmic Free Amino Acids and Sucrose Contents during Turgor Regulation. *Plant Cell Physiol* 28, 663–669.

Okihara K, Ohkawa TA, Tsutsui I, Kasai M (1991) A Ca^{2+}- and voltage-dependent Cl^--sensitive anion channel in the *Chara* plasmalemma: A patch-clamp study. *Plant Cell Physiol* 32, 593–601.

Oliveira IC, Brenner E, Chiu J, Hsieh MH, Kouranov A, Lam HM, Shin MJ, Coruzzi G (2001) Metabolite and light regulation of metabolism in plants: Lessons from the study of a single biochemical pathway. *Braz J Med Biol Res* 34, 567–575.

Opritov VA, Lobov SA, Pyatygin SS, Mysyagin SA (2005) Analysis of possible involvement of local bioelectric responses in chilling perception by higher plants exemplified by *Cucurbita pepo*. *Russ J Plant Physiol* 52, 801-808.

Opritov VA, Pyatygin SS, Vodeneev VA (2002) Direct coupling of action potential generation in cells of a higher plant (*Cucurbita pepo*) with the operation of an electrogenic pump. *Russ J Plant Physiol* 49, 142-147.

Ortega JL, Roche D, Sengupta-Gopalan C (1999) Oxidative turnover of soybean root glutamine synthetase. In vitro and in vivo studies. *Plant Physiol* 119, 1483–1496.

Ortiz-Lopez A, Chang H, Bush DR (2000) Amino acid transporters in plants. *Biochim Biophys Acta Biomembr* 1465, 275-280.

Ortiz-Ramírez C, Michard E, Simon AA, Damineli DSC, Hernández-Coronado M, Becker JD, Feijó JA (2017) GLUTAMATE RECEPTOR-LIKE channels are essential for chemotaxis and reproduction in mosses. *Nature* 549, 91–95.

Philippe F, Verdu I, Morère-Le Paven MC, Limami AM, Planchet E (2019) Involvement of *Medicago truncatula* glutamate receptor-like channels in nitric oxide production under short-term water deficit stress. *J Plant Physiol* 236, 1–6.

Price MB, Jelesko J, Okumoto S (2012) Glutamate receptor homologs in plants: functions and evolutionary origins. *Front Plant Sci* 3, 1–10.

Pyatygin SS, Opritov VA, Vodeneev VA (2008) Signaling role of action potential in higher plants. *Russ J Plant Physiol* 55, 285–291.

Qi Z, Stephens NR, Spalding EP (2006) Calcium entry mediated by GLR3.3, an Arabidopsis glutamate receptor with a broad agonist profile. *Plant physiol* 142, 963–71.

Qi Z, Stephens NR, Spalding EP (2006) Calcium entry mediated by GLR3.3, an *Arabidopsis* glutamate receptor with a broad agonist profile. *Plant Physiol* 142, 963–971.

Qiu XM, Sun YY, Ye XY, Li ZG (2019) Signaling Role of Glutamate in Plants. *Front Plant Sci* 10, 1–11.

Roelfsema M, Hedrich R (2010) Making sense out of Ca^{2+} signals: their role in regulating stomatal movements. *Plant Cell Environ* 33, 305–321.

Rousseaux CG (2008) A Review of Glutamate Receptors I: Current Understanding of Their Biology. *J Toxicol Pathol* 21, 25–51.

Sandström J, Pettersson J (1994) Amino acid composition of phloem sap and the relation to intraspecific variation in pea aphid (*Acyrthosiphon pisum*) performance. *J Insect Physiol* 40, 947–955.

Seifi HS, Van Bockhaven J, Angenon G, Höfte M (2013) Glutamate metabolism in plant disease and defense: friend or foe? *Mol Plant Microbe Interact* 26, 475–485.

Sevriukova O, Kanapeckaite A, Kisnieriene V, Ladygiene R, Lapeikaite I, Sakalauskas V (2014) Modifying action of tritium on the charophytes bioelectrical response to anthropogenic pollution. *Trace Elements and Electrolytes* 31, 60–66.

Shepherd JD, Huganir RL. 2007. The cell biology of synaptic plasticity: AMPA receptor trafficking. *Annu Rev Cell Dev Biol* 23, 613–643.

Shepherd VA, Beilby MJ, Al Khazaaly SAS, Shimmen T (2008) Mechano-perception in *Chara* cells: The influence of salinity and calcium on touch-activated receptor potentials, action potentials and ion transport. *Plant Cell Environ* 31, 1575–1591.

Shetty K, Asano Y, Oosawa K, 1992. Stimulation of in vitro shoot organogenesis in *Glycine max* (Merrill) by allantoin and amides. *J Plant Sci* 81, 245–251.

Shiina T, Tazawa M (1986) Regulation of membrane excitation by protein phosphorylation in *Nitellopsis obtusa*. *Protoplasma* 134, 60–61.

Shiina T, Tazawa M (1987) Ca^{2+}-activated Cl^- channel in plasmalemma of *Nitellopsis obtusa*. *J Membr Biol* 99, 137–146.

Shimmen M, Mimura T, Kikuyama M, Tazawa M (1994) Characean Cells as a Tool for Studying Electrophysiological Characteristics of Plant Cells. *Cell Struct Funct* 19, 263–278.

Sibaoka T (1969) Physiology of rapid movements in higher plants. *Annu Rev Plant Physiol* 20, 165–184.

Sibaoka T (1991). Rapid plant movements triggered by action potentials. *Bot Mag Tokyo* 104, 73-95.

Singh SK, Chien C Te, Chang IF (2016) The *Arabidopsis* glutamate receptor-like gene GLR3.6 controls root development by repressing the Kip-related protein gene KRP4. *J Exp Bot* 67, 1853–1869.

Sinyukhin AM, Britikov EA (1967) Action potentials in the reproductive system of plants. *Nature* 215, 1278–1280.

Sivaguru M, Pike S, Gassmann W, Baskin TI (2003) Aluminum rapidly depolymerizes cortical microtubules and depolarizes the plasma membrane: evidence that these responses are mediated by a glutamate receptor. *Plant Cell Physiol* 44, 667–675.

Soulié-Märsche I, Benammi M, Gemayel P (2002) Biogeography of living and fossil *Nitellopsis* (Charophyta) in relationship to new finds from Morocco. *Journal of Biogeography* 29, 1703–1711.

Stephens NR, Qi Z, Spalding EP (2008) Glutamate receptor subtypes evidenced by differences in desensitization and dependence on the GLR3.3 and GLR3.4 genes. *Plant Physiol* 146, 529–538.

Stolarz M, Dziubinska H (2017) Osmotic and salt stresses modulate spontaneous and glutamate-induced action potentials and distinguish between growth and circumnutation in *Helianthus annuus* seedlings. *Front Plant Sci* 8, 1–13.

Stolarz M, Król E, Dziubinska H (2010) Glutamatergic elements in an excitability and circumnutation mechanism. *Plant Signal Behav* 5, 1108–1111.

Sukhov V (2016) Electrical signals as mechanism of photosynthesis regulation in plants. *Photosynth Res* 130, 373–387.

Sukhov V, Sukhova E, Vodeneev V (2019) Long-distance electrical signals as a link between the local action of stressors and the systemic physiological responses in higher plants. *Prog Biophys Mol Biol* 146, 63–84.

Sukhov V, Vodeneev V (2009) A Mathematical Model of Action Potential in Cells of Vascular Plants. *J Membrane Biol* 232, 59–67.

Sulieman S, Fischinger SA, Gresshoff PM, Schulze J (2010) Asparagine as a major factor in the N-feedback regulation of N2 fixation in *Medicago truncatula*. *Physiol Plant* 140, 21–31.

Ta TC, Joy KW (1986) Metabolism of some amino acids in relation to the photorespiratory nitrogen cycle of pea leaves. *Planta* 169, 117–122.

Taira M, Valtersson U, Burkhardt B, Ludwig RA (2004) *Arabidopsis thaliana* GLN2-encoded glutamine synthetase is dual targeted to leaf mitochondria and chloroplasts. *Plant Cell* 16, 2048–2058.

Tapken D, Anschütz U, Liu LH, Huelsken T, Seebohm G, Becker D, Hollmann M (2013) A plant homolog of animal glutamate receptors is an ion channel gated by multiple hydrophobic amino acids. *Sci Signal* 6, ra47.

Tapken D, Hollmann M (2008) *Arabidopsis thaliana* Glutamate Receptor Ion Channel Function Demonstrated by Ion Pore Transplantation. *J Mol Biol* 383, 36–48.

Tazawa M, Kikuyama M (2003). Is Ca^{2+} release from internal stores involved in membrane excitation in characean cells? *Plant Cell Physiol*, 44, 518-526.

Teardo E, Formentin E, Segalla A, Giacometti GM, Marin O, Zanetti M, Lo Schiavo F, Zoratti M, Szabò I (2011) Dual localization of plant glutamate receptor AtGLR3.4 to plastids and plasmamembrane. *Biochim Biophys Acta* 1807, 359–67.

Thiel G, Dityatev AE (1998) Transient activity of excitatory Cl^- channels in *Chara*: Evidence for quantal release of a gating factor. *J Membr Biol* 163, 183-191.

Thiel G, Homann U, Gradmann D (1993) Microscopic elements of electrical excitation in *Chara*: Transient activity of Cl^- channels in the plasma membrane. *J Membr Biol* 134, 53–66.

Thiel G, Homann U, Plieth C (1997) Ion channel activity during the action potential in *Chara*: new insights with new techniques. *J Exp Bot* 48, 609–622.

Thiel G, MacRobbie EA, Hanke DE (1990). Raising the intracellular level of inositol 1,4,5-trisphosphate changes plasma membrane ion transport in characean algae. *EMBO J* 9, 1737-1741.

Toyota M, Spencer D, Sawai-Toyota S, Jiaqi W, Zhang T, Koo AJ, Howe GA, Gilroy S (2018) Glutamate triggers long-distance, calcium-based plant defense signaling. *Science* 361, 1112–1115.

Traynelis SF, Wollmuth LP, McBain CJ, Menniti FS, Vance KM, Ogden KK, Hansen KB, Yuan H, Myers SJ, Dingledine R (2010) Glutamate Receptor

Ion Channels: Structure, Regulation, and Function. *Pharmacol Rev* 62, 405–496.

Trebacz K, Dziubinska H, Krol E (2006) Electrical signals in long-distance communication in plants. *Communication in Plants: Neuronal Aspects of Plant Life* 277–290.

Trebacz K, SimonisW, Schönknecht G (1994) Cytoplasmic Ca^{2+},K^{+},Cl^{-},and NO^{-3} activities in the liverwort *Conocephalum conicum* L. at rest and during action potentials. *Plant Physiol* 106,1073–1084.

Tsutsui I, Ohkawa T, Nagai R and Kishimoto U (1987) Role of Calcium Ion in the Excitability and Eiectrogenic Pump Activity of the *Chara corallina* Membrane: I. Effects of La^{3+}, Verapamil, EGTA, W-7, and TFP on the Action Potential. *J Membr Biol* 96, 65–73.

Vatsa P, Chiltz A, Bourque S, Wendehenne D, Garcia-Brugger A, Pugin A (2011) Involvement of putative glutamate receptors in plant defence signaling and NO production. *Biochimie* 93, 2095–2101.

Vincill ED, Bieck AM, Spalding EP (2012) Ca^{2+} conduction by an amino acid-gated ion channel related to glutamate receptors. *Plant Physiol* 159, 40–46.

Vincill ED, Clarin AE, Molenda JN, Spalding EP (2013) Interacting glutamate receptor-like proteins in Phloem regulate lateral root initiation in *Arabidopsis*. *Plant Cell* 25, 1304–1313.

Vodeneev V, Akinchits E, Sukhov V (2015) Variation potential in higher plants: Mechanisms of generation and propagation. *Plant Signal Behav* 10, 1–7.

Wacke M, Thiel G (2001) Electrically triggered all-or-none Ca^{2+}-liberation during action potential in the giant alga *Chara*. *J Gen Physiol* 118, 11-22.

Wacke M, Thiel G, Hütt MT (2003) Ca^{2+} dynamics during membrane excitation of green alga *Chara*: model simulations and experimental data. *J Membr Biol* 191, 179–192.

Walch-Liu P, Liu LH, Remans T, Tester M, Forde BG (2006) Evidence that L-glutamate can act as an exogenous signal to modulate root growth and branching in *Arabidopsis thaliana*. *Plant Cell Physiol* 47, 1045–1057.

Wayne R (1994) The excitability of plant cells: With a special emphasis on characean internodal cells. *Bot Rev* 60, 265–367.

Wayne R, Staves MP (1991) The Density of the Cell Sap and Endoplasm of *Nitellopsis* and *Chara*. *Plant Cell Physiol* 32, 1137–1144.

Weiland M, Mancuso S, Baluska F (2016) Signalling via glutamate and GLRs in *Arabidopsis thaliana*. *Funct Plant Biol* 43, 1–25.

Werdin-Pfisterer NR, Kielland K, Boone RD (2009) Soil amino acid composition across a boreal forest successional sequence. *Soil Biol Biochem* 41, 1210–1220.

Williamson RE (1975) Cytoplasmic streaming in *Chara*: a cell model activated by ATP and inhibited by cytochalasin B. *J Cell Sci* 17, 655-668.

Williamson RE, Ashley CC (1982) Free Ca^{2+} and cytoplasmic streaming in the alga *Chara*. *Nature* 296, 647–651.

Winter U, Kirst GO, Grabowski V, Heinemann U, Plettner I, Wiese S (1999) Salinity tolerance in *Nitellopsis obtusa*. *Aust J Bot* 47, 337–346.

Wudick MM, Michard E, Oliveira Nunes C, Feijó JA (2018) Comparing plant and animal glutamate receptors: Common traits but different fates? *J Exp Bot* 69, 4151–4163.

Yang H, Postel S, Kemmerling B, Ludewig U (2014) Altered growth and improved resistance of *Arabidopsis* against *Pseudomonas syringae* by overexpression of the basic amino acid transporter AtCAT1. *Plant Cell Environ* 37, 1404–1414.

Yao X, Zhu G, Cai L, Zhu M, Zhao L, Gao G, Qin B (2012) Geochemical Characteristics of Amino Acids in Sediments of Lake Taihu, A Large, Shallow, Eutrophic Freshwater Lake of China. *Aquat Geochem* 18, 263–280.

Yoshida R, Mori I, Kamizono N, Shichiri Y, Shimatani T, Miyata F, Honda K, Iwai S (2016) Glutamate functions in stomatal closure in *Arabidopsis* and fava bean. *J Plant Res* 129, 39–49.

Young VR, Ajami AM (2000) Glutamate: An Amino Acid of Particular Distinction. *J Nutr* 130, 892S–900S.

Zeier J (2013) New insights into the regulation of plant immunity by amino acid metabolic pathways. *Plant Cell Environ* 36, 2085–2103.

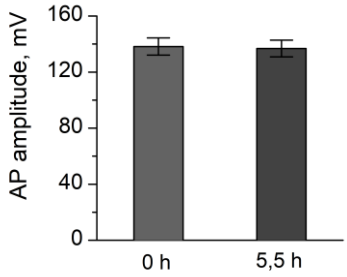

Fig S3a Average AP amplitude during repeated measurements in control solution (APW), n=5. No significant differences were observed.

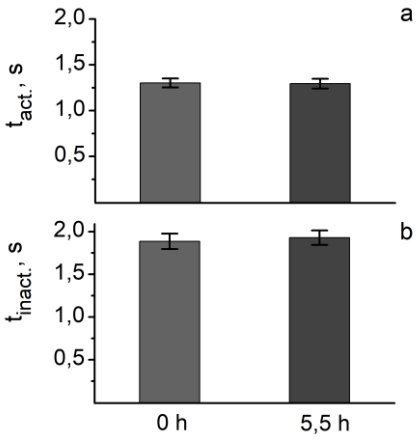

Fig S3b Average Cl^- efflux at -90 mV activation duration $t_{act.}$ (a) and corresponding inactivation duration $t_{inact.}$ (b) during repeated measurements in control solution (APW), n=5. No significant differences were observed.

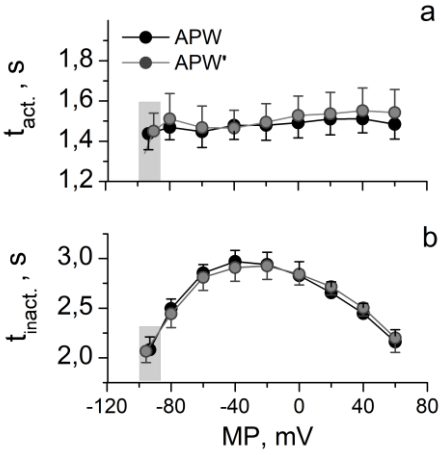

Fig S3c Average Cl^- efflux $t_{act.}$ – efflux activation duration (a) and $t_{inact.}$ - inactivation duration (b) in all voltages of clamped MP in control solution (APW) and after exposure to 1 mM of additional Cl^-. -90 mV membrane potential is indicated in grey background, n=9.

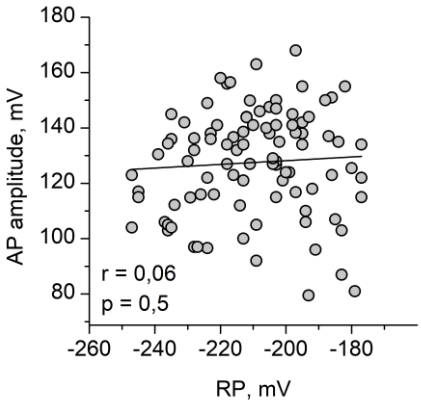

Fig S3d RP values and corresponding AP amplitudes of each cell in control solution (APW), n=93.

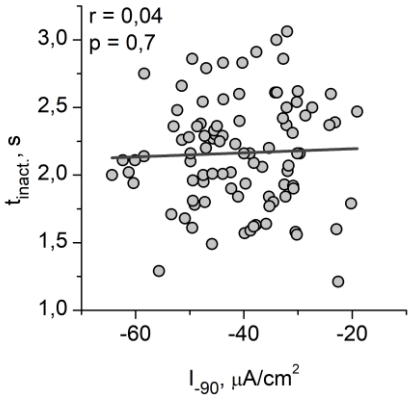

Fig S3e I_{-90} values and corresponding $t_{inact.}$ values of each cell in control solution (APW), n=93.

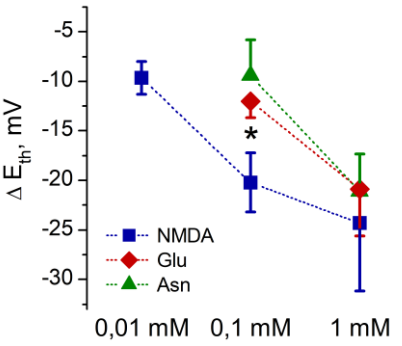

Fig S3f Average hyperpolarizations of E_{th} after exposure to 0,1-1 mM Glu or Asn and 0,01-1 mM NMDA. The asterisk indicates significant differences between the effects of AA and the effect of NMDA, n=3-9 for each treatment set. K_M for NMDA is 0,016 mM, Glu – 0,16 mM and Asn– 0,1 mM.

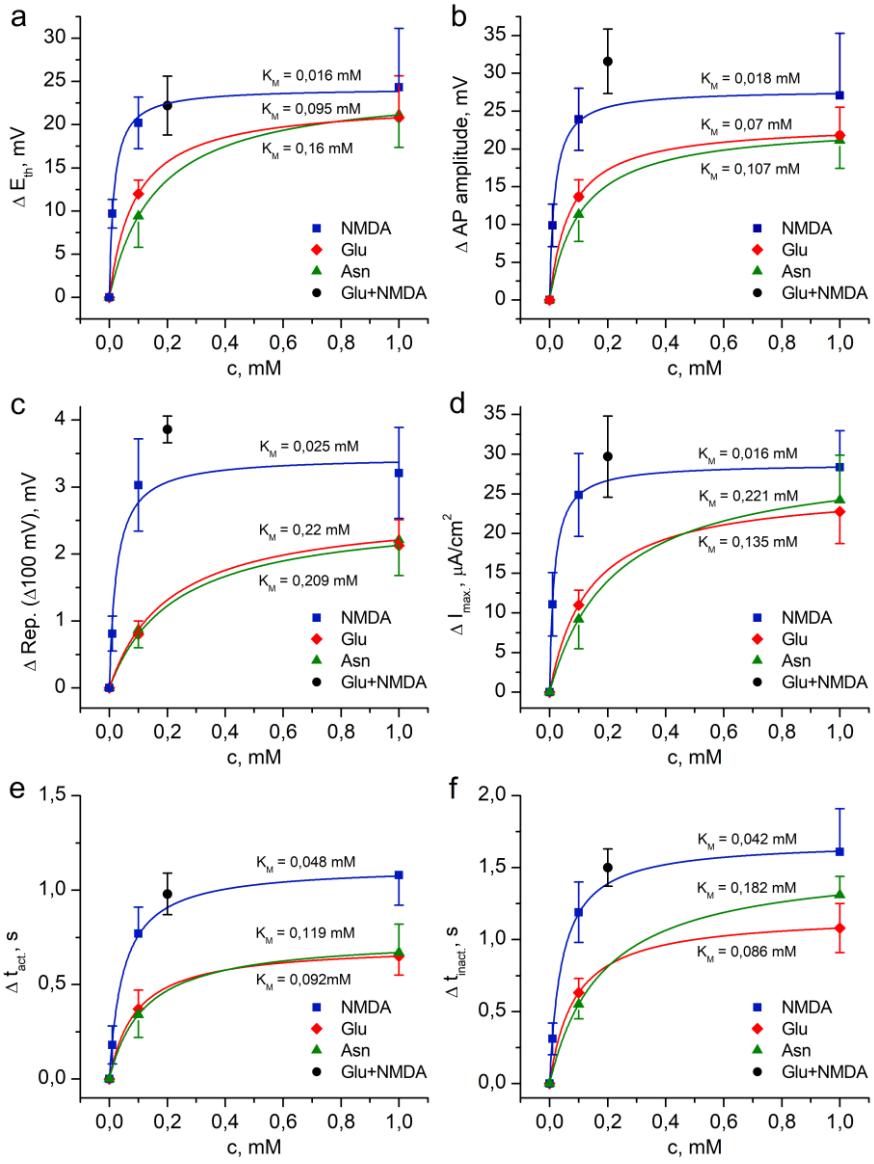

Fig S3g Electrophysiological parameters' changes (upon Asn, Glu, NMDA treatment) aproximations with Michaelis–Menten kinetics: $\Delta = \Delta_{max} * [X] / (K_M + [X])$. Δ_{max} is a saturating difference of a parameter, [*X*] - concentration of a solution. K_M - Michaelis-Menten constant, equal to concentration [*X*] in which parameter reaches half-saturating alteration ($\Delta_{max}/2$), n=3-9 for each treatment set. Glu+NMDA marks co-treatment (0,1 mM Glu+0,1 mM NMDA).

LIST OF PUBLICATIONS

Publications regarding the dissertation:

Journal articles:

Kisnieriene V, Lapeikaite I, Pupkis V (2018) Electrical signalling in *Nitellopsis obtusa*: Potential biomarkers of biologically active compounds. *Funct. Plant Biol.* 45(2), 132-142.

Lapeikaite I, Dragunaite U, Pupkis V, Ruksenas O, Kisnieriene V (2019) Asparagine alters action potential parameters in single plant cell. *Protoplasma* 256, 511–519.

Lapeikaite I, Pupkis V, Neniskis V, Ruksenas O, Kisnieriene V (2020) Glutamate and NMDA affect cell excitability and Action Potential dynamics of single cell of macrophyte *Nitellopsis obtusa*. *Funct. Plant Biol* https://doi.org/10.1071/FP20074.

Conference Proceedings:

1) Lapeikaite I, Kisnieriene V, Sevriukova O. Glutamate and NMDA effect on single characeaen cell membrane transport systems activity. Plant transport 2014: Systems and synthetic biology, Glasgow, UK, 2014.
2) Kisnieriene V, Lapeikaite I, Sevriukova O. Daktariunas A., Ruksenas O. *Nitellopsis obtusa* as model system for environmental impact investigation: current and voltage clamp approaches. 3rd International Symposium on Plant Signaling and Behavior, Paris, 2015, p. 99.
3) Kisnieriene V, Lapeikaite I, Pupkis V. Neuroactive compounds and electrical signaling in "green axon" *Nitellopsis obtusa*. 4th International Symposium on Plant Signaling and Behavior, 2016, St. Petersburg, p. 57.
4) Lapeikaite I, Dragunaite U, Kisnieriene V. Asparagine effect on single Characean cell action potential parameters. 4th International Symposium on Plant signaling and Behavior, 2016, St. Petersburg, p. 59.
5) Kisnierienė V and Lapeikaite I. Mechanisms of aluminium toxicity: from plants to humans. 3rd international conference Evolutionary medicine: pre-existing mechanisms and patterns of current health issues, 2016, Vilnius, p. 61.
6) Pupkis V, Lapeikaite I, Kisnieriene V. Effect of blockers on ion channels in the tonoplast of *Nitellopsis obtusa* investigated using patch clamp technique. XVth International Conference of the Lithuanian Biochemical Society, 2018, Dubingiai, p. 41.
7) Lapeikaite I, Pupkis V, Kisnieriene V. Changes of *Nitellopsis obtusa* Action Potential properties in response to exogenous L-asparagine. 2nd

International scientific conference “Plant cell biology and biotechnology”, Minsk, 2018.

8) Pupkis V, Lapeikaite I, Kisnieriene V. Investigation of plant electrical signaling: biophysical approaches. Baltic Biophysics Conference, 2018, Kaunas, p. 41.

9) Kisnieriene V, Pupkis V, Lapeikaite I. Exploring electrical signalling alterations of *Nitellopsis obtusa* cells in response to modulators of ion channels. Joint 12th EBSA congress and 10th ICBP – IUPAP congress, 2019, Madrid (Spain), *European Biophysics Journal with Biophysics Letters* 48 (1 Supplement), p. S162.

10) Pupkis V, Lapeikaite I, Kisnieriene V. Electrophysiological Examination of the Effects of Classical Pharmacological Agent Verapamil in Plant-Based Model System. 64th Annual meeting of the Biophysical Society, 2020, San Diego (USA), *Biophysical Journal* 118 (3 Supplement 1), p. 591A.

Other publications:

Journal articles:

Bariseviciute R, Skipityte R, Pukiene R, Lapeikaite I, Kakaras I, Remeikis V (2017) Climatic sensitivity of $\delta^{13}C$ in tree rings of Quercus robur L., Populus tremula L. and Pinus sylvestris L. in Vilnius region (eastern Lithuania). *Dendrobiology* 78.

Kisnieriene V, Lapeikaite I, Pupkis V, Beilby MJ (2019) Modeling the Action Potential in Characeae *Nitellopsis obtusa*: Effect of Saline Stress. *Frontiers in Plant Science*, 10, 1–15.

Kisnieriene V, Lapeikaite I, Sevriukova O, Ruksenas O (2016) The effects of Ni^{2+} on electrical signaling of *Nitellopsis obtusa* cells. *Journal of Plant Research* 129.

Kisnieriene V, Lapeikaite I (2015) When chemistry meets biology: The case of aluminium - A review. *Chemija* 26.

Book chapter:

Kisnieriene, V, Lapeikaite, I and Pupkis, V (2018). Neurotransmitters in Characeaen Electrical Signaling in Ramakrishna, A. and Roshchina, V.V. (eds.). Neurotransmitters in Plants: Perspectives and Applications, CRC Press; pp. 181-200.

ORCID ID: https://orcid.org/0000-0001-7323-1721

ABOUT THE AUTHOR

Professional Experience:

The author from 2015 has worked as a research assistant at the Department of Neurobiology and Biophysics, Institute of Biosciences, Vilnius University, since 2018 in joint Lithuanian-Polish project "Long-distance electrical signalling systems in plants – adaptation to the change from water to terrestrial environment" (S-LL-18-1) (DAINA). The author also conducted laboratory work, assisted final exams, advised and supervised students' final theses in Vilnius University:

Dragunaite U (2016). Asparagine effect on characean cells electrical properties. Master's thesis in Biophysics, Vilnius, Vilnius University.

Neniskis V (2017). Investigation of the effect of NMDA receptor ligands on electrophysiological properties of plant cell. Master's thesis in Neurobiology, Vilnius, Vilnius University.

Education:

Ph.D in Biophysics 2014 – 2019
M.Sc in Biophysics 2012 – 2014 (*magna cum laude*)
B.Sc in Biophysics 2008 – 2012
Vilnius University, Lithuania

Member of:

Federation of European Neuroscience Societies (FENS) since 2013
Lithuanian Neuroscience Association (LNA) since 2013
The Botanical Society of Japan since 2015
European Biophysical Societies' Association (EBSA) since 2019

The author also has given science-promoting lectures at the Vilnius University and other education facilities in Lithuania since 2015.

Courses/training:

School for young scientists "Plant cell biology: from theory to practice", Minsk, 2018

ACKNOWLEDGEMENTS

My appreciation and gratitude goes towards the department of Neurobiology and Biophysics for sympathetic environment, support, willingness to share and life lessons granted during the road of knowledge-seeking. I thank prof. Osvaldas Rukšėnas for established opportunities and trust. Heart-warming environment provided by Algis Daktariūnas and other members of the department is much cherished.

The deepest respect and gratefulness navigates to Vilma Kisnierienė, my supervisor, mentor and long-term example. I thank the present and the ex-members of plant electrophysiology laboratory: Vilmantas Pupkis for editing this thesis and goodwill, Vidmantas Sakalauskas for valuable lessons during my first attempts at scientific research.

Deepest gratitude goes to my family - for all the foundations and the notion of the love for knowledge. I'm grateful to my foremost formal teachers - Dalia Vėželienė and Daiva Puodžiukienė.

For all the support and adventures they caused I thank all the friends and cousins of mine.

Vilnius University Press
9 Saulėtekio Ave., Building III, LT-10222 Vilnius
Email: info@leidykla.vu.lt, www.leidykla.vu.lt
Print run copies 14